Phytol and Tocopherol Metabolism in *Arabidopsis thaliana*

Dissertation

zur

Erlangung des Doktorgrades (Dr. rer. nat.)

der

Mathematisch-Naturwissenschaftlichen Fakultät

der

Rheinischen Friedrich-Wilhelms-Universität Bonn

vorgelegt von

Katharina vom Dorp

aus

Bonn

Bonn, Mai 2015

Angefertigt mit Genehmigung der Mathematisch-Naturwissenschaftlichen Fakultät der Rheinischen Friedrich-Wilhelms-Universität Bonn.

Erster Gutachter: Prof. Dr. Peter Dörmann
Zweiter Gutachter: Prof. Dr. Lukas Schreiber
Tag der Promotion: 12.10.2015
Erscheinungsjahr: 2015

Table of Contents

Table of Figures

Abbreviations

% (v/v)	Percent volume per volume (ml per 100 ml)
% (w/v)	Percent weight per volume (g per 100 ml)
ACP	Acyl-carrier protein
CHAPS	3-[(3-Cholamidopropyl)dimethylammonio]-1-propanesulfonate
CID	Collision-induced dissociation
CoA	Coenzyme A
COG	Cluster of orthologous genes
CTAB	Cetyltrimethylammonium bromide
DAG	Diacylglycerol
ddH_20	Double deionized water
DGAT	Diacylglycerol acyltransferase
DGDG	Digalactosyldiacylglycerol
DMAPP	Dimethylallyl-pyrophosphate
DNA	Deoxyribonucleic acid
dNTPs	Deoxyribonucleotide triphosphates (dATP, dCTP, dTTP, dGTP)
DUF	Domain of unknown function
EDTA	Ethylenediaminetetraacetic acid
ELT	Esterase-lipase-thioesterase
ER	Endoplasmic reticulum
ESI	Electrospray ionization
et al.	Lat.: *et alii* = and others
FAME	Fatty acid methyl ester
FID	Flame ionization detector
FLD	Fluorescence light detector
GC-FID	Gas chromatography-flame ionization detection
GC-MS	Gas chromatography-mass spectrometry
GFP	Green fluorescent protein
GG-P/-PP	Geranylgeranyl-phosphate/-pyrophosphate
GGR	Geranylgeranyl reductase
HPLC	High pressure liquid chromatography
HPT	Homogentisate phytyltransferase
IPP	Isopentenyl-pyrophosphate
I.S.	Internal standard
LB medium	Luria-Bertani medium
LC-MS	Liquid chromatography coupled to mass spectrometry
MGDG	Monogalactosyldiacylglycerol
mol%	Molar percentage
MOPS	3-Morpholinopropane-1-sulfonic acid
MS	Mass spectrometry
MS medium	Murashige and Skoog medium
MSTFA	N-Methyl-N-(trimethylsilyl) trifluoroacetamide
NADPH	Nicotinamide adenine dinucleotide phosphate
NTPs	Ribonucleotide triphosphates (ATP, CTP, UTP, GTP)
OD	Optical density
ORF	Open reading frame
P	Phosphate
PC	Phosphatidylcholine
PC-8	Plastochromanol-8
PDAT	Phospholipid:diacylglycerol acyltransferase
PES	Phytyl Ester Synthase
Phytyl-P/-PP	Phytyl-phosphate/-pyrophosphate
PP	Pyrophosphate
PPH	Pheophytin pheophorbide hydrolase

PPK	Phytyl-phosphate kinase
Q-TOF MS	Quadrupole Time-of-Flight Mass Spectrometer
RNA	Ribonucleic acid
ROS	Reactive oxygen species
rpm	Revolutions per minute
RT	Room temperature
RT-PCR	Reverse transcription PCR
SD	Standard deviation
SPE	Solid phase extraction
TLC	Thin layer chromatography
Tris	Tris(hydroxymethyl)aminomethane
UDP	Uridine diphosphate
VTE	Vitamin E deficient
woTP	Without transit peptide for translocation to plastids
WT	Wild type

Abbreviation for Lipids and Isoprenoids:

In this work, fatty acids and alcohols are abbreviated as follows:

X:Yz, where X indicates the number of C-atoms, Y indicates the number of double bonds and z is substituted by "ol" if the compound is an alcohol. For glycerolipids (TAGs, phospholipids and galactolipids) that contain more than one fatty acid, the C atoms and double bonds for the fatty acid moieties are summarized, e.g. 36:6-PC stands for phosphatidylcholine with two 18:3-fatty acids.

1 Introduction

Plants are photoautotrophic organisms. Therefore, they can synthesize all structural and functional components of the cell (Benedict and Benedict, 1978). Energy fixation and carbon assimilation in plants is mediated by photosynthesis. Photosynthesis represents a redox reaction accompanied with the production of oxygen (O_2) and consumption of carbon dioxide (CO_2) (Scheibe, 1991). Photosynthesis is localized to plant chloroplasts, organelles derived from the endosymbiosis of a photosynthetic bacterium and an early eukaryotic cell (Whatley and Whatley, 1981; Dyall *et al.,* 2004). They are separated from the cytosol by two membranes, the outer and inner envelopes (Gunning, 1965; Block *et al.,* 1983). An intricate structure of internal membranes (thylakoids) is localized to the stroma of chloroplasts. The photosystems I and II as well as light harvesting complex II (LHCII) are embedded in the thylakoid membranes (Anderson and Melis, 1983). These photosystems harbor the components for the electron transfer chain: chlorophyll, pheophytin, phylloquinone (vitamin K1), plastoquinone, carotenoids and ferredoxin. Thylakoids also contain the galactolipids monogalactosyldiacylglycerol (MGDG) and digalactosyldiacylglycerol (DGDG). Furthermore, starch granules and plastoglobules are found in chloroplasts, for deposition of starch and non-polar lipids, respectively (Steinmüller and Tevini, 1985; Tevini and Steinmüller, 1985). Chlorophyll, prenyl-quinones (phylloquinone, plastoquinone and tocochromanols) and fatty acid phytyl esters are isoprenoid-derived, nonpolar lipids and play a major role in plastid metabolism. Plastoglobules are plastid-specific subcompartments which harbor electron-dense structures. Purified plastoglobule fractions contain a variety of non-polar lipids, including triacylglycerol (TAG), tocochromanols (vitamin E), plastoquinone and plastoquinol (Steinmüller and Tevini, 1985; Tevini and Steinmüller, 1985; Vidi *et al.*, 2006). Moreover, fatty acid phytyl esters are stored in plastoglobules (Vidi *et al.,* 2006; Gaude *et al.,* 2007). During senescence and under conditions of stress, the size of plastoglobules strongly increases.

1.1 Isoprenoid Metabolism in Plants

1.1.1 Isoprenoid *de novo* Synthesis

All isoprenoids (also called terpenoids) are derived from the C5 isoprene units isopentenyl-PP (IPP) and dimethylallyl-PP (DMAPP) (Lichtenthaler *et al.,* 1997). However, the origin of these precursors differs between cell compartments in plants (Figure 1). The mevalonic acid pathway is present in all eukaryotes (Lichtenthaler *et al.,* 1997; Rohmer, 1999; Lange *et al.,* 2000). The first step of the mevalonic acid pathway is the synthesis of 3-hydroxy-3-methylglutaryl-coenzyme A

(HMG-CoA) from acetyl-CoA and acetoacetyl-CoA (Rogers, 1983). The following deacylation of HMG-CoA to mevalonic acid using NADPH as reducing agent is the first committed step of the mevalonic acid pathway (Linn, 1967; Rogers, 1983). HMG-CoA reductase is localized in the endoplasmic reticulum (ER) (Re *et al.,* 1997). Mevalonic acid is converted to IPP via hydrolysis of ATP and decarboxylation. The C5 unit IPP can be isomerized to DMAPP by isopentenyl-PP isomerase (Ogura *et al.,* 1968; Jedlicki *et al.,* 1972; Phillips *et al.,* 2008a). In plastids of plants and in bacteria, the same reaction products, IPP and DMAPP, can also be produced via another pathway, the non-mevalonic acid or methylerythritol-4-phosphate (MEP) pathway (Rohmer, 1999). Here, the starting point of the pathway is the synthesis of 1-deoxy-D-xylulose-5-phosphate (DOXP) from glyceraldehyde-3-phosphate and pyruvate via a condensation reaction, catalyzed by 1-deoxy-D-xylulose-5-phosphate (DOXP) synthase (Lichtenthaler, 1999; Rodríguez-Concepción and Boronat, 2002). The enzyme 1-deoxy-D-xylulose-5-phosphate (DOXP) reductoisomerase converts 1-deoxy-D-xylulose-5-phosphate (DOXP) to methylerythritol-4-phosphate (MEP). The enzyme 4-diphosphocytidyl-2C-methyl-D-erythritol cytidylyltransferase adds a cytosine monophosphate group from cytosine triphosphate to DOXP, generating 4-diphosphocytidyl-2C-methyl-D-erythritol. Finally, IPP is synthesized by 4-hydroxy-3-methylbut-2-enyl diphosphate synthase and reductase (Hunter, 2007; Phillips *et al.,* 2008b).

The precursors IPP and DMAPP (C5, hemiterpenes) can be condensed in a head-to-tail manner to generate C10, C15 and C20 isoprenyl-PPs. These condensation reactions are carried out by isoprenyl-PP synthases (Chen *et al.,* 1994; Zhu *et al.,* 1997; Wang, 2000; Schmidt and Gershenzon, 2007). Geranyl-PP is formed from two C5 units, farnesyl-PP from three C5 units and geranylgeranyl-PP (GG-PP) is formed by combination of four C5 units. The isoprenoids that derive from these precursors are organised according to the number of C-atoms: monoterpenes are derived from geranyl-PP (C10), sesquiterpenes from farnesyl-PP (C15) and diterpenes are derived from GG-PP (C20) (Figure 2).

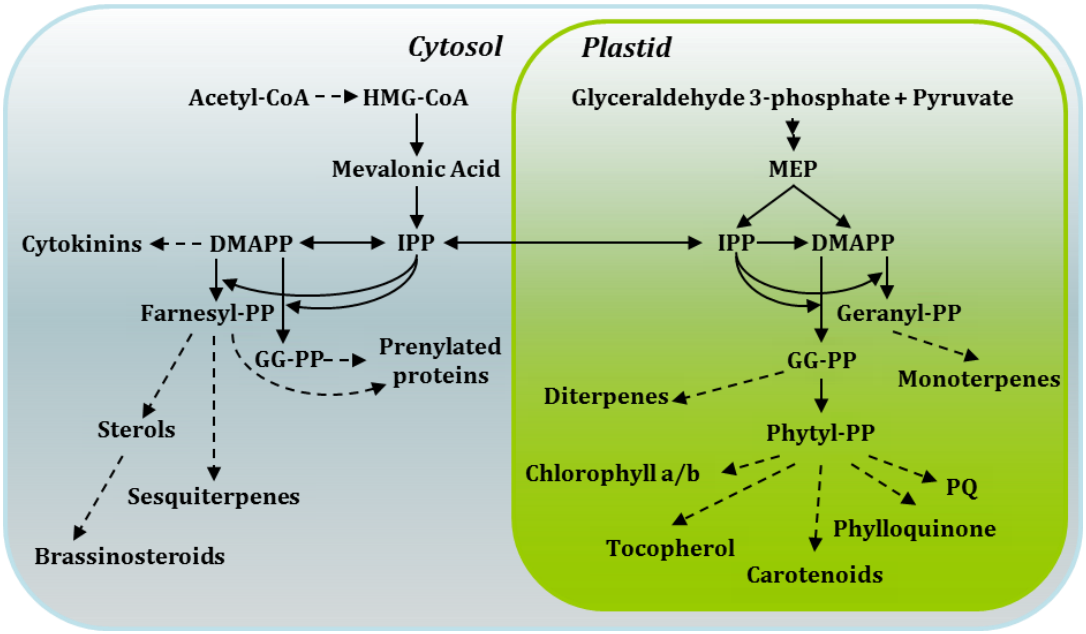

Figure 1 Compartmentalization of Isoprenoid *de novo* Synthesis in Plants.

The precursors for isoprenoids in plants, IPP and DMAPP, can be synthesized via a plastidial pathway (MEP pathway) from condensation of glyceraldehyde-3-phosphate and pyruvate or via a non-plastidial pathway (mevalonic acid pathway) starting from acetyl-CoA and acetoacetyl-CoA. In the plastid, these C5 precursors are mainly used to synthesize compounds important for photosynthetic activity, such as pigments (chlorophyll, carotenoids) or components of the electron transport chain (phylloquinone, plastoquinone). Modified from Rodríguez-Conceptión and Boronat (2002).

The group of isoprenoids comprises both primary and secondary metabolites. Primary metabolites derived from isoprenoid synthesis are plant hormones (e.g. cytokinins), photosynthetic pigments or electron carriers for photosynthesis. Secondary metabolites that are produced from isoprenoids are mainly specialized compounds, including anti-herbivoric or anti-pathogenic compounds or bio-attractant compounds that accumulate in certain plant organs (Keeling and Bohlmann, 2006a; Keeling and Bohlmann, 2006b; Erbilgin *et al.,* 2006). Conifers produce bioactive terpenoids as components of their oleoresin which is exuded to deter herbivores. Pathogen attack up-regulates transcript levels of isoprenyl-PP synthases (Nagel *et al.,* 2014). Phytol is produced by the reduction of GG-PP to phytyl-PP catalyzed by the plastid-localized enzyme geranylgeranyl reductase (GGR) (Keller *et al.,* 1998; Tanaka *et al.,* 1999) (Figure 2). Keller *et al.* (1998) showed that GGR can reduce the geranylgeraniol moiety of both GG-PP and geranylgeranylated chlorophyll (chlorophyll-GG). Phytyl-PP is used for the prenylation of tocopherol and phylloquinone and for the synthesis of chlorophyll.

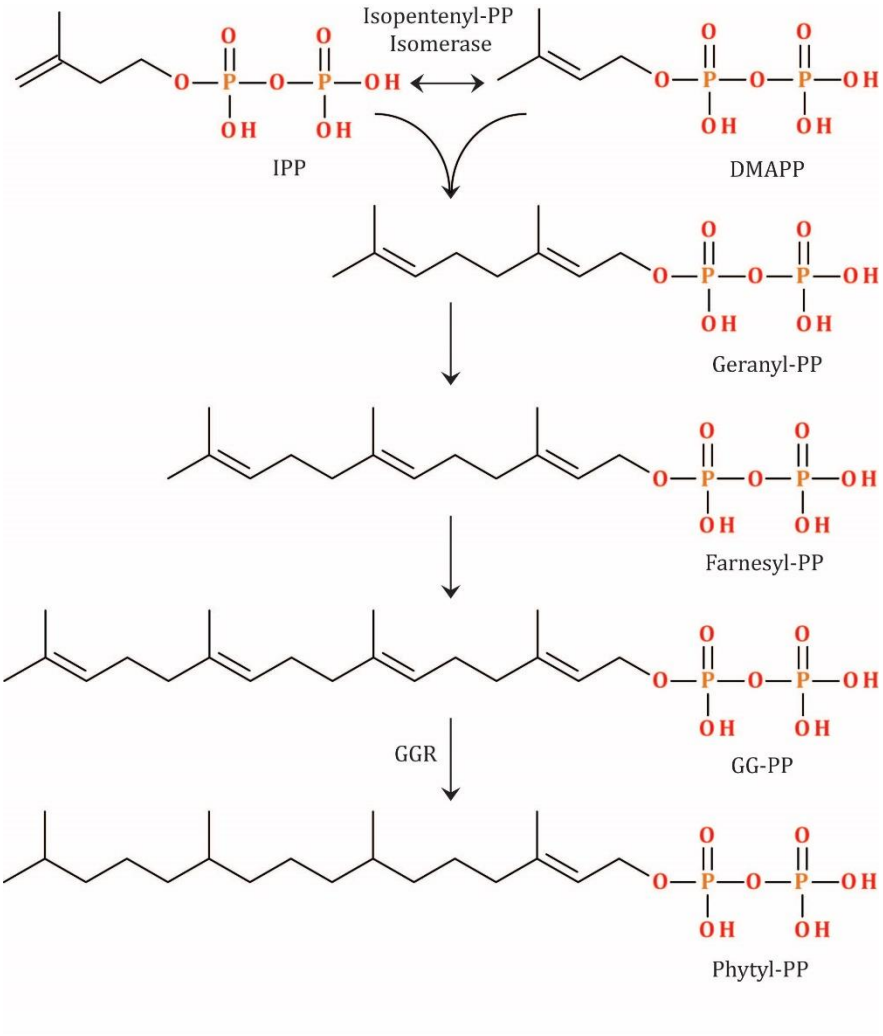

Figure 2 Synthesis of Phytyl-PP by Condensation of C5 Isoprene Units and Reduction.

Synthesis of long-chain isoprenyl-phosphates via condensation reactions catalyzed by isopentenyl-PP synthases. The conversion of GG-PP to phytyl-PP is catalyzed by GG-PP reductase (GGR; Keller *et al.*, 1998).

1.1.2 Chlorophyll Synthesis and Turnover in Plants

Chlorophyll is considered the most abundant molecule in nature. Therefore, its synthesis and turnover need to be tightly regulated. Chlorophyll can be synthesized via esterification of chlorophyllide (Chlide) using phytyl-PP as prenyl donor by chlorophyll synthase (ChlG) or by reduction of chlorophyll-GG by GGR (Oster *et al.,* 1997; Keller *et al.,* 1998; Eckhardt *et al.,* 2004; Shalygo *et al.,* 2009; Kim *et al.,* 2013). Chlorophyllide is derived from the tetrapyrrole pathway (Kim *et al.,* 2013).

Chlorophyll is degraded during leaf senescence (Csupor, 1971). In addition, there are many more conditions under which chlorophyll degradation is induced, including pathogen attack and nutrient deprivation (Hendry *et al.,* 1987; Yao *et al.,* 2002; Vailleau *et al.,* 2002; Kandlbinder *et al.,* 2004; Pageau *et al.,* 2006). Moreover, chlorophyll is degraded during fruit ripening, as recently studied in tomato (Hörtensteiner and Kräutler, 2011; Guyer *et al.,* 2014; Almeida *et al.,* 2015).

The initial steps of chlorophyll degradation are the conversion of chlorophyll b to chlorophyll a, dephytylation and removal of the magnesium (Mg) cation. The order of the last two catabolic steps is yet unclear (Hörtensteiner, 1999; Hörtensteiner, 2006; Zhang *et al.,* 2014). The removal of Mg as central ion in the tetrapyrrole ring is assigned to a non-defined Mg-chelating substance (MCS) and might be catalyzed enzymatically or occur chemically (Hörtensteiner and Kräutler, 2011). The Mg-free tetrapyrrol is called pheophytin. The enzyme responsible for the dephytylation of chlorophyll, pheophytin pheophorbide hydrolase (PPH), was recently identified (Schelbert *et al.,* 2009). Pheophorbide is converted into red chlorophyll catabolite (RCC) by pheophorbide a oxigenase (PAO) (Pružinská *et al.,* 2003; Pružinská *et al.,* 2005). RCC is the first breakdown product of chlorophyll that does not exhibit a green colour, due to the opening of the tetrapyrrole ring structure. Non-fluorescent chlorophyll catabolites are produced in subsequent degradation steps (Hörtensteiner, 2006; Hörtensteiner and Kräutler, 2011). While the degradation of the chlorophyll headgroup has been studied in detail, less is known about the fate of phytol released from chlorophyll by action of PPH or an unidentified dephytylase (Zhang *et al.,* 2014).

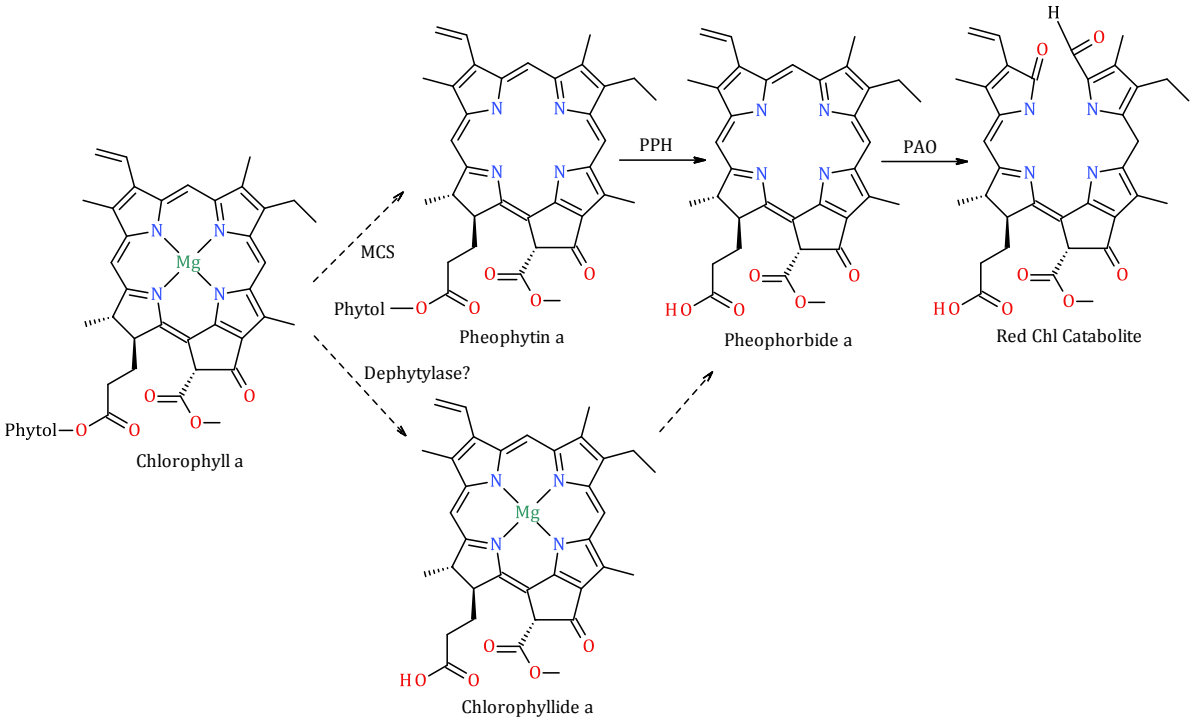

Figure 3 Degradation of Chlorophyll.

Chlorophyll degradation involves removal of the central Mg^{2+} cation by a magnesium-chelating substance (MCS) and cleavage of the phytol chain by PPH. The remaining tetrapyrrole structure is converted to a red Chl catabolite by pheophorbide a oxigenase (PAO) and further to non-fluorescent Chl catabolites in a multi-step process. An alternative pathway is the cleavage of phytol from chlorophyll by an unknown dephytylase, leading to the synthesis of chlorophyllide (Zhang *et al.*, 2014).

1.2 Metabolism of Chlorophyll-Derived Phytol in Plants

Chlorotic stress, such as nitrogen deprivation, results in severe changes in the ultrastructure of chloroplasts (Gaude *et al.,* 2007). In a healthy plant cell, the chloroplast harbors a network of thylakoid membranes (Figure 4, +N). After growth on nitrogen-deprived medium, the thylakoid membranes have vanished and instead the sizes of starch granules and plastoglobules have strongly increased (Figure 4, -N). These ultrastructural changes can be correlated with changes in the lipid composition: chlorophyll and galactolipids are degraded while non-polar lipids (TAGs, tocopherols and fatty acid phytyl esters) accumulate (Steinmüller and Tevini, 1985; Tevini and Steinmüller, 1985). It is believed that TAG, tocopherols and fatty acid phytyl esters are produced and deposited in plastoglobules to avoid the accumulation of the breakdown products of galactolipids and chlorophyll, i.e. fatty acids and phytol (Lippold *et al.*, 2012).

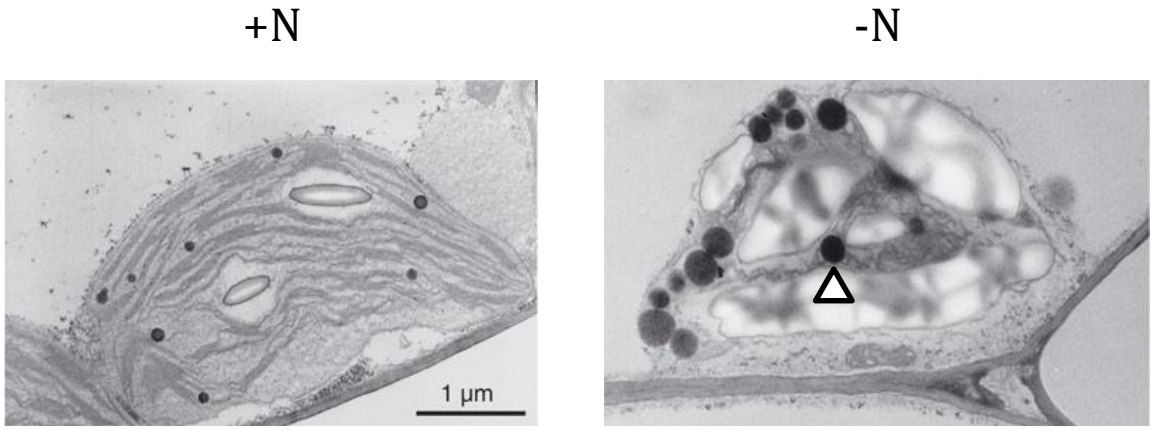

Figure 4 Ultrastructural Changes in Chloroplasts During Nitrogen Deprivation.

Electron micrographs of chloroplasts of plants grown on full nutrient medium (+N, left) and nitrogen-depleted medium (-N, right). While under normal growth conditions (+N) the thylakoid membranes dominate the chloroplast ultrastructure, they are disintegrated under –N conditions, and starch granules and plastoglobules (arrow head) strongly increase in size. Electron micrographs taken from Gaude *et al.* (2007).

Chlorophyll degradation results in the release of large amounts of free phytol (Grob and Csupor, 1967; Csupor, 1971; Lippold *et al.,* 2012; Zhang *et al.,* 2014). In the plastid, PPH is responsible for the dephytylation of chlorophyll (Schelbert *et al.,* 2009). However, recently it was shown that another enzyme (unidentified dephytylase) might be involved in catalyzing chlorophyll hydrolysis in *Arabidopsis* seeds (Zhang *et al.,* 2014). Free phytol produced by either of these enzymes is channelled into several plastidial and extraplastidial pathways. Using radioactive labeling studies, Ischebeck *et al.* (2006) showed that phytol is ultimately incorporated into chlorophyll, tocopherol and fatty acid phytyl esters. The pathway of phytol degradation has not been studied in plants in detail. Rontani *et al.* (1996) proposed a model for the chemical degradation of phytol via photooxidation. However, it is not clear to which extent this pathway contributes to phytol

degradation *in planta*. In animals on the other hand, the degradation of phytol via α- and β-oxidation is well described. Most enzymes and intermediates involved in this pathway have been identified (Wanders *et al.,* 2003; Wanders *et al.,* 2011). In animals, phytol resulting from hydrolysis of dietary chlorophyll is oxidized to phytenal and subsequently to phytenic acid. Phytenic acid is activated to phytenoyl-CoA which is transported to the peroxisomes and reduced to phytanoyl-CoA by *trans*-2-enoyl-CoA reductase (van den Brink *et al.,* 2005). The product of peroxisomal α-oxidation is pristanic acid. Pristanic acid can be broken down by several rounds of β-oxidation in the peroxisomes and mitochrondria. A similar pathway is presumably present in plants. Homologs of the genes involved in breakdown of phytol in animals have been identified in plants. Moreover, the *Arabidopsis etfqo* mutant lacking the mitochondrial electron-transfer flavoprotein:ubiquinone oxidoreductase (ETFQO) protein reveals an increased rate of chlorophyll breakdown and at the same time accumulates phytanoyl-CoA (Ishizaki *et al.*, 2005).

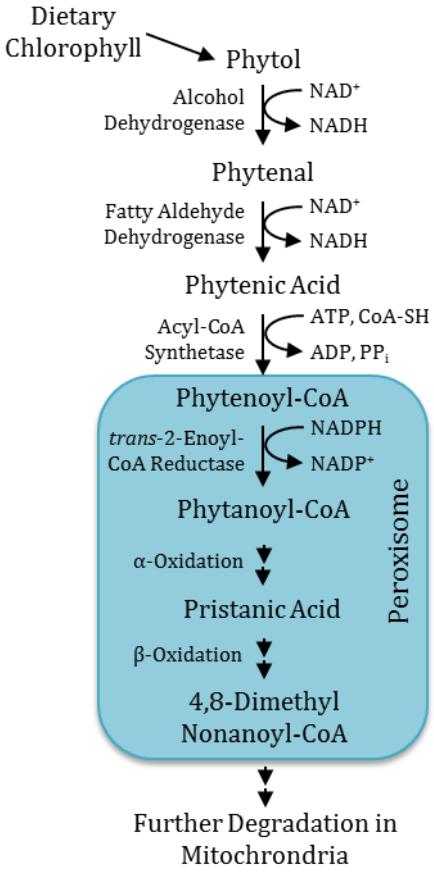

Figure 5 Degradation of Phytol Via α- and β-Oxidation in Animals.

Dietary chlorophyll is hydrolyzed and free phytol is released. Phytol is converted to phytanoyl-CoA which can enter peroxisomal α-oxidation. Pristanic acid, the reaction product of α-oxidation, can be broken down by β-oxidation in peroxisomes and mitochondria. Modified from van den Brink *et al.* (2005) and Wanders *et al.* (2011).

1.2.1 Fatty Acid Phytyl Ester Accumulation in Chlorotic Leaves

Nearly 50 years ago, fatty acid phytyl esters were first detected in chlorotic leaves of *Acer platanoides*. Grob and Csupor (1967) and Csupor (1971) showed that the bulk of phytol is bound in chlorophyll in green leaves, while it is esterified to 18:3-fatty acid in yellow leaves. They assumed a mechanism for the release of phytol from chlorophyll and subsequent acylation by independent reactions. Therefore, free phytol is predicted to occur as intermediate in these catabolic reactions. Furthermore, it was demonstrated that some marine bacteria (e.g. *Marinobacter hydrocarbonoclasticus*) synthesize fatty acid phytyl esters after feeding synthetic phytol (Rontani *et al.,* 1996; Holtzapple and Schmidt-Dannert, 2007).

Fatty acid phytyl esters are produced in *Arabidopsis* leaves during chlorotic stress, such as senescence and nitrogen deprivation (Ischebeck *et al.,* 2006; Gaude *et al.,* 2007). Another condition that stimulates fatty acid phytyl ester synthesis is cold stress (Patterson *et al.,* 1993). The fatty acid composition of fatty acid phytyl esters is distinct from the total fatty acid composition in leaves (Patterson *et al.,* 1993). Fatty acid phytyl esters contain large amounts of medium-chain fatty acids (10:0, 12:0 and 14:0) but the most abundant fatty acid in *Arabidopsis* phytyl esters is 16:3 (Patterson *et al.,* 1993; Gaude *et al.,* 2007; Lippold *et al.,* 2012).

The enzymes catalyzing the esterification of free phytol were recently characterized (Lippold *et al.,* 2012). To identify candidates for *Arabidopsis* phytyl ester synthases in a bioinformatics approach, *Arabidopsis* acyltransferases were selected with sequence similarities to wax ester synthases from the Acinetobacter-type and jojoba-type and also six acyltransferases of the esterase/lipase/thioesterase (ELT) family. The gene expression pattern was analyzed using Genevestigator (www.genevestigator.com). In fact, two acyltransferases of the ELT family were strongly upregulated under senescence, ELT1 (At1g54570) and ELT2 (At3g26840). The protein sequences also contained a predicted chloroplast transit peptide, according to analysis with TargetP (www.cbs.dtu.dk/services/). Chloroplasts are the site of fatty acid phytyl ester synthesis during senescence. ELT1 and ELT2 were selected as candidates for fatty acid phytyl ester synthesis enzymes and designated *PHYTYL ESTER SYNTHASES 1* and *2* (*PES1*, *PES2*). PES1 and PES2 localize to the chloroplast as revealed by import experiments into pea chloroplasts (Lippold *et al.*, 2012). In accordance with these findings, PES1 and PES2 were also identified in two independent proteomics studies of isolated plastoglobules (Vidi *et al.,* 2006; Ytterberg *et al.,* 2006). Therefore, PES1 and PES2 localize to chloroplasts and most likely to plastoglobules. Aslan *et al*. (2014) showed that co-expression of the full-length sequence of PES2 from *Arabidopsis* with a fatty acid reductase (FAR) in leaves of *Nicotiana benthamiana* (*N. benthamiana*) results in the production of wax esters.

The *Arabidopsis* genome harbors six members of the ELT family, ELT1 (=PES1), ELT2 (=PES2), ELT3, ELT4, ELT5 and ELT6. Several of these genes show a very high sequence similarity and are

organized in tandem: PES2 and ELT3, ELT4 and ELT5. PES1 and ELT6 are evolutionary more distant. Like PES1 and PES2, ELT3, ELT4, ELT5 and ELT6 carry an N-terminal extension which is predicted to encode a transit peptide according to TargetP (www.cbs.dtu.dk/services/).

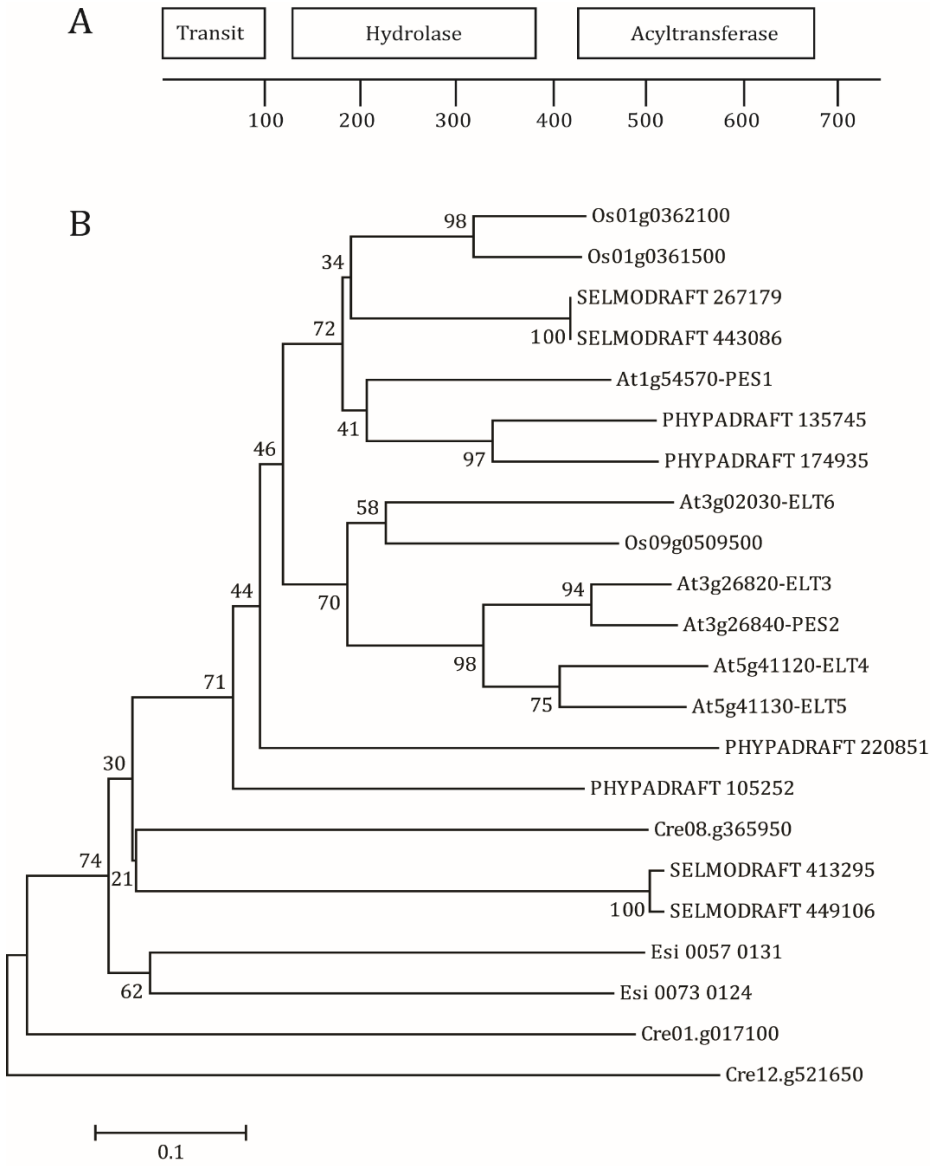

Figure 6 Protein Domains and Phylogenetic Tree of ELT Sequences.

(A) Sequences of ELT proteins exhibit two distinct domains: a hydrolase-like sequence (amino acids 120 to 380) and an acyltransferase-like sequence (amino acids 420 to 670). The predicted transit peptide spans from amino acid 1 to 100 (TargetP). (B) An unrooted phylogenetic tree was constructed using the neighbor-joining method with ELT protein sequences from *Arabidopsis* (At), rice (Os), *Selaginella moellendorffii* (SELMODRAFT), *P. patens* (PHYPADRAFT), *C. reinhardtii* (Cre), and *Ectocarpus siliculosus* (Esi) using MEGA 5.0 and the ClustalW algorithm (Thompson *et al.,* 1997; Tamura *et al.,* 2011). Bootstrap values are indicated next to the branches and were calculated from 1000 replicates (Felsenstein, 1985). In the x-dimension, branch length represents evolutionary distance based on the number of amino acid differences per site. Phylogenetic tree taken from Lippold *et al.* (2012).

In the *Arabidopsis pes1 pes2* mutant, the amount of fatty acid phytyl esters is strongly decreased, mainly due to the loss of 16:3-phytol and of medium-chain fatty acid phytyl esters. However, the amounts of some molecular species are unchanged, for example 16:0-phytol and 18:3-phytol. These fatty acid phytyl esters might be produced by the remaining ELT proteins.

Homozygous *Arabidopsis* T-DNA insertion mutants for *pes1* and *pes2* showed no changes in growth and development and only little changes in the fatty acid phytyl ester content. In the double mutant *pes1 pes2*, severe alterations in fatty acid phytyl esters can be observed. Green WT leaves contain almost no fatty acid phytyl esters, but nitrogen deprivation results in an increase in fatty acid phytyl ester content by about 5-fold. The *pes1 pes2* double mutant still shows an increase in fatty acid phytyl esters during nitrogen deprivation, but the accumulation is strongly suppressed as compared to WT. The effect is most prominent in the molecular species composition of fatty acid phytyl esters, because the reduction is mostly due to the complete loss of 16:3-phytol and medium chain fatty acid phytyl esters (Lippold *et al.,* 2012).

1.2.2 Phosphorylation of Chlorophyll-Derived Phytol

In addition to esterification to fatty acids by PES1 and PES2, free phytol derived from chlorophyll degradation can enter the “salvage pathway” for phytyl-PP synthesis. Phytyl-PP can finally be incorporated into tocopherol (Ischebeck *et al.,* 2006; Valentin *et al.,* 2006). The enzyme catalyzing the first step of the phytol phosphorylation pathway, phytol kinase or vitamin E deficient 5 (VTE5), was described by Valentin *et al.* (2006). This enzyme localizes to the chloroplasts and is encoded by the gene At5g04490. VTE5 catalyzes the conversion of phytol to phytol-P. For phytyl-PP synthesis, another enzyme, phytyl-P kinase, is required, which synthesizes phytyl-PP, presumably by phosphorylation of phytol with CTP. The presence of phytyl-P kinase activity was experimentally demonstrated in *Arabidopsis* leaves through the incorporation of radioactive phytol into phytyl-P and phytyl-PP (Ischebeck *et al.*, 2006). However, the gene encoding phytyl-P kinase was unknown.

Seeds of the phytol kinase mutant *vte5-1* contain only 20% tocopherol and accumulate free phytol. The reduction of seed tocopherol content by 80% reveals that the phytyl-PP synthesized via the phytol phosphorylation pathway strongly contributes to the total phytyl-PP pool. Alternatively, phytyl-PP can be generated by reduction of GG-PP.

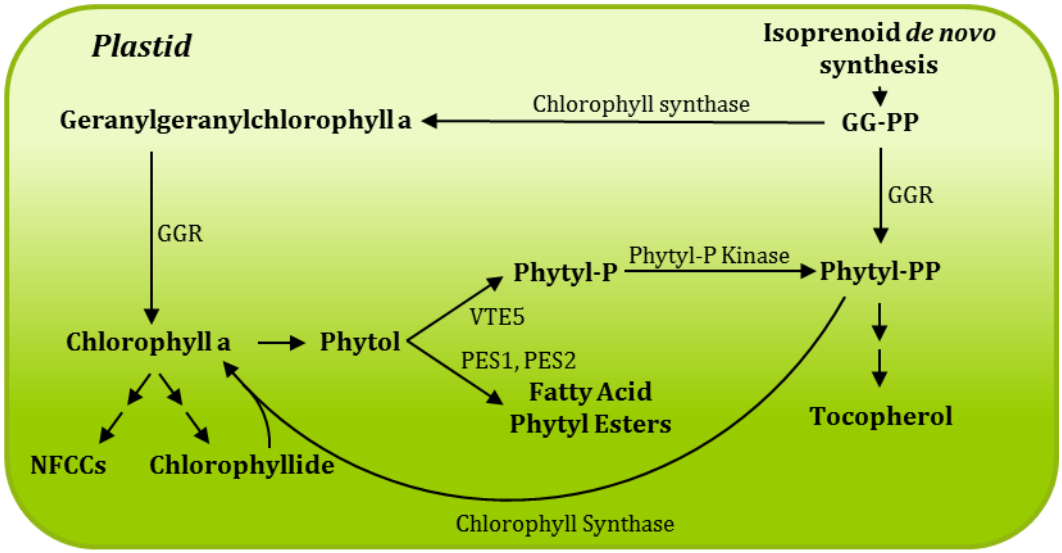

Figure 7 Metabolism of Chlorophyll-Derived Phytol in *Arabidopsis*.

One of the first steps of chlorophyll degradation is dephytylation. Phytol can be esterified to fatty acids by PES1 and PES2, or phosphorylated by VTE5 and an unknown phytyl-P kinase to give rise to phytyl-PP. Phytyl-PP is incorporated into tocopherol or used for the synthesis of chlorophyll by condensation with chlorophyllide by chlorophyll synthase.

1.2.2.1 Identification of a Candidate Gene for Phytyl-Phosphate-Kinase

The "salvage pathway" for phytyl-PP synthesis uses phytol from chlorophyll degradation and provides phytyl-PP for tocopherol biosynthesis. It is likely that enzymes catalyzing phytol phosphorylation are conserved among photoautotrophic organisms. In line with this hypothesis, Valentin *et al.* (2006) showed that homologs of the *Arabidopsis* VTE5 can be found in plants and photosynthetic bacteria. They also showed that the *Arabidopsis VTE5* genes and the *Synechocystis* open reading frame (ORF) *slr1652* encode proteins with phytol kinase activity. The fact that in bacteria, genes encoding proteins involved in a biosynthetic pathway are oftentimes organized in close proximity (e.g. in operons), helps to discover potential candidate genes that encode a putative phytyl-P kinase. The SEED database integrates whole genomes from bacteria and plants, along with the annotated functions of these genes (Overbeek *et al.,* 2005; Seaver *et al.,* 2014). This database can be used to search for similarities of genome organization patterns between different organisms across different kingdoms, and can lead to the discovery of "clusters of orthologous groups" (COGs). A set of proteins involved in isoprenoid *de novo* synthesis, long-chain isoprenyl-PP synthesis, chlorophyll metabolism and related metabolic pathways was analyzed for common associated COGs (Seaver *et al.*, 2014). This resulted in the discovery of an ORF called COG1836, which is found in several bacteria in genomic proximity to genes homologous to *Arabidopsis VTE5*. Orthologs of COG1836 were identified in *Arabidopsis* (At1g78620) and *Synechocystis* (*sll0875*).

The putative phytyl-P kinase encoded by At1g78620 contains an N-terminal extension that is predicted to be a chloroplast transit peptide of 65 amino acid length (ChloroP 1.1 Server,

Emanuelsson et al. (1999)). The sequence similarity with prokaryotic COG1836 protein sequences starts only after these first 65 amino acids (at position 66 when compared to Synechocystis slr1652). The spinach ortholog of the At1g78620 protein was previously identified in chloroplast envelopes (Ferro *et al.,* 2003).

1.3 Tocopherol Metabolism in Plants

1.3.1 Tocopherol Biosynthesis

Tocopherol biosynthesis is linked to aromatic amino acid metabolism as tyrosine is the main precursor for the tocopherol head group synthesis. Tyrosine is converted to *p*-hydroxypyruvate by tyrosine aminotransferase (Riewe *et al.,* 2012). Alternatively, *p*-hydroxyphenylpyruvate can be directly produced from prephenate (de la Torre *et al.,* 2014). Homogentisic acid (HGA) is synthesized from *p*-hydroxyphenylpyruvate by *p*-hydroxyphenylpyruvate dioxygenase (HPPD) (Norris *et al.,* 1995). HGA is the common precursor for all tocochromanols, i.e. tocopherols and tocotrienols and plastochromanol-8 (PC-8) (Whistance and Threlfall, 1970). The prenylation of HGA is catalyzed by homogentisate phytyltransferase (HPT, VTE2) or homogentisate geranylgeranyltransferase (HGGT), using phytyl-PP or GGPP as substrates, respectively (Savidge *et al.,* 2002; Collakova and DellaPenna, 2003; Cahoon *et al.,* 2003; Yang *et al.,* 2011). The products of HGA prenylation by HPT or HGGT are 2-methyl-6-phytylbenzoquinol (MPBQ) or 2-methyl-6-geranylgeranylbenzoquinol (MGGBQ), respectively. An additional methyl group is added to the chromanol ring by the methyltransferase VTE3, producing 2,3-dimethyl-6-phytylbenzoquinol (DMPBQ) and 2,3-dimethyl-6-geranylgeranylbenzoquinol (DMGGBQ). Apart from HPT and HGGT, the other enzymes of tocopherol or tocotrienol biosynthesis (VTE1, VTE3, VTE4) can use either the phytylated or geranylgeranylated substrates. Tocopherol cyclase VTE1 closes the second ring on MPBQ and DMPBQ (or MGGPQ and DMGGBQ) and thereby forms the chromanol ring (Porfirova *et al.,* 2002).

Plastochromanol-8 (PC-8) is synthesized via a related pathway. HGA is condensed with solanesyl-PP, a C45-isoprenyl-phosphate, to produce 2-methyl-6-solanesyl-1,4-benzoquinol (MSBQ) (Mène-Saffrané *et al.,* 2010). MSBQ is methylated using S-adenosylmethionine by VTE3, the reaction product is plastoquinol-9. Finally, VTE1 cyclizes plastoquinol-9 to PC-8.

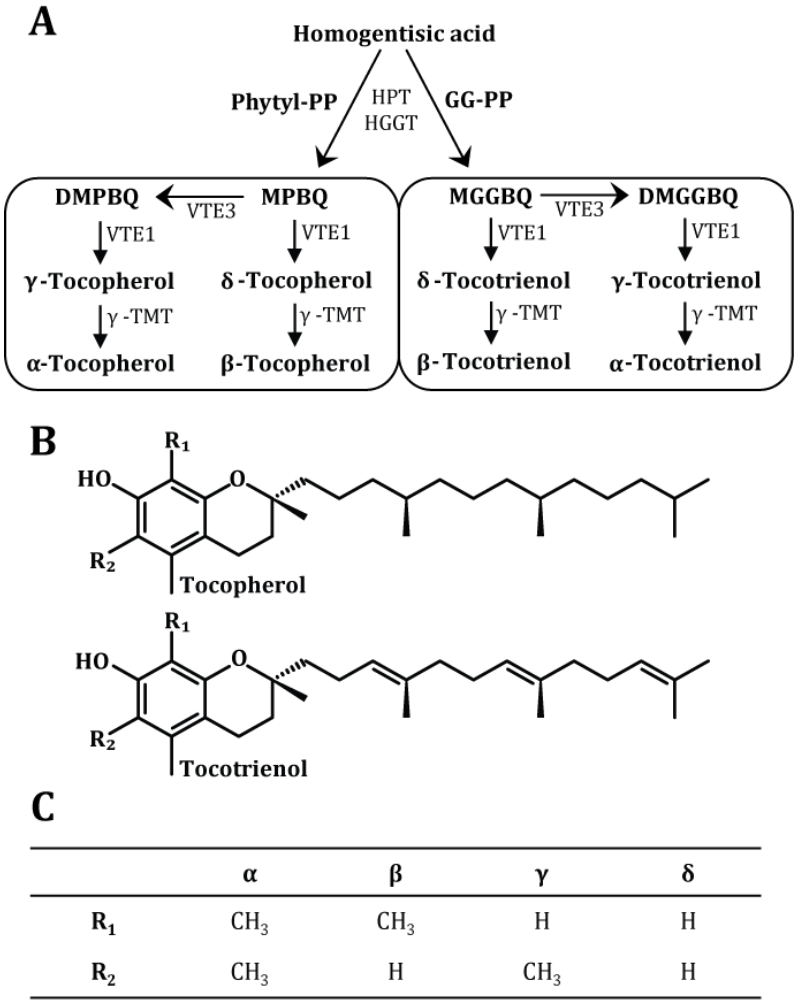

Figure 8 Biosynthesis and Structures of Tocochromanols (Vitamin E).

(A) The condensations of HGA with phytyl-PP or with GG-PP are the first steps in tocopherol or tocotrienol biosynthesis, respectively. The products, MPBQ (or MGGBQ), are either directly converted to δ- and β-tocochromanol by VTE1, or can be further methylated to DMPBQ (or DGGPBQ), which can be converted to γ- and α-tocochromanols by VTE1. (B+C) Tocopherol and tocotrienol differ in the prenyl chain bound to the chromanol ring. Tocopherol carries a saturated chain, while the prenyl chain of tocotrienol carries three double bonds. Four different forms of tocochromanols, α, β, γ and δ are distinguished based on their degree of methylation and position of the methyl group on the chromanol ring.

1.3.2 Structure and Biological Function of Tocopherol

The term "Vitamin E" encompasses the four forms of tocopherols and tocotrienols: α, β, γ and δ as well as PC-8. The different forms are distinguished by the degree of methylation of the chromanol ring and by the length and the number of double bonds of the nonpolar side chain (Figure 8). α-Tocopherol and α-tocotrienol have the highest degree of methylation. Tocopherols contain a saturated side chain while the side chain of tocotrienols carries three double bonds, derived from the prenylation of homogentisate with phytyl-PP or GG-PP, respectively.

Tocochromanols are lipid-soluble antioxidants which protect cells from reactive oxygen species (ROS). Tocochromanols can transfer the hydrogen atom of the hydroxyl group to free radicals (e.g.

peroxyl radicals) and render them inactive (Liebler, 1993; Liebler *et al.,* 1996). This is important to protect lipids, especially polyunsaturated fatty acids (PUFAs), from oxidation by ROS (Girotti, 1998). Vitamin E activity is determined by a set of methods using animal test systems, for example rats, chicken and guinea pigs (Leth and Søndergaard, 1977; Chow, 1991). Most of these methods rely on the severe defect during embryo development that is caused by vitamin E deficiency. The highest vitamin E activity was determined for the naturally occurring form of *α*-tocopherol, the other tocopherol and tocotrienol forms are less active (Leth and Søndergaard, 1977). One international unit (IU) of vitamin E activity was defined as the vitamin E activity of 1 mg of synthetic all-racemic α-tocopherol-acetate (Valentin and Qi, 2005; Karunanandaa *et al.,* 2005). The activity of α-tocopherol from biological origin (RRR-*α*-tocopherol) is 1.5-fold higher than synthetic α-tocopherol-acetate.

When *α*-tocopherol is exposed to ROS, a tocopheroxyl radical is formed, which can be further converted to *α*-tocopheroylquinone (α-TQ) and α-tocopherylhydroquinone (α-tocopherylquinol, α-TQH_2) (Liebler *et al.,* 1996; Kobayashi and DellaPenna, 2008). A yet unknown dehydratase introduces a double bond in the side chain, producing either 2,3,5-trimethyl-6-phytyl-1,4-benzoquinone (TMPBQ) or 2,3,5,trimethyl-6-phytyl-1,4-benzoquinol ($TMPBQH_2$). $TMPBQH_2$ is structurally very similar to DMPBQ and therefore serves as substrate for the tocopherol cyclase VTE1, leading to the synthesis of α-tocopherol and completing the detoxification cycle (Kobayashi and DellaPenna, 2008).

In plants, different functions are assigned to tocopherols in seeds and in leaves. In leaves, tocopherols are synthesized at the plastidial envelopes and plastoglobules and stored in plastoglobules (Lichtenthaler *et al.,* 1981; Soll *et al.,* 1985; Vidi *et al.,* 2006). In the chloroplasts, they protect the photosynthetic membranes from oxidation, caused by ROS derived from photosynthesis (Munné-Bosch, 2005; Havaux *et al.,* 2005). In seeds, tocopherols are crucial to prevent chemical lipid peroxidation during seed storage and germination (Sattler *et al.,* 2004).

Furthermore, tocopherol is involved in the adaptation to low temperature growth. The *vte2* mutant of *Arabidopsis* shows reduced growth associated with callose deposition at plasmodesmata and increased carbohydrate accumulation in the leaves after long-term exposure to the cold (Maeda *et al.,* 2008). This cold response is independent from oxidative stress. Furthermore, the *Arabidopsis vte2* mutant shows an altered content of PUFAs in phospholipids under low temperature (Maeda *et al.,* 2008). This effect is most prominent in phosphatidylcholine (PC), because cold treatment leads to an increased content of 18:3-containing PC in WT, but not in *vte2*, where the relative proportion of 18:2-containing PC is higher than in WT. This change in the degree of desaturation of PC acyl groups is causally linked with the cold response, because this response was suppressed in the double mutant *fad2 vte2* deficient in ER-dependent 18:2 desaturation (Maeda *et al.,* 2008; Mehrshahi *et al.,* 2013). The mechanism of the cold-stress response in *vte2*, and the link with the 18:2 desaturation, remain enigmatic.

1.4 Objectives

Chlorophyll is one of the most abundant molecules in nature and is continuously synthesized and degraded during chlorophyll turnover in photosynthetic membranes. Chlorophyll degradation strongly increases during senescence or chlorotic stress, such as exposure to darkness or nitrogen deprivation. The tetrapyrrole ring of chlorophyll is converted into non-fluorescent chlorophyll catabolites in many independent steps. The enzymes catalyzing chlorophyll degradation have been described in the last decade. However, much less is known about the fate of phytol, a C20-isoprenoid alcohol, which represents the non-polar tail of the chlorophyll molecule.

The aim of this work was to investigate the metabolism of free phytol after cleavage from chlorophyll during chlorotic stress, with a focus on two pathways: (i) esterification of phytol to fatty acid phytyl esters and (ii) phosphorylation to phytyl-P and phytyl-PP. Phytyl-PP is the precursor for tocopherol biosynthesis. In addition, comprehensive phytyllipid and glycerolipid profiles were generated for *Arabidopsis* wild type and mutant plants affected in phytol metabolism grown under chlorotic stress conditions.

To study phytol metabolism in *Arabidopsis* WT and in the mutants, sensitive methods for the quantification of fatty acid phytyl esters and isoprenyl-phosphates (e.g. phytyl-P and phytyl-PP) were developed using liquid chromatography mass spectrometry (LC-MS). The enzymes catalyzing the acylation of phytol were recently identified (Lippold *et al.,* 2012): Phytyl Ester Synthases 1 and 2 (At1g54570 and At3g26840). In the present work, growth and development of the double mutant of *Arabidopsis pes1 pes2* was characterized. A candidate gene for *PHYTYL-P KINASE* was identified by the use of the SEED database (Overbeek *et al.,* 2005; Seaver *et al.,* 2014), and employed to study the phytol phosphorylation pathway. This work includes the characterization of *Arabidopsis* insertional mutants for this novel gene on the physiological and biochemical level.

2 Materials and Methods

2.1 Equipment

Blade-type tissue homogenizer	Homogenizer HO 4/A	Edmund Bühler GmbH (Hechingen, D)
Bead-beating-type tissue homogenizer	Precellys®24	PeQlab (Erlangen, D)
Mortar-pestle tissue grinder	Potter-Elvehjem tissue grinder with PTFE pestle	Sigma-Aldrich (Taufkirchen, D)
Table-top centrifuge	5810 R	Eppendorf (Hamburg, D)
Microcentrifuge	5417 R	Eppendorf (Hamburg, D)
Ultracentrifuge		Beckman-Coulter (Krefeld, D)
Mortar-pestle tissue grinder	Potter-Elvehjem tissue grinder with PTFE pestle	Sigma-Aldrich (Taufkirchen, D)
Incubation shaker	Multitron 28570	INFORS (Bottmingen, CH)
Phytochamber Incubator for plants on MS plates	SIMATIC OP17	York International (York, USA)
Spectrophotometer	Nanodrop 1000	PeQlab (Erlangen, D)
Spectrophotometer	Specord 205	Analytik Jena (Jena, D)
Gas Chromatograph (GC) with Flame Ionization Detector (FID)	6890 Series	Agilent (Böblingen, D)
High Pressure Liquid Chromatography (HPLC) with Fluorescent Light Detector (FLD)	1100 Series	Agilent (Böblingen, D)
Liquid Chromatography-Mass Spectrometry (LC-MS)	6530 Series Accurate-Mass Quadrupole Time-of-Flight (Q-TOF) LC/MS	Agilent (Böblingen, D)
Water bath		Köttermann Lab Devices (Uetze/Hänigsen, D)
Vortex	Certomat®MV	Braun (Melsungen, D)
pH Meter	pH-Level 1	InoLab WTW (Weilheim, D)
Sterile bench	Holten LaminAir Model 1.8	ThermoScientific (Schwerte, D)

2.2 Materials

2.2.1 Consumables

Glass vials with thread	8 ml	VWR (Darmstadt, D)
Glass vials with thread	40 ml	Schmidlin (Neuheim, CH)
PTFE screw caps for 8 ml glass vials		Schott (Mainz, D)
Plastic screw caps for 40 ml glass vials		Schmidlin (Neuheim, CH)
Teflon septa for screw caps	13.3 and 22.4 mm	Schmidlin (Neuheim, CH)
Glass vials without thread	8 ml	VWR (Darmstadt, D)
Pasteur (glass) pipettes	150 and 225 mm	Brand (Wertheim, D)

Sample vials (GC and LC)	Vials with inserts and screw caps with teflon-septa	Macherey and Nagel (Düren, D)
TLC plates	Silica 60 Durasil (with concentration zone)	Macherey and Nagel (Düren, D)
SPE columns	Strata Si-1 silica, 55 µm, 70 Å, 500 mg/6 ml and 100 mg/1 ml	Macherey and Nagel (Düren, D)
Petri dishes	94x16 and 145x20 mm	Labomedic (Bonn, D)
Plastic tips for micropipettes		Labomedic (Bonn, D)
Pots for plant cultivation		Pöppelmann (Lohne, D)
Soil for plant cultivation	"Einheitserde Classic VE"	Rolfs (Siegburg, D)

2.2.2 Chemicals

1 N HCl in Methanol	Supelco/Sigma-Aldrich (Taufkirchen, D)
3-[(3-Cholamidopropyl)dimethylammonio]-1-propanesulfonate (CHAPS)	AppliChem (Darmstadt, D)
32% NH_4OH	AppliChem (Darmstadt, D)
Acetic acid	AppliChem (Darmstadt, D)
Acetone	AppliChem (Darmstadt, D)
Acetone	VWR (Darmstadt, D)
Acetonitrile (for Q-TOF)	Roth (Karlsruhe, D)
Acetosyringone	Sigma-Aldrich (Taufkirchen, D)
Agarose	PeQlab (Erlangen, D)
NH_4OAc (Ammonium acetate)	Sigma-Aldrich (Taufkirchen, D)
Bacto-Agar	BD (Heidelberg, D)
Bovine serum albumin (BSA)	Sigma-Aldrich (Taufkirchen, D)
Cetyltrimethylammonium bromide (CTAB)	Roth (Karlsruhe, D)
Chloroform (for Q-TOF)	VWR (Darmstadt, D)
Citric acid	Sigma-Aldrich (Taufkirchen, D)
Diethylether	Grüssing (Filsum, D)
Dimethylsulfoxide	AppliChem (Darmstadt, D)
Dithiothreitol (DTT)	AppliChem (Darmstadt, D)
Ethanol	Merck (Darmstadt, D)
Ethidium bromide	Roth (Karlsruhe, D)
Fe-EDTA	Sigma-Aldrich (Taufkirchen, D)
Formaldehyde	AppliChem (Darmstadt, D)
Glucose	Duchefa (Haarlem, NL)
Isoascorbate	Sigma-Aldrich (Taufkirchen, D)
Isopropanol	AppliChem (Darmstadt, D)
KH_2PO_4	Merck (Darmstadt, D)
Lysozyme	AppliChem (Darmstadt, D)
Methanol (for Q-TOF)	J.T. Baker/VWR (Darmstadt, D)
MS salts including vitamins	Duchefa (Haarlem, NL)
n-Hexane	Merck (Darmstadt, D)
N-Methyl-N-(trimethylsilyl) trifluoroacetamide (MSTFA)	Roth (Karlsruhe, D)
Paq polymerase	DNA Cloning Service (Hamburg, D)
Peptone	ForMedium (Norfolk, UK)
Pfu Polymerase	ThermoScientific (Schwerte, D)
Sodium orthovanadate	Sigma-Aldrich (Taufkirchen, D)
Sorbitol	AppliChem (Darmstadt, D)
Sucrose	Duchefa (Haarlem, NL)

Taq polymerase	DNA Cloning Service (Hamburg, D)
Tertiary butylmethylether (MTBE)	Roth (Karlsruhe, D)
Trichloroacetonitrile	Sigma-Aldrich (Taufkirchen, D)
Triethylamine	Sigma-Aldrich (Taufkirchen, D)
Tris base	Duchefa (Haarlem, NL)
Triton X-100	Sigma-Aldrich (Taufkirchen, D)
Tryptone	AppliChem (Darmstadt, D)
Yeast extract	Duchefa (Haarlem, NL)
Yeast nitrogen base	BD (Heidelberg, D)

For Q-TOF measurements, solvents of different suppliers were tested and those with highest purity were used for analysis ("for analysis", "HPLC grade"). For the handling of solvents involved in Q-TOF sample processing, only glass ware was used.

2.2.3 Antibiotics

All antibiotics were obtained from Duchefa (Haarlem, The Netherlands). Stock solutions for ampicillin (Amp), streptomycin (Sm) and spectinomycin (Sp) were prepared in water, rifampicin was dissolved in dimethylsulfoxide (DMSO). Stock solutions were stored at -20°C.

2.2.4 Kits and Enzymes

First Strand cDNA Synthesis Kit	Fermentas (St. Leon-Rot, D)
Universal RNA Purification Kit	Roboklon (Berlin, D)
Ambion TURBO DNA-free™ Kit	Thermo Fisher Scientific (Karlsruhe, D)
SuperScript III First Strand Synthesis Kit	Life Technologies (Invitrogen) (Darmstadt, D)
High-Speed Plasmid Mini Kit	DNA Cloning Cervice (Hamburg, D)
CloneJET PCR Cloning Kit	Thermo Fisher Scientific (Karlsruhe, D)
T_4 DNA Ligase	Fermentas (St. Leon-Rot, D)
DCS DNA Polymerase	DNA Cloning Service (Hamburg, D)
Pfu DNA polymerase	Thermo Fisher Scientific (Karlsruhe, D)
Paq 5000 HotStart PCR Master Mix	Agilent (Böblingen, D)

2.2.5 Synthetic Oligonucleotides

Oligonucleotides used in this study are shown in Table 15 and were obtained from IDT Genomics (Leuven, BE).

2.2.6 *Arabidopsis* Ecotypes and Insertion Lines

Table 1 ***Arabidopsis*** **Ecotypes and Insertion Lines.**

Genotype	Ecotype	Gene	Stock Center Code	Origin
Wild type	Col-0			
Ds3-390-1	No-0		N8521, donor for pst15134	RIKEN (Ibaraki, JP)
Ds 389-13	No-0		N8518, donor for pst00121	RIKEN (Ibaraki, JP)
pes1 pes2	Col-0	At1g54570 At3g28640		Lippold et al., 2012
vte6-1	No-0	At1g78620	pst15134	RIKEN (Ibaraki, JP)
vte6-2	No-0	At1g78620	pst00121	RIKEN (Ibaraki, JP)
vte5-2	No-0	At5g04490	pst12490	RIKEN (Ibaraki, JP)
vte5-2 vte6-1	No-0	At5g04490 At1g78620		Dr. Georg Hölzl, University of Bonn (D)
pao1	Col-0	At3g44880	SALK_111333.47.60	Dr. Stefan Hörtensteiner, University of Zurich (CH)

Arabidopsis ecotype Columbia-0 (Col-0) was used as WT control for all experiments. The background of the transposon insertion lines for *vte6-1* and *vte6-2* are two donor lines, Ds3-390-1 and Ds 389-13, is *Arabidopsis* ecotype Nossen-0 (No-0) (Table 1). Growth and lipid content of these lines were indistinguishable to WT Col-0. Therefore Col-0 was used as control for *vte6-1* and *vte6-2*.

2.2.7 Microorganisms

Table 2 **Bacterial and Algal Strains Used in this Study.**

Strain	Organism	Description	Reference
Electroshox	*E. coli*	Electrocompetent cells	Bioline
BL21(DE3) pLysS	*E. coli*	Chemically competent cells	Stratagene
INVSc1	*S. cerevisiae*	Electrocompetent cells	Invitrogen
GV3101-pMP90	*A. tumefaciens*	Electrocompetent cells	DNA Cloning Service, Hamburg (D)
CC-124	*C. reinhardtii*	WT strain	Dr. Simone Zäuner, IMBIO, University of Bonn/ Dr. Christoph Benning, Michigan State University East Lansing (USA)

2.2.8 Vectors and Recombinant Plasmids

Table 3 Cloning Vectors (* selection in bacteria, ** selection in yeast).

Vector	Target organism	Selectable Marker	Reference
pJet	*E. coli*	Amp^R*	Fermentas
pET22b	*E. coli*	Amp^R*	Novagen (EMD Millipore)
pDR196	*S. cerevisiae*	Amp^R*, URA3**	Rentsch et al. (1995)
pL-35s-DsRed	*A. tumefaciens*	Sm/Sp^R*	Dr. Georg Hölzl, IMBIO, University of Bonn, unpublished

Table 4 Recombinant Plasmids.

Construct	Description	Protein	Vector	Destination	Stock Number
pET-VTE6woTP47	Expression in *E. coli*	VTE6woTP	pET22b	*E. coli* BL21(DE3) pLysS	bn528
pET-VTE6woTP67	Expression in *E. coli*	VTE6woTP	pET22b	*E. coli* BL21(DE3) pLysS	bn529
pDR-VTE6woTP67	Expression in yeast	VTE6woTP	pDR196	*S. cerevisiae*	bn563
pda00492	RIKEN cDNA clone	VTE6	Bluescript derivative	*E. coli* Chemoshox	bn52
pL-35S-VTE6-DsRed	Expression in plants	VTE6	pL-35S-DsRed	*A. tumefaciens* GV3101-pMP90	
pL-35S-VTE6-TAP-DsRed	Expression in plants	VTE6, TAP	pL-35S-DsRed	*A. tumefaciens* GV3101-pMP90	

2.3 Methods

2.3.1 Cultivation of Plants and Microorganisms

2.3.1.1 Cultivation and Transformation of E. coli

Escherichia coli (*E. coli*) cells were grown on solid or in liquid Luria-Bertani (LB) medium at 37°C. Liquid cultures were shaken at 180 rpm for aeration. Antibiotics were added in the appropriate concentration for selection (Amp, 100 µg ml^{-1}; Sm, 100 µg ml^{-1}; Sp, 100 µg ml^{-1}). For heat-shock mediated transformation of BL21(DE3) pLysS cells (Table 2), 50 µl of competent cells were thawed on ice, mixed with 5 µl plasmid DNA and incubated for 5 min on ice. The Eppendorf tube containing cells and DNA was placed into a water bath at 42°C for 50 s. Afterwards, the cells were cooled in ice. After 5 min, the cells were suspended in 800 mL of LB medium and incubated for 1 h at 37°C while shaking. Finally, the cells were plated on LB with antibiotics and grown over night.

For electroporation of Electroshox cells (Table 2), 100 µl of competent cells were thawed on ice, mixed with 5 µl of plasmid DNA and incubated for 5 min on ice. The cell/DNA mixture was transferred to a pre-cooled electroporation cuvette and a pulse of 1800 V was applied. Quickly, the cells were suspended in 800 µl ice-cold LB medium and incubated for 1 h at 37°C while shaking. Finally, the cells were plated on LB with antibiotics and grown over night.

LB Medium

10 g l^{-1}	Tryptone
5 g l^{-1}	Yeast extract
10 g l^{-1}	NaCl
15 g l^{-1}	Agar
	pH 7.2 (NaOH)

2.3.1.2 Cultivation and Transformation of A. tumefaciens

A. tumefaciens cells of the strain GV3101-pMP90 were grown on solid YEP medium with antibiotics for 2 days at 28°C. Single colonies were picked to inoculate 5 ml cultures of liquid YEP with antibiotics, which were grown overnight at 28°C while shaking.
Electrocompetent *A. tumefaciens* cells were transformed as described for *E. coli* (2.3.1.1), apart from using YEP medium instead of LB medium.

YEP Medium

10 g l^{-1}	Peptone
10 g l^{-1}	Yeast extract
5 g l^{-1}	NaCl
15 g l^{-1}	Agar
	pH 6.8 (NaOH)

2.3.1.3 Cultivation of C. reinhardtii

C. reinhardtii cultures were provided by Dr. Simone Zäuner (IMBIO, University of Bonn) (Moellering and Benning, 2010; Zäuner *et al.,* 2012). Liquid cultures of *C. reinhardtii* were grown in Tris-Acetate-Phosphate (TAP) medium at 22°C in continuous light with an intensity of 50-75 µmol m^{-2} s^{-1} until an OD_{560} of 1 was reached. The WT strain CC-124 was used in this work.
For nitrogen-deprivation experiments, N stock was omitted from the Tris-Acetate-Phosphate (TAP) medium. Cells were transferred to –N medium and grown for 3 days before harvesting.

Tris-Acetate-Phosphate (TAP) Medium (1 l)

100 ml	TAP Base
10 ml	N Stock
1 ml	P Stock
1 ml	Hutner's Trace Element Solution (1000 x)
	total volume: 1 l

TAP Base (10x)

1 g	$MgSO_4$ x $7H_2O$
0.5 g	$CaCl_2$ x $2H_2O$
24.2 g	Tris Base
10 ml	Acetic Acid
	pH 7-7.5
	total volume: 1 l

N Stock (100x)

180 g	NH_4Cl
	total volume: 1 l

P Stock (1000x)

180 g	K_2HPO_4
90 g	H_2PO_4
	total volume: 1 l

Hutner's Trace Element Solution (1000x)

50 g	EDTA
22 g	$ZnSO_4$
11.4 g	H_3BO_3
5.06	$MnCl_2$ x $4H_20$
1.61 g	$CoCl_2$ x $6H_20$
1.57 g	$CuSO_4$ x $5H_20$
1.1 g	$(NH_4)_6Mo_7O_{24}$ x $4H_20$
4.99 g	$FeSO_4$ x $7H_20$
	total volume: 1 l

2.3.1.4 Cultivation of Arabidopsis thaliana

Arabidopsis Growth on Synthetic Medium

Arabidopsis thaliana WT plants were grown at 16 h day and 8 h night, at a temperature of 21°C, humidity of 60% and a light intensity of 120 µmol m^{-2} s^{-1}. For surface sterilization, seeds were immersed in sterilization solution containing ddH_20/ethanol/12% sodium hypochlorite (21:25:4, v/v/v) and mixed for 20 min. Afterwards, the sterilization solution was completely removed and the seeds were quickly washed three times with ethanol (technical grade). All remaining ethanol was removed after the last washing step and the seeds were dried before sowing. Seeds were plated on MS medium containing 2% sucrose (Murashige and Skoog, 1962) and were left over night at 4°C for stratification.

For nitrogen deprivation experiments, plants were first grown on MS sucrose medium for 2 weeks and then transferred to synthetic *Arabidopsis* nutrient medium (+N) or nutrient medium depleted of nitrogen sources (-N).

Synthetic Arabidopsis Nutrient (2 x strength)

0.8% (w/v)	Agarose
1%	Sucrose
2.5 mM	KNO_3*
1 mM	$MgSO_4$
1 mM	$Ca(NO_3)_2$*
1 mM	KH_2PO_4
1 mM	NH_4NO_3*
25 µM	Fe-EDTA
Micronutrients:	35 µM H_3BO_3, 7 µM $MnCl_2$, 0.25 µM $CuSO_4$, 0.5 µM $ZnSO_4$, 0.1 µM Na_2MoO_4, 5 µM NaCl, 5 nM $CoCl_2$
*	for nitrogen starvation experiments, KNO_3, $Ca(NO_3)_2$ and NH_4NO_4 were replaced with 2.5 mM KCl and 1 mM $CaCl_2$.

Arabidopsis Growth on Soil

Arabidopsis plants were germinated on MS sucrose medium as described above. After about 7 days, seedlings were transferred to 10 cm pots containing soil/vermiculite (2:1, v/v). Five plants were transferred to one pot. Plants were grown at 150 µmol m^{-2} s^{-1} light at 16 h light per day, 20 °C and 55% relative humidity in phytochambers.

Stable Transformation of Arabidopsis by Floral Dipping

Arabidopsis WT Col-0 plants were transformed by floral dipping with a suspension of transgenic *Agrobacteria* carrying the pL-35S-VTE6-DsRed plasmid as previously described (Clough and Bent, 1998). *Arabidopsis* plants were transformed with the empty vector (pL-35S-DsRed) as control. Transgenic seeds were selected by fluorescent microscopy based on the expression of the DsRed marker gene.

2.3.1.5 Cultivation of Nicotiana benthamiana

Growth conditions for N. benthamiana

N. benthamiana seeds were directly sown on 15 cm pots containing soil/vermiculite (2:1, v/v) and grown at 150 µmol m^{-2} s^{-1} light at 16 h light per day, 25 °C and 55% relative humidity in phytochambers. Ten days after germination, seedlings were transferred to fresh pots, with only one plant per pot. After 6-10 weeks, plants were used for leaf infiltration.

Transient transformation of N. benthamiana with A. tumefaciens

Transgenic *Agrobacteria* were grown as described in 2.3.1.2. A liquid culture (5 ml) was inoculated from a single colony and grown overnight at 28°C. On the next day, the bacteria were harvested and suspended in infiltration medium to a final OD_{600} of 0.8. Leaves of 4-6 week old *N. benthamiana* were used for transient transformation. To this end, the bacterial suspension was infiltrated into the spongy mesophyll through the lower leaf surface using a 5 ml plastic syringe. The whole leaf was infiltrated or the infiltrated areas were indicated with a pencil.

For heterologous expression of At1g78620 with TAP-tag, leaves of 4 weeks old *N. benthamiana* plants were infiltrated with *A. tumefaciens* carrying the pL-35S-VTE6-TAP plasmid. For suppression of transgene silencing by *N. benthamiana*, *A. tumefaciens* expressing the p19 protein was co-infiltrated.

Infiltration Medium

20 mM	Citric acid
2%	Sucrose
100 µM	Acetosyringone (500 mM stock in dimethylsulfoxide (DMSO))
	pH 5.2 (NaOH)

2.3.2 Methods in Molecular Biology

2.3.2.1 Isolation of Genomic DNA from Arabidopsis

For isolation of genomic DNA, 1 leaf of *Arabidopsis* grown on soil or on MS medium was harvested, frozen in liquid nitrogen and ground to a fine powder using the Precellys homogenizer. Without thawing the frozen tissue, 1 ml of cetyltrimethylammonium bromide (CTAB) buffer was added and the sample was incubated for 10 min at 65°C while shaking. Afterwards, 0.4 ml of chloroform was added and the sample was centrifuged to achieve a phase separation. The lower, aqueous, phase was transferred to a fresh tube containing 0.7 ml of isopropanol, the sample was mixed and incubated on ice for 10 min for precipitation of genomic DNA. After precipitation, the DNA was spun down and washed with pre-cooled 70% (v/v) ethanol. Finally, 20-50 µl of ddH_20 were added to dissolve the DNA.

CTAB Buffer for Isolation of Genomic DNA

140 mM	Sorbitol
220 mM	Tris-HCl, pH 8
22 mM	EDTA
800 mM	NaCl
0.8%	CTAB
	pH 8

2.3.2.2 Isolation of Plasmid DNA from E. coli

Plasmid DNA was isolated from a 5 ml overnight liquid culture of *E. coli* grown in LB medium. To this end, the cells were harvested by centrifugation and the pellet was resuspended in 200 µl BF buffer and 10 µl of lysozyme (20 mg ml^{-1} in water, stored at -20°C). The suspension was incubated for 1 min at 95°C and afterwards placed on ice for 1 min. The sample was centrifuged and the supernatant was transferred to a fresh tube containing 480 µl IS mix to precipitate the plasmid DNA. The plasmid DNA was spun down and washed with 75% (v/v) ethanol. The ethanol was completely removed and the dried DNA was dissolved in 50 µl ddH_20.

BF Buffer

8% (w/v)	Sucrose
0.5% (w/v)	Triton X-100
50 mM	EDTA, pH 8
10 mM	Tris-HCl, pH 8

IS Mix

400 µl	Isopropanol
80 µl	5 M Ammonium Acetate

2.3.2.3 Polymerase-Chain-Reaction (PCR)

PCR was used for genotyping of *Arabidopsis* insertion lines as well as for the cloning of DNA fragments. DNA was amplified using the heat-stable *Taq* polymerase from *Thermus aquaticus* as well as the *Paq* polymerase from *Pyrococcus*. Paq polymerase was used only for genotyping of *vte5-2*. The combinations of oligonucleotides for genotyping of *vte6-1*, *vte6-2*, *vte5-2* and *vte5-2 vte6-1* are indicated in Table 6. Oligonucleotide sequences are listed in Table 15.

Genotyping of Arabidopsis Insertion Lines

Reaction Setup for Taq Polymerase

1 µl DNA
0.2 µl DCS *Taq*- Polymerase (5 U μl^{-1})
1.5 µl Buffer B (10x)
1.5 µl $MgCl_2$ (25 mM)
0.3 µl dNTPs (10 mM)
1.5 µl Forward Primer (10 pmol μl^{-1})
1.5 µl Reverse Primer (10 pmol μl^{-1})
1.5 µl Insertion Primer (10 pmol μl^{-1})
H_2O ad 15 µl

Reaction Setup for Paq Polymerase

0.5 µl DNA
5 µl *Paq* master mix
1.5 µl Forward Primer (10 pmol μl^{-1})
1.5 µl Reverse Primer (10 pmol μl^{-1})
1.5 µl Insertion Primer (10 pmol μl^{-1})
H_2O ad 10 µl

Table 5 Oligonucleotides for Genotyping of *Arabidopsis* Insertion Lines.

The oligonucleotide sequences are presented in Table 15.

Target	Forward Primer	Reverse Primer	Insertion Primer	Product size [bp]
VTE5	bn771	bn772		1352
vte5-2	bn771		bn232	1080
VTE6	bn233	bn234		1255
vte6-1		bn234	bn232	970
vte6-2		bn234	bn130	1230

Table 6 Temperature Program for Genotyping of *Arabidopsis* Insertion Lines.

Temperature	Function	Duration	
95°C	Initial Denaturation	1 min	
94°C	Denaturation	30 s	37 cycles
55°C, *vte6-1*	Annealing	30 s	
57°C, *vte6-2*			
56°C, *vte5-2*			
72°C	Elongation	1 min (*vte6-1*, *vte5-2*)	
		3 min (*vte6-2*)	
8°C	Pause	∞	

Cloning of Constructs for Functional Analysis of VTE6

Reaction Setup for Pfu PCR

2 µl Plasmid DNA (1 ng µl^{-1})
1 µl *Pfu* Polymerase
5 µl 10x-Buffer + $MgSO_4$
1 µl dNTPs (10 mM stock)
1.5 µl Forward Primer (10 pmol µl^{-1})
1.5 µl Reverse Primer (10 pmol µl^{-1})
Total volume: 50 µl

Table 7 Oligonucleotides for Cloning of VTE6 Expression Constructs.

The oligonucleotide sequences are presented in Table 15.

Amplicon	Function	Restriction Sites
VTE6	VTE6 for overexpression in plant vector pL-35S-DsRed	*XbaI*, *SalI*
VTE6-woTP	VTE6-woTP for expression in yeast vector pDR196	*EcoRI*, *SalI*
VTE6-woTP	VTE6-woTP for expression in *E. coli* vector pET22b	*BamHI*, *SalI*

* Omitting the predicted N-terminal transit peptide of 46 amino acids.
** Omitting the predicted N-terminal transit peptide of 65 amino acids.

Table 8 Temperature Program for *Pfu* PCR.

Temperature	Function	Duration	
95°C	Initial Denaturation	5 min	
94°C	Denaturation	30 s	35 cycles
58°C	Annealing	45 s	
72°C	Elongation	4 min	
8°C	Pause	∞	

2.3.2.4 Agarose Gelelectrophoresis

DNA fragments were separated via gel electrophoresis on a 1% (w/v) agarose gel. Agarose gels were prepared in 1x Tris-Acetate-EDTA (TAE) buffer. Ethidium bromide was added to the liquid agarose in Tris-Acetate-EDTA (TAE) buffer, the final concentration was 0.01 µg ml^{-1}. Ethidium bromide intercalates with DNA and thereby can be used to visualize DNA under UV light. DNA was loaded on agarose gels in DNA loading buffer.

50X Tris-Acetate-EDTA (TAE) Buffer (1 l)
2 M Tris base
50 mM Acetic acid
1 M EDTA, pH 8
pH 8.5 (HCl)

6X DNA Loading Buffer
30% (v/v) Glycerol
0.25% (w/v) Bromophenol blue
0.25% (w/v) Xylene cyanol FF

2.3.2.5 RT-PCR

RNA was isolated from *Arabidopsis* leaves using the Roboklon RNA extraction kit according to the instructions. An additional DNase digest was performed using the Ambion Kit. The quality of RNA was tested using a formaldehyde agarose gel. 250-1000 ng RNA were used for cDNA synthesis with the First-Strand cDNA Synthesis kit (Fermentas).

Formaldehyde Agarose Gel (1.5%)

1.5% (w/v)	Agarose
6% (w/v)	Formaldehyde
1X	MOPS buffer

10X MOPS Buffer

0.2 M	MOPS
50 mM	Sodium acetate
10 mM	Na-EDTA
	pH 7 (NaOH)

Formaldehyde Electrophoresis Buffer

10% (v/v)	Formaldehyde
1X	MOPS buffer

Semi-Quantitative RT-PCR

Semi-quantitative RT-PCR was done for *PES1*, *PES2*, *VTE5*, *VTE6* and *Actin* (*ACT2*, housekeeping gene). The employed oligonucleotides are listed in Table 15. Conditions were as described (Lippold *et al.,* 2012).

Quantitative RT-PCR (qPCR)

For quantitative analysis of gene expression, the StepOnePlus™ Real-Time PCR System (Applied Biosystems) was employed with the help of Philipp Gutbrod (AG Grundler, INRES Institute, University of Bonn). Three technical and three biological replicates were performed. *ACT*2 and *UBIQUITIN* (*UBI*) were used as reference genes to calculate the relative gene expression according to the ΔΔCT method (Livak and Schmittgen, 2001).

The primer amplification efficiency of each primer pair was evaluated before quantification, using the slope determined as shown in Figure 10 (Livak and Schmittgen, 2001) and the formula:

$$\text{Efficiency (\%)} = (10^{(-1/\text{slope})^{-1}})*100$$

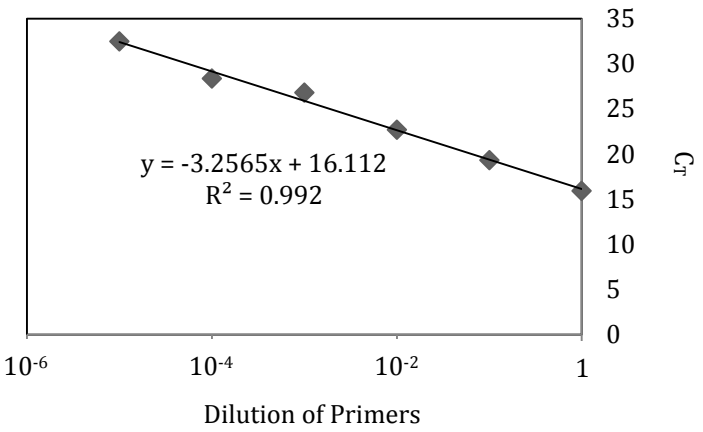

Figure 9 Standard Curve for Primer Efficiency.

Primer pairs were mixed 1:1 (v/v), diluted and used for the amplification of their respective target from *Arabidopsis* WT cDNA. The C_T values (y-axis) are plotted against the primer dilutions (x-axis). A regression line and the coefficient of determination (R^2) were calculated from the diagram using Microsoft Office Excel.

Reaction Setup for qPCR		*Fast SYBR® Green Master Mix*
10 µl	Fast SYBR® Green Master Mix	*(Thermo Fisher Scientific) (2X)*
5 µl	cDNA (1:100, v/v)	AmpliTaq® Fast DNA Polymerase
5 µL	Forward and Reverse Primer Mix (1:1, v/v; 1 µM each)	SYBR® Green I dye dNTPs Uracil-DNA Glycosylase (UDG)

2.3.3 Methods in Biochemistry

2.3.3.1 Phytyl-P-Kinase Assay with Recombinant VTE6 Proteins

Extraction of proteins for phytyl-P-kinase assay from *E. coli*, yeast and *N. benthamiana* was done as described by Ischebeck *et al.* (2006).

Radioactive Phytyl-P-Kinase Assay

To produce the radioactive substrate for the phytyl-phosphate-kinase assay, 10 µl (1 mCi) of gamma-^{32}P-adenosine triphosphate (γ-^{32}P-ATP, Hartmann Analytik, Braunschweig) was incubated with 44 µl H_2O, 10 µl 100mM $MgCl_2$, 30 µl 100mM CDP (Sigma-Aldrich) in 100 mM Tris-HCl (pH 7.4), 5 µl 1M Tris-HCl (pH 7.4) and 1 µl nucleoside 5'-diphosphate kinase (10U/µl, Sigma-Aldrich) to synthesize gamma-^{32}P-cytosine triphosphate (γ-^{32}P-CTP). For the assay, 40 µl protein extract, 8 µl CHAPS assay buffer, 2 µl 1% phytyl-P in ethanol, 7 µl ddH_20 and 3 µl of ^{32}P-Mix were mixed and incubated for 30 min at 30°C while shaking. The reaction was stopped by the addition of 100 µl methanol. Isoprenyl-phosphates were extracted from the assay mixture with 100 µl water-saturated butanol. For evaluation of the assay, 80 µl of the butanol extract were loaded on a TLC plate (Macherey & Nagel) and developed in a glass container. The solvent system was isopropanol/ammonium hydroxide/H_20 (6:3:1, v/v/v). The TLC plate was dried, transferred to an

autoclave bag and the radiation of the plate was exposed to a phosphorimager screen (BioRad) for 3-4 days. The screen was developed using a Molecular Imager FX System phosphorimager (BioRad).

Non-Radioactive Phytyl-P-Kinase Assay

For the non-radioactive phytyl-P-kinase assay, γ-^{32}P-CTP was replaced by an equimolar mix of NTPs (10 mM each of ATP, UTP, GTP and CTP). For the assay, 30 µl 5 mM phytyl-P in ethanol were transferred to a 1.5 ml Eppendorf tube and dried under air flow. Afterwards, 150 µl leaf extract, 40 µl CHAPS assay buffer and 5 µl of 10 mM NTPs in extraction buffer were mixed and incubated for 30 or 60 min at 30°C while shaking. The reaction was stopped by the addition of 200 µl isopropanol/50 mM KH_2PO_4 pH 7.2/acetic acid (200:200:5, v/v/v). Isoprenyl-phosphates were extracted from the assay mixture. For evaluation of the assay, the purified isoprenyl-phosphates were dissolved in 100 µl of methanol and analysed using LC-Q-TOF-MS/MS as described.

Protein Extraction Buffer

100 mM	Tris-HCl, pH 7.5
1 mM	EDTA, pH 8.5
2.5 mM	Dithiothreitol (DTT)
1 mM	$MgCl_2$
1 mM	Isoascorbate
1 mM	KCl
0.1%	Bovine serum albumin (BSA)
	pH 7.5 (HCl)

Assay Buffer

0.25%	CHAPS
20 mM	$MgCl_2$
50 mM	Sodium orthovanadate

2.3.3.2 Preparation of Chloroplast Membranes from Arabidopsis

Isolation of Intact Chloroplasts

Chloroplast membranes were prepared as described by Hiltbrunner *et al.* (2001) and Vidi *et al.* (2006) with modifications. All experiments were done in the cold room at 4°C or on ice. Exposure of the leaves and isolated chloroplasts to light was minimized to avoid light damage.

Arabidopsis seeds were densely sown on 10 cm pots with soil/vermiculite (2:1, v/v) and seedlings grown under normal conditions for 2 weeks. The plants were placed into the dark in the evening and harvested in the next morning to minimize the accumulation of starch in the leaves. Leaves were collected in ice-cold tap water and incubated for 30 min. Afterwards, the leaves were transferred to a 150 ml glass vessel (Edmund Bühler GmBH) with 100 ml of cold HB buffer and ground three times at 1500 rpm using the tissue homogenizer (Edmund Bühler GmBH). The sample was filtered through two layers of Miracloth and collected in 500 ml centrifuge tubes (Nalgene). Chloroplasts were harvested by centrifugation (2 min, 2200 rpm, 4°C) in a pre-cooled JA-14 rotor using the Sorvall centrifuge. The supernatant was collected as control (cytosol, other organelles) and stored at -20°C. The chloroplast pellet was carefully suspended in 1 ml RB buffer

with a marten hair brush. This suspension was loaded on top of a percoll step gradient (40% and 85%, v/v, in RB buffer) and centrifuged (10 min, 4000 rpm, 4°C) in a Beckman-Coulter ultracentrifuge using an SW28 swing-out rotor for 35 ml tubes. Intact chloroplasts were harvested from the interphase between 40% and 85% percoll. The chloroplasts were washed with 10 volumes of RB buffer and suspended in 1 ml TE buffer. Chlorophyll was measured in 5-10 µl of the sample as described in 2.3.3.7, but at a wavelength of 652 nm (chlorophyll concentration in mg/ml = OD_{652} x dilution factor/36). After chlorophyll determination, the sample was filled up to a volume of 10 ml and chloroplasts were harvested again by centrifugation.

Fractionation of Chloroplast Membranes on a Sucrose Gradient

For the preparation of chloroplast membranes, the chloroplast pellet was suspended in 0.6 M sucrose in TE buffer to a final concentration of 1.2 mg/ml chlorophyll and incubated on ice for 10 min. Afterwards the suspension was frozen at -80°C for 1-2 h and thawed at room temperature. Then the sample was diluted with 0.6 M sucrose in TE buffer to a final volume of 50 ml. To rupture the chloroplasts, the sample was ground with a Potter-Elvehjem homogenizer with polytetrafluorethylene (PTFE) pestles of decreasing sizes and increasing homogenization strengths: 45 ml, 8 ml and 3 ml. For homogenization, 20 strokes were carefully performed for each pestle. The lysed chloroplasts were centrifuged in the SW28 swing-out rotor (27.000 rpm, 1 h, 4°C) after each homogenization step. The supernatant resulting from centrifugation after the first homogenization step (45 ml Potter-Elvehjem homogenizer) contains the stroma and can be stored at -20°C. The pellet resulting from centrifugation after the final homogenization step was resuspended in 45% sucrose in TE buffer, the concentration should be 2-3 mg chlorophyll/ml. This suspension was layered on top of a sucrose gradient of 5, 15, 20 and 38 % sucrose in TE buffer (v/v) and centrifuged for 16 h at 27.000 rpm at 4°C in an SW28 swing-out rotor. Fractions of 1 ml were collected from the gradient from top to bottom and stored at -20°C. Plastoglobules accumulate at the top of the gradient in the 5% sucrose layer and were visible as a milky white emulsion.

TE Buffer

50 mM	Tricine-HCl, pH 7.5
2 mM	EDTA, pH 8
2 mM	Dithiothreitol (DTT)

Two-Step Percoll Gradient

85% (v/v)	percoll in HB buffer
40% (v/v)	percoll in HB buffer

HB Buffer

450 mM	Sorbitol
20 mM	Tricine/KOH, pH 8.4
10 mM	EDTA, pH 8.5
10 mM	$NaHCO_3$
1 mM	$MnCl_2$

RB Buffer

300 mM	Sorbitol
20 mM	Tricine/KOH, pH 8.4
2.5 mM	EDTA, pH 8.5
1 mM	$MgCl_2$

Sucrose Gradient

5% (w/v)	sucrose in TE buffer
15% (w/v)	sucrose in TE buffer
20% (w/v)	sucrose in TE buffer
38% (w/v)	sucrose in TE buffer

2.3.3.3 Internal Standards for Q-TOF MS/MS

Table 9 Internal Standards for Lipid Quantification Using GC-FID, GC-MS and Q-TOF MS/MS.

Analyte	Internal Standards	Standard amount per sample	Supplier
Triacylglycerol	tri10:0	1 nmol	Larodan (Malmö, SE)
	tri11:1	1 nmol	Synthesized in house
	tri20:0	2 nmol	Larodan (Malmö, SE)
	tri22:1	2 nmol	Larodan (Malmö, SE)
Tocopherol	rac-Tocol	1.3 nmol, 500 ng	Biotrend (Destin, USA)
Phytyl Esters	17:0-phytol	1 nmol	Synthesized in house
Phytol	Octadecenol (18:1ol)	10 nmol	Sigma-Aldrich (Taufkirchen, D)
Isoprenyl-Phosphates	10:0-P	1 nmol	Synthesized in house
	10:0-PP	1 nmol	
	16:0-P	1 nmol	
	16:0-PP	1 nmol	
	18:0-P	1 nmol	
	18:0-PP	1 nmol	
	20:0-P	1 nmol	
	20:0-PP	1 nmol	
Fatty Acids	15:0	19.5 nmol, 5 µg	Sigma-Aldrich (Taufkirchen, D)

2.3.3.4 Synthesis of Lipid Standards for Q-TOF Mass Spectrometry

Synthesis of Fatty Acid Phytyl Esters

The internal standard for the quantification of phytyl esters was synthesized as described in Gellerman *et al.*, 1975. Briefly, 0.2 mmol of heptadecanoic acid (17:0, Sigma Aldrich, Taufkirchen, D) were dissolved in 1 ml of toluene and 0.28 mmol of oxalyl chloride were added. The mixture was incubated for 2 h at 60°C and dried under air flow. Next, 1 ml of dried diethylether, 0.2 mmol of phytol and 0.25 ml of dried pyridine were added and the mixture was incubated for 2 h at 80°C. The synthesized phytyl esters were extracted from the mixture with hexane and purified via solid-phase-extraction as described in 2.3.3.6.

Synthesis of Triacylglycerols

The monounsaturated internal standard for triacylglycerols, tri11:1$^{\Delta cis}$, was synthesized as described for fatty acid phytyl esters by Helga Peisker (IMBIO Institute, University of Bonn). Instead of 17:0 fatty acid 11:1$^{\Delta cis}$ fatty acid (Larodan) was used, and phytol was replaced with glycerol.

Synthesis of Alcohol-Phosphates and Alcohol–Pyrophosphates

Alcohol-phosphates and alcohol-pyrophosphates were synthesized from phytol and decanol (10:0ol). Octadecenol and decanol occur in very low amounts in plants. For the synthesis of alcohol-phosphates, a protocol modified from Joo *et al.*, 1973 and Cramer *et al.*, 1962 was used. First, di-(triethylammonium) phosphate was synthesized. To this end, 19.6 g H_3PO_4 was dissolved in 100 ml of acetonitrile. Then 40.4 g triethylamine and 2 ml H_20 were added to dissolve the precipitating salt. The solution was filled up to 250 ml with acetonitrile. Next, 2 mmol of phytol, 10:0ol or another long-chain alcohol were dissolved in 15 mmol of trichloroacetonitrile. 45 ml of the freshly prepared di-(triethylammonium) phosphate solution were added dropwise over a period of 3 h at RT to the alcohol solution. The mixture was stirred overnight at RT and diluted with 50 ml acetone on the next day. Then concentrated aqueous ammonium hydroxide was added dropwise until no more precipitation occurred. Afterwards the solution was kept at 0°C for several hours. The white precipitate was harvested by centrifugation and washed with acetone. Then the precipitate was resuspended in 50 ml of 0.28 M methanolic ammonium hydroxide, prepared by dissolving 1 ml 32% ammonium hydroxide solution in 50 ml of methanol. After centrifugation, the methanol-soluble supernatant which contains alcohol-P was dried. The methanol-insoluble material, which contains alcohol-PP was washed first with 10 ml of 0.28 M methanolic ammonium hydroxide to remove residual phytyl-P. Then the alcohol-PP was extracted with a premixed solution of 10 ml of chloroform with 2 ml of methanol/ddH_20 (10:9, v/v). The suspension was centrifuged and the supernatant containing alcohol-PP was harvested and dried. Alcohol-P and alcohol–PP were purified by TLC separation with the solvent isopropanol/32% ammonium hydroxide solution/H_20 (6:3:1, v/v/v).

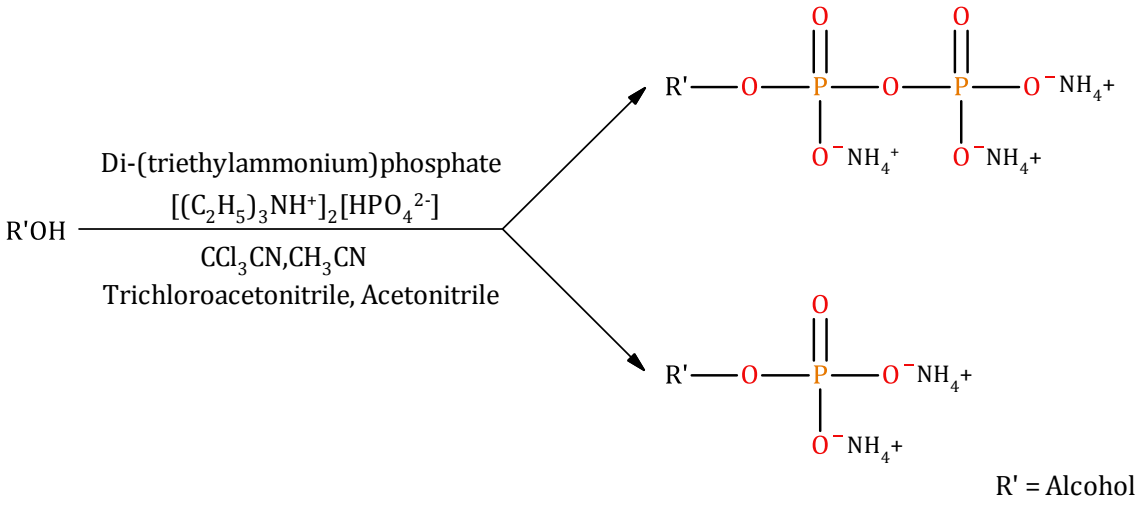

Figure 10 Synthesis of Alcohol-P and Alcohol-PP from Free Alcohol.

Alcohol-P and alcohol–PP were synthesized from phytol and 10:0ol (=R'). The reaction products were ammonium salts of the alcohol-phosphates (M=NH_4^+).

2.3.3.5 Quantification of Lipid Standards

Spectrophotometric Determination of Tocol

For the quantification of *rac*-tocol (Biotrend, Destin, USA), a working stock of 1 µg µl^{-1} in 100% ethanol was prepared. The concentration was confirmed by spectrophotometric measurement. 1 ml of the working stock was measured in a quartz cuvette against pure ethanol at a wavelength of 298 nm. The extinction coefficient 90 was taken from (Schüep and Rettenmeier, 1994).
An absorption of A_{298nm} 90 represents a concentration of 1 µg µl^{-1}.

Gas Chromatography-Flame Ionization Detection (GC-FID)

The concentration of the synthetic 17:0-phytol (3.3.3.4.1) was determined by quantification of the fatty acid moiety using GC-FID. To this end, 17:0-phytol and 5 µg of 15:0 (internal standard) were transmethylated by incubation with 1 ml 1 N HCl in methanol for 20 min at 80°C in a water bath. After methylation, 1 ml of 0.9% NaCl (in water) was added and the FAMEs were extracted with 1 ml of hexane. The FAMEs were separated and quantified using the Agilent Gas Chromatograph with flame ionization detection (FID) by comparing the peak areas of the phytyl ester-derived FAMEs to that of the internal standard 15:0-methyl ester. Internal standards for triacylglycerol were quantified similarly. As triacylglycerols consist of 3 fatty acid moieties, the amount of FAME has to be divided by 3 to obtain the amount of triacylglycerol.

Table 10 Column Parameters for GC-FID.

Parameter	Setting
Column	Supelco SP-2380
Column length	30 m
Carrier gas	Helium
Flow rate	7 ml/min

Oven Ramp	Temperature
Initialization	100°C
25°C min^{-1}	to 160°C
10°C min^{-1}	to 220°C
25°C min^{-1}	to 100°C

Gas Chromatography-Mass Spectrometry (GC-MS)

Exact amounts of standards for alcohol-phosphates (C10-C20), dissolved in methanol, and 10 nmol sorbitol in 100% ethanol were dried under air flow. 80 µl of MSTFA were added and the lipids were derivatized for 30 min at 80°C. Afterwards, MSTFA was evaporated under air flow and the sample was dissolved in *n*-hexane and transferred to glass sample vials for analysis. GC-MS conditions were modified from Roessner *et al.* (2000) (Table 11).

Table 11 Column Parameters for GC-MS.

Parameter	Setting
Column	Agilent HP-5MS
Column length	30 m
Carrier gas	Helium
Flow rate	7 ml/min

Oven Ramp	Temperature
Initialization	70°C
5°C min^{-1}	to 310°C
Hold 1 min	310°C
Equilibration	70°C

2.3.3.6 Preparation of Lipid Extracts from Arabidopsis Seeds and Leaves

Extraction of Phospholipids and Galactolipids from Arabidopsis Leaves

For phospholipid and galactolipid analysis, 20 mg of leaf tissue were harvested, transferred to a 2 ml Eppendorf tube and immediately frozen in liquid nitrogen to prevent degradation by phospholipase activity. The tissue was ground to a fine powder using the Precellys homogenizer. Lipids were extracted from the ground material using 2 vol chloroform/methanol/formic acid (1:1:0.1, v/v/v) and 1 vol 1 M KCl/0.2 M H_3PO_4. Phase separation was achieved by centrifugation (5 min at 2500 rpm). The lower phase was transferred to a fresh glass vial. The extraction was repeated twice with chloroform/methanol (2:1, v/v) and the extracts were combined. The solvent was evaporated and the extracted lipids were dissolved in 1 ml of chloroform/methanol/300 mM ammonium acetate (300:665:35, v/v/v). 20 µl of the extract were mixed with 20 µl of internal standard mix (Welti *et al.,* 2002; Gasulla *et al.,* 2013) and diluted with 160 µl of chloroform/methanol/300 mM ammonium acetate (300:665:35, v/v/v).

Extraction of Non-Polar Lipids from Arabidopsis Seeds and Leaves

For the extraction of non-polar lipids from seeds or leaves, 20 mg of seeds or 100 mg of leaf tissue were used for analysis via HPLC-FLD (tocopherol), GC-MS (phytol) or Q-TOF MS/MS (fatty acid phytyl esters). The tissue was harvested, frozen in liquid nitrogen and ground to a fine powder as described above. Non-polar lipids were extracted using 2 vol diethylether and 1 vol 1 M KCl/0.2 M H_3PO_4. The sample was centrifuged (5 min at 2500 rpm) and the upper phase was harvested. The extraction procedure was repeated twice and the pooled extracts were dried under air flow. Tocopherols were measured directly in non-polar extracts, phytol and fatty acid phytyl esters were further purified using solid-phase-extraction.

Solid-Phase-Extraction of Lipids from Non-Polar Leaf Extracts

Solid-phase extraction was performed as described in vom Dorp *et al.* (2013). Normal-phase silica columns (100 mg) were used for separation of the lipid classes. For elution of the different lipid fractions, 3 ml of each solvent were used. Lipids were separated into 3 fractions based on their polarity. Non-polar lipids were eluted with chloroform, glycolipids with acetone/2-propanol (1:1) and polar lipids with methanol. When non-polar lipids were of low abundance in the analyzed tissue, a second solid-phase-extraction step was applied to enrich these non-polar lipids (http://www.cyberlipid.org). To this end, the chloroform fraction was dried and the non-polar lipids were dissolved in *n*-hexane. Lipids were again loaded to a silica SPE column (100 mg) equilibrated in *n*-hexane. Fatty acid phytyl esters and sterol esters were eluted from the column using *n*-hexane/diethylether (99:1, v/v), TAGs and tocopherol were eluted with *n*-

hexane/diethylether (95:5, v/v), phytol was eluted with *n*-hexane/diethylether (92:8, v/v) and DAGs were eluted with 100% diethylether.

Extraction of Isoprenyl-Phosphates from Seeds and Leaves

The extraction protocol for isoprenyl-phosphates was modified from Larson and Graham (2001). Plant tissue (20 mg) was harvested in 2 ml Eppendorf tubes, frozen in liquid nitrogen and ground to a fine powder using the Precellys homogenizer. 200 µl isopropanol/50 mM KH_2PO_4 pH 7.2/acetic acid (200:200:5, v/v/v) were pipetted to the powder as well as 50 µl of the internal alcohol-phosphate standard mix (Table 9), and the sample was thoroughly vortexed. Non-polar lipids were removed from the sample by washing three times with 200 µl of n-hexane saturated with isopropanol/H_20 (1:1, v/v). Proteins were removed by precipitation after addition of 5 µl saturated $(NH_4)_2SO_4$ solution and 600 µl methanol/chloroform (2:1, v/v) and incubation for 20 min at RT. The precipitate was removed by centrifugation for 2 min at maximum speed. The supernatant was dried, the residual alcohol-phosphates dissolved in 100 µl of methanol and transferred to Q-TOF sample vials for analysis.

2.3.3.7 Analytical Tools for Lipid Quantification

Quantification of the Chlorophyll Content in Leaves

The chlorophyll content of leaves was determined as described in Porra *et al.* (1989). Leaves were frozen in liquid nitrogen and ground to a fine powder using the Precellys homogenizer. Chlorophyll was extracted with 1 ml 80% (v/v) acetone, the extract was centrifuged at maximum speed and the supernatant was transferred to a quartz cuvette. The absorbances at the wavelengths of 663.3, 646.6 and 750 nm were measured with a spectrophotometer. The following formulas were used to calculate the amount of chlorophyll:

Chlorophyll a (µg/ml) = 12.25 * (A663.6-A750) - 2.55 * (A646.6-A750)

Chlorophyll b (µg/ml) = 20.31 * (A646.6-A750) - 4.91 * (A663.6-A750)

The absorbance measured at 750 nm was subtracted from A663.6 and A646.6 to remove background signals.

Tocopherol Analysis Using HPLC-FLD

For tocopherol analysis, lipids were extracted as described in 2.3.3.6, dissolved in *n*-hexane and measured quickly after extraction as described in Balz *et al.* (1992). Briefly, the different forms of tocopherol were separated on a LiChrospher diol column (Knauer, 250 x 3 mm, 2.1 µm particle size) by isocratic elution with *n*-hexane/tertiary butylmethylether (96:4, v/v) at a flow rate of 0.75 ml min^{-1}. Chromatography was carried out using an Agilent 1100 series HPLC system with fluorescent light detector (FLD).

Quantification of Phytol Using GC-MS

For the quantification of free phytol, non-polar lipids were isolated and phytol was purified by SPE as described in 2.3.3.6. Oleyl alcohol (18:1ol, 10 nmol) were added during the extraction procedure. Phytol was silylated and measured by GC-MS as described in Ischebeck et al. (2006). Parameters were used for GC-MS as described in 2.3.3.5.

2.3.3.8 Analysis of Lipids via Q-TOF MS/MS

Direct Infusion Q-TOF MS/MS

Fatty acid phytyl esters, triacylglycerol and phospholipids/galactolipids were analyzed by direct infusion Q-TOF MS/MS. To this end, lipid extracts were prepared as described (2.3.3.6) and the purified lipids were dissolved in chloroform/methanol/300 mM ammonium acetate (300:665:35, v/v/v) (Welti *et al.,* 2002). Samples were delivered to the Q-TOF MS using an Agilent Series 1100/1200 nanopump and HPLC-Chip Cube MS interface. The flow rate was 1 µl/min. The Chip Cube was equipped with a flow infusion chip that exhibits a small diameter needle which produces a spray of fine, charged droplets (containing the analytes) at the tip. Lipids were analyzed in the positive ion mode via MS/MS experiments on an Agilent 6530 Series Accurate-Mass Q-TOF LC/MS. Other instrumental parameters were used as described in Table 12. Lipids were quantified by precursor ion scanning or neutral loss scanning after collision-induced-dissociation (CID). Details are given in 7.3.

Table 12 Parameters for Direct Infusion Q-TOF MS/MS Analysis.

Parameter	Setting
Drying gas	8 l/min N_2
Fragmentor voltage	200 V
Gas temperature	300 °C
HPLC-Chip V_{cap}	1700 V
Scan rate	1 spectrum/s

Contribution of $^{13}C_2$ Isotopes

During direct infusion mass spectrometry, lipids that contain 2 ^{13}C atoms will give rise to a m/z value increased by two as compared to the compound containing only ^{12}C atoms. This peak will overlap with the m/z of a related lipid that lacks one double bond. The isotope distribution pattern for a given molecule is calculated by the use of the Agilent MassHunter Isotope Distribution Calculator. The relative contribution of the $^{13}C_2$ isotope of a compound to the abundance of a compound that is larger by two m/z units (i.e. equivalent to a related compound lacking one fatty acid double bond) is calculated and the total peak abundance is adjusted accordingly.

Analysis of Isoprenyl-Phosphates via LC-Q-TOF MS/MS

Isoprenyl-phosphate HPLC separation and detection using Q-TOF MS/MS were modified from Miriyala *et al.* (2010) and Nagel *et al.* (2012). For the separation of isoprenyl-phosphates, a Macherey & Nagel Nucleodur C8 column (50x4.6 mm, 2.1 µm particle size) was used. Isoprenyl-phosphates were eluted from the column using a gradient of solvent A (5 mM ammonium bicarbonate) and solvent B (acetonitrile), starting with 20% B and increasing to 100% B in 25 min. Afterwards, the column was equilibrated with 20% B for 5 min. The separation was carried out using an Agilent 1100 Series binary pump coupled to an Agilent 6530 Series Accurate-Mass Q-TOF LC/MS. Isoprenyl-phosphates were analyzed in negative ion mode after collision-induced-dissociation, by precursor ion scanning for fragment F_1 (Figure 13) with m/z 78.9591 (phytyl-P, m/z 375.2664; phytyl-PP, m/z 455.2328, GG-P, m/z 369.2195, GG-PP, m/z 449.1858) as described before (Valentin *et al.*, 2006). Peak areas were normalized against the peak areas of the internal standards 10:0ol-P/10:0ol-PP, and nmol values were calculated as described in 3.1.2. No correction for isotopic overlap was necessary as all target compounds were separated from each other by chromatography and the target molecular ions differ by more than 2 m/z units.

Table 13 Parameters for LC-Q-TOF MS/MS Analysis.

Parameter	Setting
Drying gas	8 l/min N_2
Fragmentor voltage	200 V
Gas temperature	300°C
V_{cap}	3500 V
Scan rate	1 spectrum/s

Data Evaluation

Data recorded using direct infusion Q-TOF MS/MS were evaluated using the Agilent MassHunter Qualitative Analysis software. Neutral loss scanning or precursor ion scanning for fragments of a defined m/z value was performed on the mass spectra. The details for each lipid class are indicated in 7.3 (Appendix). The resulting data were processed in Microsoft Office Excel. For data recorded

using LC-ESI-Q-TOF MS/MS, the Agilent MassHunter Quantitative Analysis software was employed and peak areas were calculated based on precursor ion scanning for isoprenyl-phosphate headgroups (7.3, Appendix). These data were further processed in Microsoft Office Excel.

2.3.4 Statistical Methods

Mean and standard deviation (SD) were calculated using Microsoft Office Excel. For the determination of statistical significance, Student's t-test was performed. Data were significantly different from the control if $P < 0.05$, indicated by a single asterisk (*).

3 Results

3.1 Quantification of Phytyl Lipids Via Q-TOF MS/MS

The focus of this work is the characterization of metabolites and enzymes involved in the incorporation of phytol into different end products in *Arabidopsis*. In particular, the acylation and the phosphorylation of free phytol, leading to the synthesis of fatty acid phytyl esters and tocopherol, respectively, will be analyzed. Therefore, a broad spectrum of analytical methods has to be established. Previously, methods for the quantification of tocopherol via fluorescence HPLC and for the quantification of free phytol and fatty acid phytyl esters via GC-MS were established or adapted in our laboratory (Balz *et al.,* 1992; Ischebeck *et al.,* 2006; Gaude *et al.,* 2007; Zbierzak *et al.,* 2010). However, the amount of fatty acid phytyl esters is extremely low in leaves and in non-green tissues, e.g. in seeds under normal growth conditions. In these samples, signals obtained after GC-MS analysis of fatty acid phytyl esters were below the detection limit. Moreover, in some *Arabidopsis* mutants with a growth defect, the sample amount is limited. Therefore, a more sensitive method for the detection of fatty acid phytyl esters was required (3.1.1). The Agilent 6530 Accurate Mass Q-TOF MS provides a very sensitive means for detection of low abundant compounds. Fatty acid phytyl esters were purified by a protocol originally described for steryl esters (2.3.3.6, http://www.cyberlipid.org/). A method for the measurement of isoprenyl phosphates (phosphorylated forms of phytol or geranylgeraniol) in *Arabidopsis* had not been established to date. Therefore, a quantitative analysis method for isoprenyl-phosphates from plant samples and from in vitro enzyme assays was developed (3.1.2).

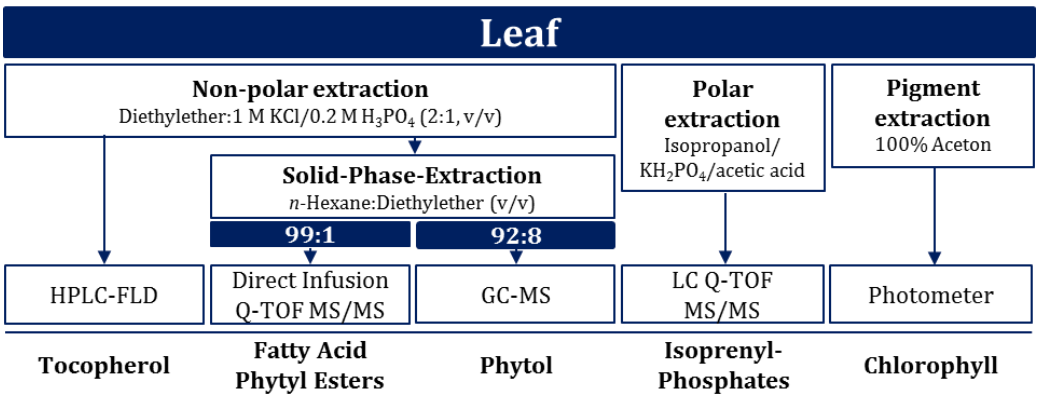

Figure 11 Extraction and Quantification of Phytyl Lipids from *Arabidopsis* Leaf Tissue.

A comprehensive profile of phytyl lipids can be obtained using different extraction procedures and analysis methods. A non-polar lipid extract can be used to directly measure tocopherol or it can be further purified by SPE on silica columns to obtain fatty acid phytyl esters or phytol. Isoprenyl-phosphates were isolated using isopropanol/50 mM KH_2PO_4/acetic acid (200:200:5, v/v/v). Chlorophyll is extracted with 80% (v/v) acetone.

3.1.1 Fatty Acid Phytyl Ester Analysis Using Direct Infusion Q-TOF MS/MS

For the quantification of fatty acid phytyl esters, an internal standard was synthesized (17:0-phytol, 2.3.3.4) which was added at the beginning of the extraction. Fatty acid phytyl esters were purified as described (2.3.3.6) from non-chlorotic tissues (e.g. green leaves and seeds) and from chlorotic tissues (senescent leaves and leaves from plants grown under –N conditions). 5 µl of the sample were infused into the Agilent Accurate Mass Q-TOF MS. Thus, fatty acid phytyl esters could be easily measured in the positive mode after fragmentation even in tissues where these lipids were not detectable using the GC-MS method (e.g. seeds). When ionized at the HPLC-ChipCube/MS interface, fatty acid phytyl esters form ammonium adducts ($[M+NH_4]^+$). The list of masses of the fatty acid phytyl ester ammonium adducts is shown in Table 18.

Different voltages were tested for collision-induced dissociation (CID) of fatty acid phytyl esters. Fragmentation of the molecular ion $[M+NH_4]^+$ results in the production of one or several fragments (F) that can be specific for the molecule of interest. Furthermore, the neutral loss (mass difference of molecular ion and fragment ion) can be used for compound identification. The signal intensity of the specific fragment ion must be high because it is used for quantification. A collision energy of 5 V was finally selected for fatty acid phytyl esters. In the mass spectrum produced by CID of the ammonium adduct of 16:3-phytol at 5 V, the parental ion (m/z 546.5250) is clearly visible. The fragment ion m/z 268.2276 represents the ammonium adduct of the 16:3-fatty acid (F_1) after neutral loss of the phytol moiety. Higher collision energies (>20 V) result in the production of many small fragment ions from the carbon chain ($(CH_2)_n$) and cause a reduced peak height of the main fragment ion F_1.

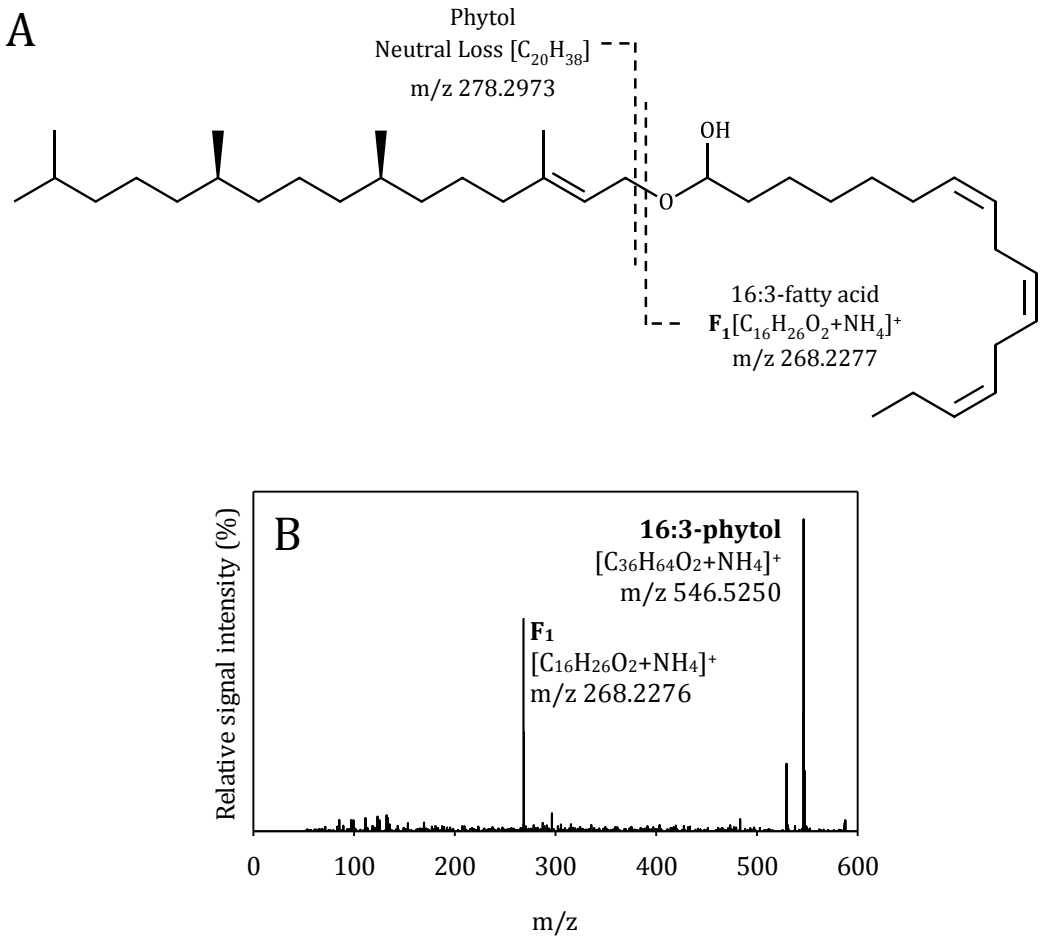

Figure 12 Structure and Fragmentation Pattern of Fatty Acid Phytyl Esters.

(A) Fatty acid phytyl esters are composed of a phytyl moiety and a fatty acid moiety. The most abundant fatty acid phytyl ester in chlorotic *Arabidopsis* leaves is 16:3-phytol. (B) CID of fatty acid phytyl esters results in a fragment ion of the fatty acid moiety as ammonium adduct (F_1) as well as the residual parental ion (ammonium adduct of 16:3-phytol).

3.1.2 Isoprenyl-Phosphate Analysis Using LC Q-TOF MS/MS

Isoprenyl-phosphates are key intermediates in the biosynthesis of a variety of isoprenoids, e.g. tocopherol/tocotrienol (Vitamin E), chlorophyll, sterols and carotenoids. GG-PP is produced via the isoprenoid *de novo* synthesis from condensation of four isoprene units. During tocopherol synthesis, homogentisate is prenylated using phytyl-PP. Methods for the chromatographic separation of isoprenyl-phosphates were previously described, mainly for synthetic standards, reaction products of enzyme assays or for mammalian tissues (Zhang and Poulter, 1993; Valentin *et al.,* 2006; Tong *et al.,* 2008; Miriyala *et al.,* 2010). Nagel *et al.* (2014) designed a method to analyze geranyl-PP (C10), farnesyl-PP (C15) and GG-PP in spruce bark and needles, starting with 750 mg of sample tissue. Until now there was no comprehensive method for the quantification of C20-isoprenyl-phosphates from *Arabidopsis*. *Arabidopsis* mutants for the genes involved in tocopherol biosynthesis (*vte1*, *vte2*, *vte3* and *vte4*) as well as for other isoprenoid-related metabolic steps have been isolated. HPT/VTE2 uses phytyl-PP for the synthesis of MPBQ, GGR

catalyzes the reduction of GG-PP to phytyl-PP. The enzymatc activities of HPT/VTE2 and GGR were corroborated by *in vitro* assays. However it was not possible to determine the actual levels of the isoprenyl-phosphates *in planta*.

In this work, several mutants of phytol metabolism are characterized, including mutant plants presumably affected in the activity of phytyl-P kinase. Phytyl-P kinase phosphorylates phytyl-P to produce phytyl-PP. In addition, phytyl-PP can be synthesized by reduction of GG-PP. Phytyl-P kinase might have a side activity for the phosphorylation of GG-P to GG-PP (Valentin *et al.,* 2006; Shpilyov *et al.,* 2013). A sensitive and reproducible LC-MS/MS method for the detection of C20-isoprenyl-phosphates in minute amounts of sample is required for the understanding of isoprenoid-metabolism.

Firstly, the extraction procedure for isoprenyl-phosphates from *Arabidopsis* was optimized. Isoprenyl-phosphates contain one or two phosphate groups and are therefore polar. For this reason, an isolation protocol based on chloroform/methanol extraction could not be used. Several protocols described for the isolation of polar metabolites were tested, but only two protocols gave satisfying results for the isolation of isoprenyl-phosphates: method A which was originally developed to isolate phosphorylated sphingolipids from *Arabidopsis* leaves (Markham *et al.,* 2006) and protocol B previoulsy used for the isolation of acyl-CoAs from *Arabidopsis* seeds and seedlings (Larson and Graham, 2001). To test the extraction efficiency of the two protocols, *Arabidopsis* leaves were extracted according to the respective method. At the beginning of the extraction, chemically synthesized phytyl-P and phytyl-PP were added to the leaves (Joo *et al.,* 1973). Measurement of these extracts by direct infusion Q-TOF MS/MS revealed that the extraction efficiency of isoprenyl-phosphates strongly depends on the degree of phosphorylation, i.e. quantitative extraction of the isoprenyl-PPs from plants depends on the use of a polar solvent (Figure 14A). Phytyl-P is equally well extracted using either of the two extraction protocols. In contrast, phytyl-PP can only be efficiently isolated using protocol B (isopropanol/50 mM KH_2PO_4 pH 7.2/acetic acid; Larson *et al.*, 2001). Therefore, protocol B was used for all further experiments. This experiment demonstrates the need of using internal standards for the extraction of isoprenyl-monophosphates and isoprenyl–diphosphates to compensate for the differences in recovery. Therefore, a set of standards was synthesized using phytol, decanol (10:0ol), hexadecanol (16:0ol), octadecanol (18:0ol) and eicosanol (20:0ol) using the method described above, producing the mono- and diphosphates of these alcohols. 10:0-P/-PP was used as internal standard, the other standards were used to optimize LC separation or to determine the dynamic range of isoprenyl-phosphate measurements using Q-TOF MS.

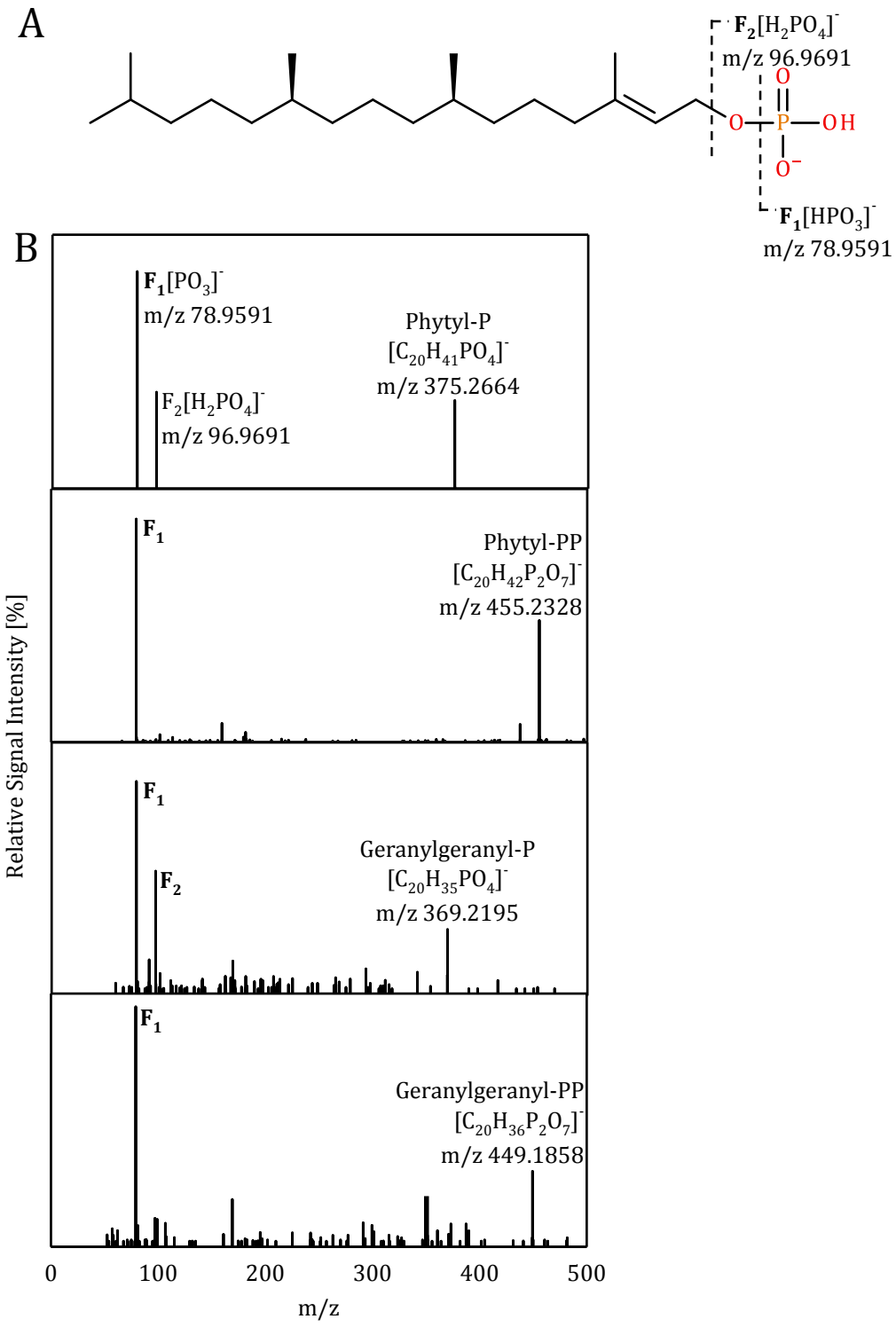

Figure 13 Fragmentation Pattern of *Arabidopsis* C20-Isoprenyl-Phosphates.

(A) Structure of phytyl-P and fragmentation pattern. (B) After CID at a collision energy of 25 V, isoprenyl-phosphates generate two different fragment, F1 and F2, which are derived from the single phosphate group of phytyl-P and GG-P, and from the outer phosphate group of phytyl-PP and GG-PP.

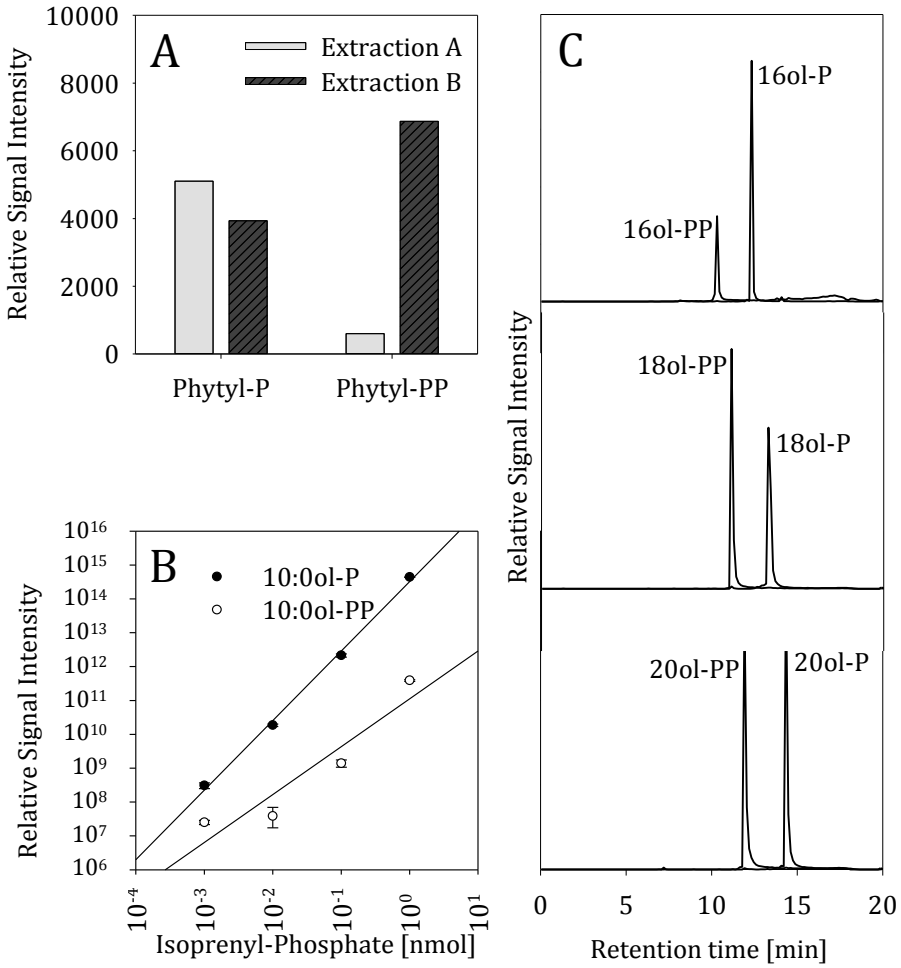

Figure 14 Optimization of Isoprenyl-Phosphate Measurements Using Q-TOF MS/MS.

(A) Extraction efficiency of isoprenyl-phosphates: synthetic standards for phytyl-P and phytyl-PP were used to determine the extraction efficiency of these compounds with different polar solvents. Extraction A: lower phase of isopropanol/hexane/H_20 (Markham *et al.*, 2006); Extraction B: Isopropanol/50 mM KH_2PO_4 pH 7.2/acetic acid (Larson *et al.*, 2001). (B) Standard curve for isoprenyl-phosphate quantification (double logarithmic plot): the signal intensity of the internal standards 10:0ol-P and 10:0ol-PP was determined at different amounts injected: 1, 0.1, 0.01 and 0.001 nmol. Afterwards, a regression line and R^2 were calculated from the data using SigmaPlot12.5. The R^2 were 1 for 10:0ol-P and 0.99 for 10:0-PP. Data represent the mean and SD of 3 replicates. (C) Separation of synthetic alcohol-phosphates of different chain lengths (16:0ol, 18:0ol, 20:0ol) using Nucleodur C8 Gravity column (Macherey & Nagel) with 5 mM ammonium acetate and acetonitrile. The alcohol phosphates were measured in negative ionization mode and the depicted peaks were generated by scanning for mass transitions of the molecular ions (m/z shown in Table 17) to the precursor ion $[HPO_3]^-$ m/z 78.9591.

A standard curve was generated using dilutions of 10:0ol-P and 10:0ol-PP (1, 0.1, 0.01 and 0.001 nmol each) (Figure 14B). A regression line shows that the linear range of 10:0ol-P is wide (R^2 = 0.99), while that of 10:0ol-PP is narrower (R^2 = 0.88). Therefore, the optimal amount of internal standard added to the sample for quantification was 0.1 nmol.

Different chromatographic conditions were tested based on the previously published protocols. Optimal separation was obtained using a Nucleodur C8 Gravity column (Macherey & Nagel) and a

gradient of solvent A, 5 mM ammonium acetate and solvent B, acetonitrile. Using this separation program, isoprenyl-phosphates could be separated based on the chain length of the alcohol moiety and the degree of phosphorylation (Figure 14C). Thus, isoprenyl-phosphates can nicely be separated, identified and quantified in extracts from *Arabidopsis* seeds and leaves. The chromatographic separation is presented in Figure 45 (Appendix).

Using this method, levels of C20-isoprenyl-phosphates in seeds and leaves from *Arabidopsis* WT were determined (Figure 15). In both seeds and leaves, phytyl-PP is the most abundant isoprenyl-phosphate. The amount of phytyl-PP is much higher in seeds than in leaves (250 and 40 nmol g FW^{-1}), respectively. GG-PP accounts for 40 nmol g FW^{-1} in seeds and 10 nmol g FW^{-1} in leaves. Monophosphates are much less abundant in the two tissues. Phytyl-P levels are 5 and 0.25 nmol g FW^{-1} in seeds and leaves, respectively, and the amounts of GG-P are even lower (0.2 and 0.05 nmol g FW^{-1}).

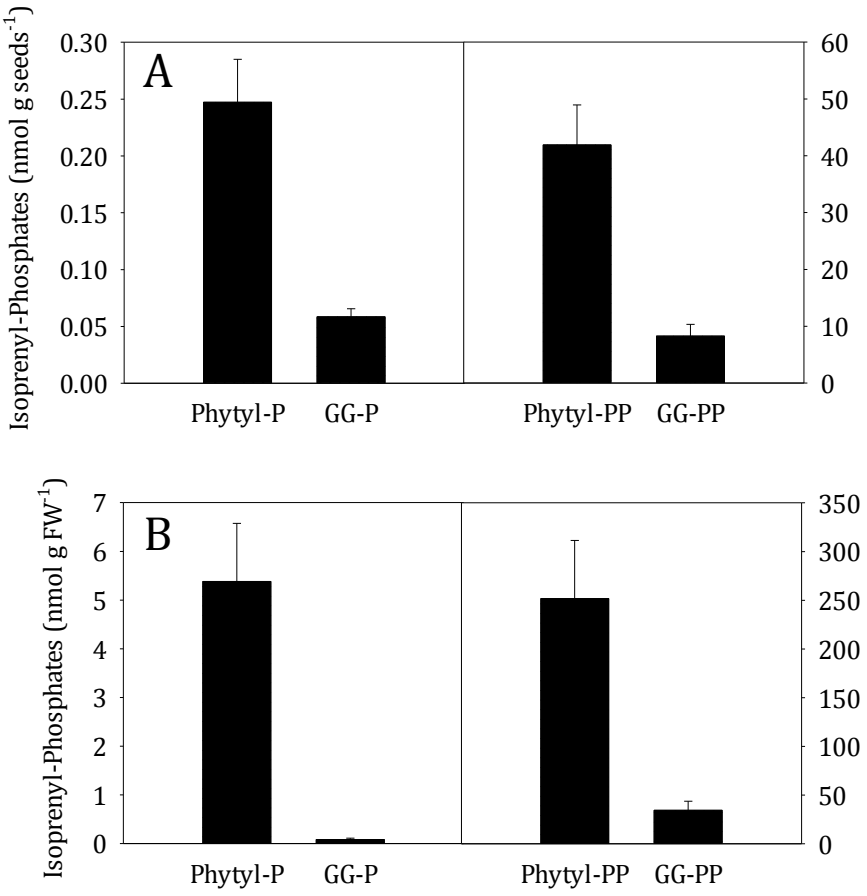

Figure 15 C20-Isoprenyl-Phosphates in *Arabidopsis* Seeds and Leaves.

Phytyl-P, GG-P, phytyl-PP and GG-PP were analysed in polar extracts from *Arabidopsis* (A) WT leaves and (B) seeds using LC-Q-TOF MS/MS as described. In seeds the total amount of isoprenyl-phosphates is much higher than in leaves. The phytylated isoprenyl-monophosphates and isoprenyl-diphosphates are considerably more abundant than the geranylgeranylated forms. Data represent the mean and SD of 4-5 replicates.

3.2 Metabolism of Phytol Released from Chlorophyll Degradation

3.2.1 Phytyl Ester and Tocopherol Accumulation in Leaves Depends on Phytol Released from Chlorophyll Degradation

During chlorotic stress, for example during natural senescence, nitrogen deprivation or dark-induced senescence, large amounts of chlorophyll as well as thylakoid membrane lipids are degraded. Degradation products are converted into other metabolites or further degraded. A green leaf contains about 1 µmol g FW^{-1} of chlorophyll. Therefore, approximately the same amount of phytol is released when all chlorophyll is degraded. Ischebeck *et al.* (2006) described that in *Arabidopsis* leaves, free phytol can be incorporated into fatty acid phytyl esters, and after phosphorylation, into tocopherol and ultimately also into chlorophyll. Moreover, free phytol was proposed to be employed for the synthesis of tocopherol in seeds after phosphorylation (Valentin *et al.*, 2006). To test the *in vivo* relevance of these pathways, fatty acid phytyl esters, tocopherol and chlorophyll were determined in the leaves (Kanwischer, 2006; Lippold *et al.,* 2012; this work) and seeds (this work) of the stay-green mutant *pheophorbide a oxigenase* (*pao1*) (provided by Dr. Stefan Hörtensteiner, University of Zurich). Leaves were detached and exposed to darkness on wet filter paper for 5 days. During this time, chlorophyll was degraded while fatty acid phytyl esters and tocopherol accumulated in the WT leaves. In *pao1* leaves, chlorophyll levels were unchanged after 5 days of darkness. Interestingly, no accumulation of fatty acid phytyl esters and tocopherol could be observed in *pao1* leaves (Kanwischer, 2006). This lead to the conclusion that the phytol moieties of fatty acid phytyl esters and tocopherol are derived from chlorophyll degradation. In seeds of the *pao1* mutant, fatty acid phytyl ester and tocopherol levels are decreased by 57 and 43% (Figure 16). These results show that synthesis of fatty acid phytyl esters and tocopherol almost entirely depends on chlorophyll-derived phytol in the leaves, and that about half of the fatty acid phytyl esters and of tocopherol is produced from chlorophyll-derived phytol in the seeds.

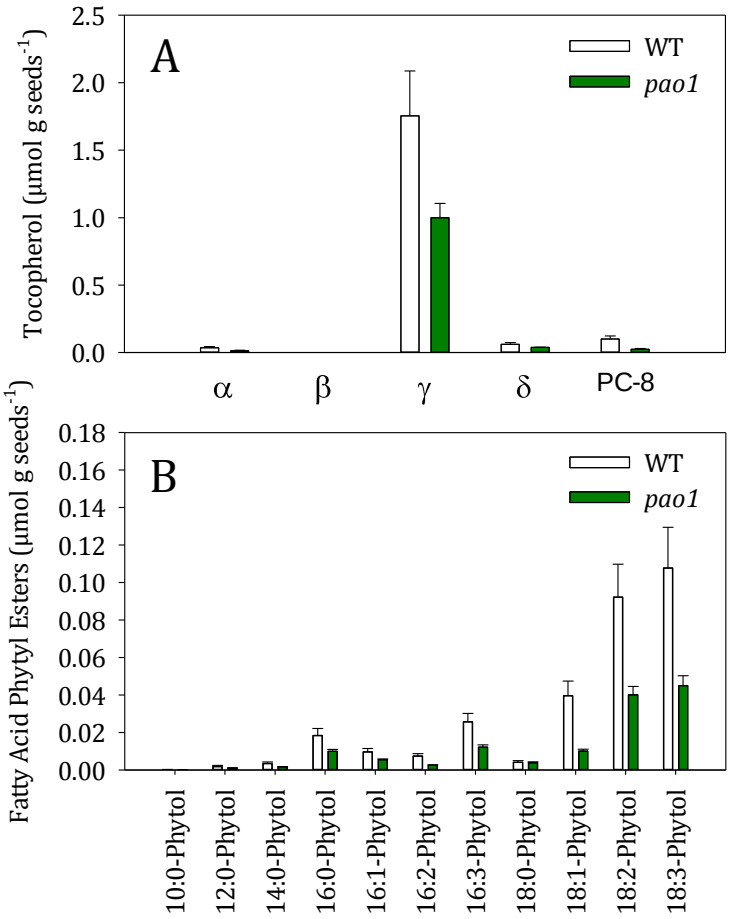

Figure 16 Phytyl Lipid Content in Seeds of the Stay-Green Mutant *pao1*.

(A) Tocopherol and (B) fatty acid phytyl esters were quantified in seeds of WT and *pao1* using HPLC-FLD and direct infusion Q-TOF MS/MS, respectively. Data represent the mean and SD of 3 replicates.

3.2.2 Reversibility of Fatty Acid Phytyl Ester and Tocopherol Synthesis during Stress

Plants can survive periods of unfavorable growth conditions by a variety of protective measures. Fatty acid phytyl esters and tocopherol play important roles in the protection of the plant during chlorotic stress. One important function is the removal of free phytol and free fatty acids from the thylakoid membranes, which have a detrimental effect on membrane stability. Tocopherols are especially important for plants during stress as they can detoxify ROS. To test whether fatty acid phytyl esters and tocopherols can be re-utilized for plant metabolism when conditions have improved, plants were first exposed to chlorotic stress (-N conditions) and then returned to normal growth conditions (+N), and chlorophyll, fatty acid phytyl esters and tocopherol were measured. Seeds were germinated on MS medium and the plants were grown on synthetic medium (+N) for 10 days. Afterwards, the plants were transferred onto nitrogen-depleted synthetic medium until the leaves were yellow (-N) (7-10 days). At this point, the plants were re-

transferred to nitrogen-repleted medium (-+N), where they were grown for 3 more days. Samples were taken before (+N), after nitrogen depletion (-N), and after returning the plants to full nitrogen medium (-+N). Chlorophyll was measured photometrically, fatty acid phytyl esters were quantified using direct infusion Q-TOF MS/MS and tocopherol was analyzed using HPLC-FLD. After 10 days of growth on –N medium, chlorophyll was reduced by 97%. Three days after transfer to +N medium, the leaves regained some green colour. The chlorophyll content was 50% of that under normal conditions. As expected, fatty acid phytyl ester and tocopherol levels increased under –N conditions. During nitrogen deprivation, the increase in fatty acid phytyl esters is mostly due to 16:3-phytol and, and the increase in tocopherols is due to α-tocopherol (data not shown). When the plants were returned to normal growth conditions (-+N), fatty acid phytyl ester and tocopherol contents decreased. While tocopherol levels were similar under +N and -+N conditions, fatty acid phytyl esters did not reach +N levels but remained at 60% of the –N levels.

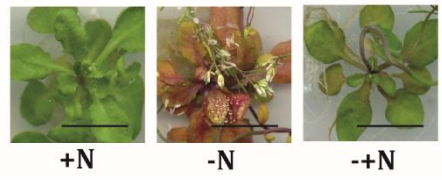

Figure 17 Growth of *Arabidopsis* During Nitrogen Deprivation.

Photos of plants on +N, -N and transfer back on nitrogen (-+N). *Arabidopsis* WT plants were grown on synthetic medium for 10 days (+N), transferred to nitrogen-deplete medium (-N) for 7-10 days until the leaves were devoid of chlorophyll and afterwards transferred to medium with full nutrition for 3 more days until the leaves were green again (-+N). The black bars represent 1 cm.

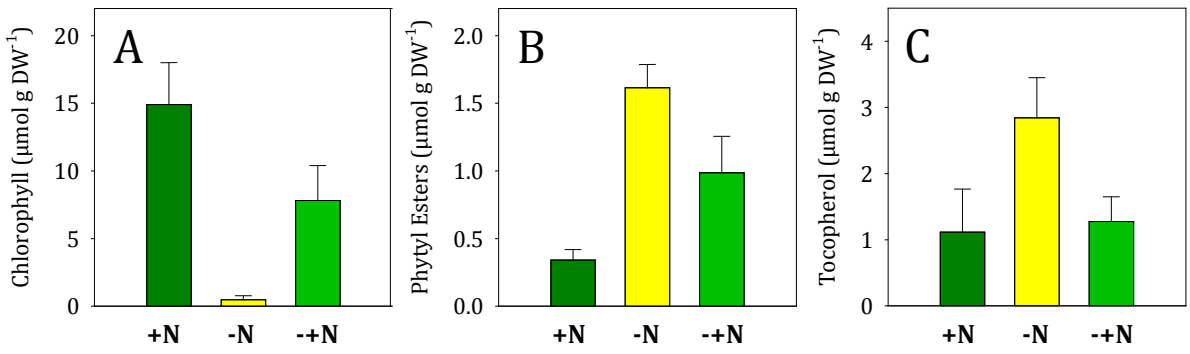

Figure 18 Phytyl Lipid Content and Composition After Nitrogen Deprivation.

(A) Chlorophyll, (B) fatty acid phytyl esters and (C) tocopherol in leaves of plants grown under +N, -N and -+N conditions. Data represent the mean and standard deviation of 4-5 replicates.

3.3 Characterization of *Arabidopsis* Phytyl Ester Synthases 1 and 2

The enzymes responsible for fatty acid phytyl ester synthesis, *Phytyl Ester Synthase 1 and 2* (*PES1* and *PES2*) belong to a family of esterases/lipases/thioesterases (ELT) with 6 genes in *Arabidopsis*, *ELT1* (=*PES1*), *ELT2* (=*PES2*), *ELT3*, *ELT4*, *ELT5* and *ELT6* (Lippold *et al.,* 2012).

3.3.1 *Arabidopsis pes1 pes2* Mutant

In agreement with results obtained by *in silico* analysis using Genevestigator (www.genevestigator.com), semiquantitative RT-PCR showed that the expression of *PES1* and *PES2* is strongly upregulated under nitrogen deprivation. The *pes1 pes2* mutant shows no residual expression of *PES1* and *PES2* under +N or –N conditions (Figure 19A). The *pes1 pes2* plants grow similarly as WT on synthetic medium with or without nitrogen. The plants are fully green on +N medium, and they show a chlorotic phenotype on -N medium.

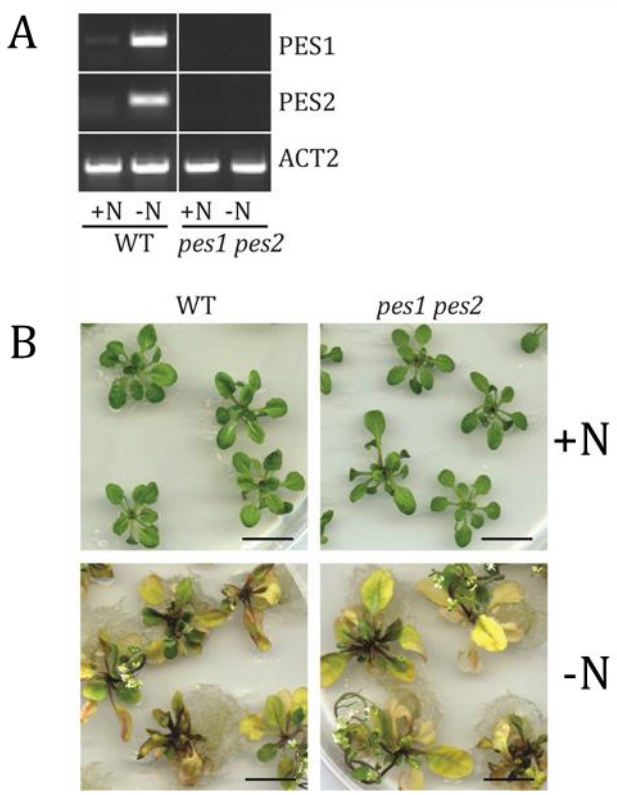

Figure 19 ***Arabidopsis pes1 pes2*** **Mutant.**

(A) Semi-quantitative RT-PCR showed that expression of *PES1* and *PES2* was up-regulated under nitrogen deprivation and not detectable in *pes1 pes2.* (B) WT and *pes1 pes2* grow normally on +N medium and suffer from chlorosis after transfer to –N medium.

Dark-induced senescence represents an alternative means for the stimulation of chlorotic stress. To this end, leaves of *Arabidopsis* WT and *pes1 pes2* grown under normal conditions on soil were detached from the plant and incubated on wet filter paper in darkness for 5 days. Chlorophyll

levels were determined spectrophotometrically to monitor the degradation of chlorophyll. After 5 days of darkness, WT leaves look pale yellow and the chlorophyll content is reduced to about 10%. This reduction in chlorophyll is less severe in leaves of *pes1 pes2*: after 5 days of darkness. The leaves are still slightly green and the chlorophyll content is about 50% of fresh *pes1pes2* leaves. Therefore chlorophyll degradation is affected in *pes1 pes2* during dark-induced senescence, but not during nitrogen deprivation (Figure 19).

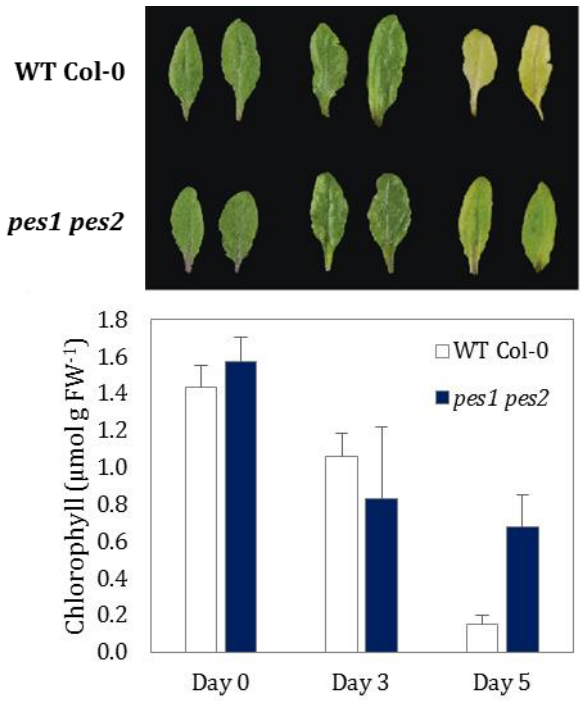

Figure 20 Chlorophyll Degradation After Dark-Induced Senescence in WT and *pes1 pes2*.

Detached leaves of WT and *pes1 pes2* were incubated on wet filter paper for 5 days. During that time, chlorophyll was degraded in WT and *pes1 pes2*, but in *pes1 pes2* chlorophyll levels remained at 50% of that in fresh *pes1 pes2* leaves, while WT leaves were nearly deplete of chlorophyll. Chlorophyll was determined photometrically. Data represent mean and standard deviation of 5 replicates. Two independent experiments were carried out.

3.3.2 Fatty Acid Phytyl Ester Synthesis in *pes1 pes2* After Feeding of Synthetic Phytol

Fatty acid phytyl ester synthesis in *pes1 pes2* in response to nitrogen starvation is strongly decreased (Lippold *et al*., 2012). To enhance the accumulation of fatty acid phytyl esters, WT and *pes1 pes2* plants were first grown on MS medium and then incubated in MES buffer containing 0.1% (v/v) phytol for 48 h. Fatty acid phytyl esters were measured in these plants using GC-MS as described by Ischebeck *et al.* (2006). In WT, phytol feeding results in five-fold increased levels of fatty acid phytyl esters compared to control conditions (WT –phytol). The molecular species composition of fatty acid phytyl esters differed from that measured in WT during nitrogen starvation: 12:0-phytol was the most abundant fatty acid phytyl ester. The other molecular species

were present in similar amounts. In *pes1 pes2*, fatty acid phytyl esters accumulated as well after feeding of synthetic phytol. However the total amount of fatty acid phytyl esters was less than 50% of WT levels. Fatty acid phytyl esters in *pes1 pes2* after phytyl feeding were exclusively 16:0-phytol and 18:1-phytol.

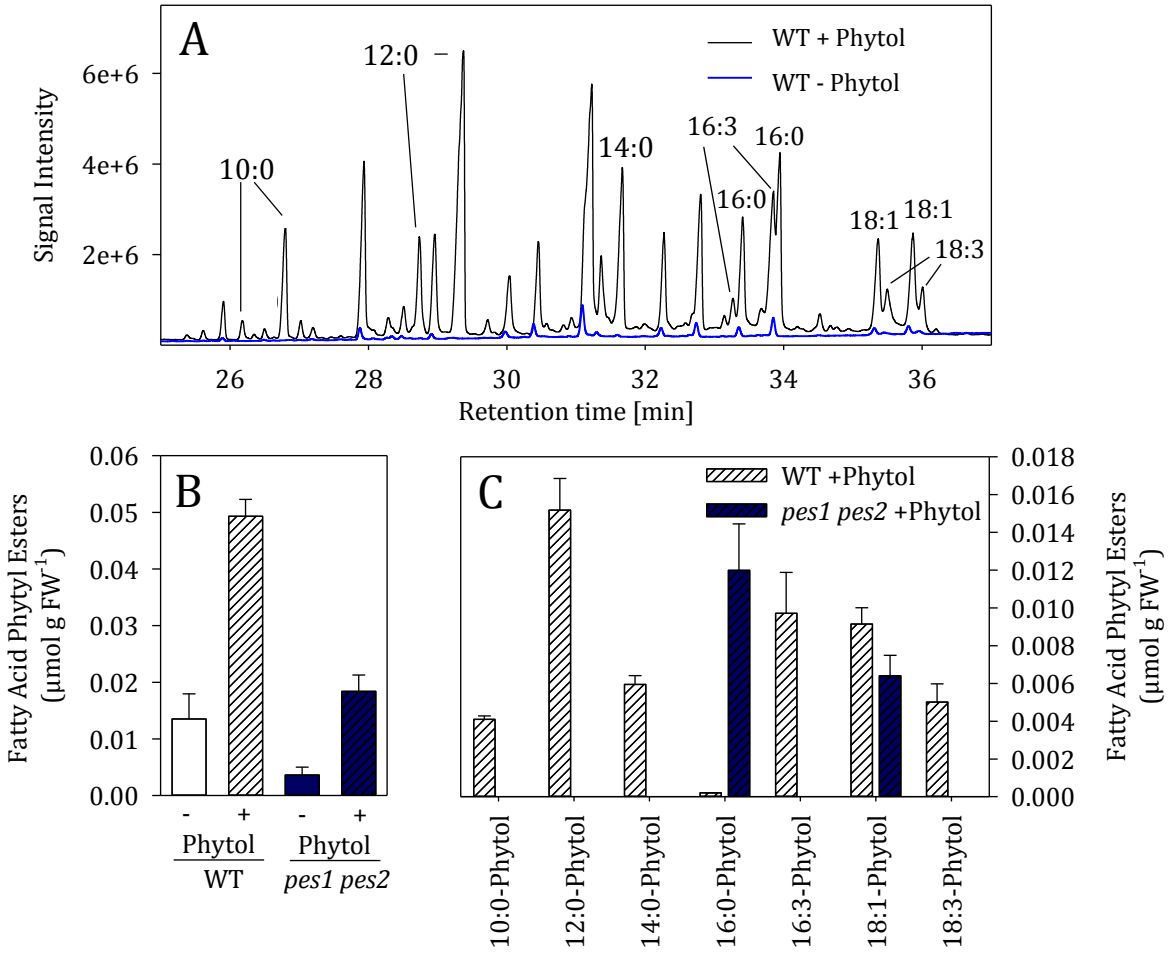

Figure 21 Fatty Acid Phytyl Esters Synthesis After Feeding of Phytol to WT and *pes1 pes2*.

WT and *pes1 pes2* were grown on MS medium for 2 weeks. Afterwards the seedlings were transferred to 20 mM MES buffer with and without 0.1% (v/v) phytol. The substrate was a mixture of the trans- and cis-isoform of phytol. Therefore, two peaks for each fatty acid phytyl ester containing either cis- or trans-phytol were detected. (A) GC-MS chromatogram of fatty acid phytyl esters in leaf extracts of WT and *pes1 pes2* after feeding of phytol. (B) Fatty acid phytyl ester content in WT and *pes1 pes2* with and without phytol feeding. (C) Fatty acid phytyl esters produced in WT and *pes1 pes2* with and without phytol feeding.

3.3.3 Fatty Acid Phytyl Esters Are Reduced in Plastoglobules of *pes1 pes2*

Fatty acid phytyl esters are stored mainly in the plastoglobules of plastids in plants (Gaude *et al.,* 2007). Small amounts of phytyl esters can also be detected in envelope and thylakoid fractions. This is likely due to fact that plastoglobules are closely connected to thylakoids and might also be attached to the envelopes (Austin *et al.,* 2006). In chlorotic leaves of the *pes1 pes2* mutant, the contents of fatty acid phytyl esters are decreased to below 20% of WT levels. Therefore, phytyl

ester content might as well be reduced in isolated plastoglobule fractions. Plastoglobules were isolated from chloroplasts of *Arabidopsis* WT and *pes1 pes2* leaves (2.3.3.2) by density gradient centrifugation and measured using direct infusion Q-TOF MS/MS. In isolated plastoglobule fractions of *pes1 pes2*, the decrease in phytyl esters was even more severe than in total leaf extracts: fatty acid phytyl esters were reduced by 97% compared to WT. The molecular species distribution of WT fatty acid phytyl esters was similar in leaves and plastoglobules, but it strongly differed between plastoglobules of WT and *pes1 pes2.* The remaining 3% of fatty acid phytyl esters in *pes1 pes2* plastoglobules contained mainly C18-fatty acids and were devoid of 16:3-phytol.

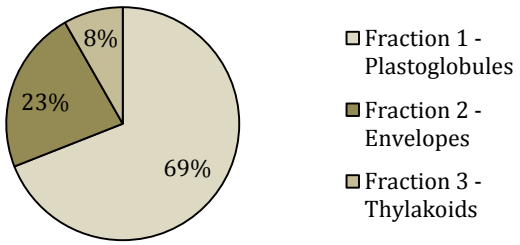

Figure 22 Distribution of Fatty Acid Phytyl Esters Between Chloroplast Membranes.

Chloroplasts were harvested from WT leaves (plants grown on soil) and their membranes fractionated as described in 2.3.3.2. Fatty acid phytyl esters were extracted from 0.5 ml of each fraction and measured using direct infusion Q-TOF MS/MS. The distribution of phytyl esters was calculated based on the volumes of the three membrane fractions after density gradient centrifugation.

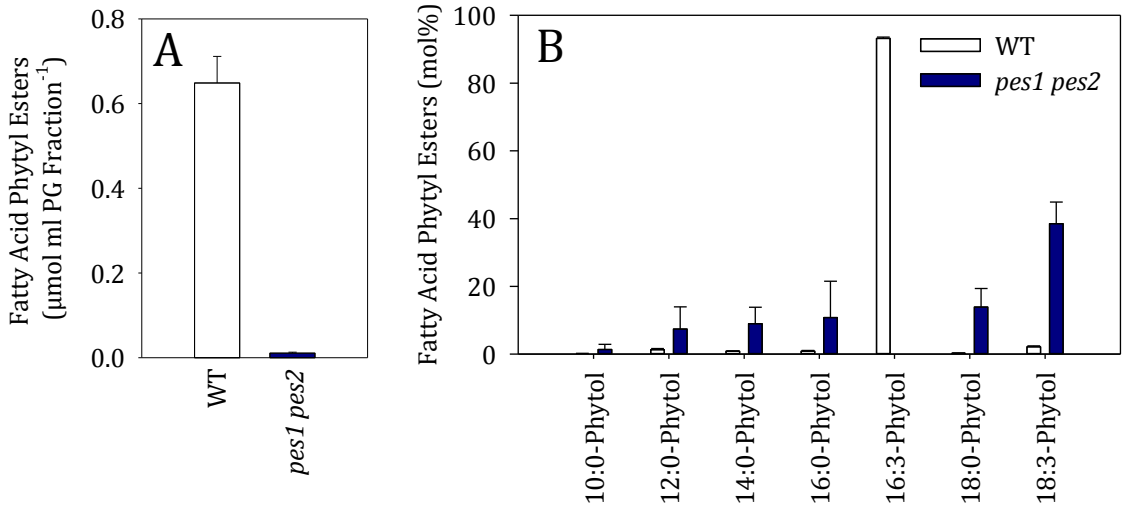

Figure 23 Fatty Acid Phytyl Ester Content in Plastoglobules of WT and *pes1 pes2*.

WT and *pes1 pes2* plants were grown on soil. Plastoglobules were isolated by density gradient centrifugation. Fatty acid phytyl esters were measured by direct infusion Q-TOF MS/MS. (A) Total amount of fatty acid phytyl esters in WT and *pes1 pes2* plastoglobules. PG, plastoglobules. (B) Molecular species distribution (mol%) of fatty acid phytyl esters in WT and *pes1 pes2* plastoglobules. Data represent the mean and SD of 3 replicates.

3.3.4 Lipid Biosynthesis in *pes1 pes2* During Nitrogen Deprivation

In plants, TAG is mainly found in seeds, providing carbon and energy for seed germination and seedling development. TAG is also present in minute amounts in green leaves. TAG accumulates in chlorotic leaves and is stored in the oil bodies in the cytosol and in the plastoglobules that strongly increase in size (Figure 4) (Steinmüller and Tevini, 1985; Tevini and Steinmüller, 1985; Gaude *et al.,* 2007). Expression of *PES1* and *PES2* is upregulated under nitrogen starvation and the two proteins localize to plastoglobules (Lippold *et al.*, 2012), pointing towards a possible involvement of PES1 and PES2 in plastidic phytyl ester and TAG accumulation. To address the question whether PES1 and PES2 are involved in chloroplastidic TAG synthesis, *Arabidopsis* WT and *pes1 pes2* plants were grown on MS medium for 2 weeks and then transferred to +N or –N medium, where they were grown for another 10-14 days. Rosette leaves were harvested and TAG was purified and quantified by direct infusion Q-TOF MS/MS. The total TAG content in leaves of the *pes1 pes2* mutant plants grown without N was reduced by 30% (Figure 24). This suggests that a fraction of TAG accumulating during N-deprivation in leaves is produced by PES1 and PES2. All molecular species of TAG are reduced by a similar extent, indicating no chain-length specific effect.

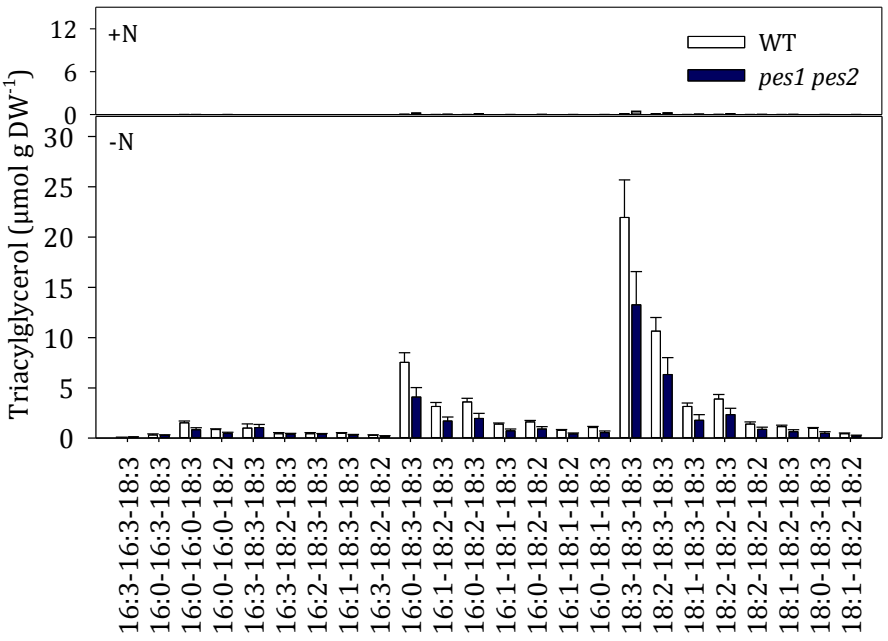

Figure 24 Molecular Species of TAG in WT and *pes1 pes2* During Nitrogen Deprivation.

Lipids were measured in leaves of plants grown in synthetic medium with and without nitrogen. TAG was measured using direct infusion Q-TOF MS/MS. Data represent the mean and SD of 4 replicates.

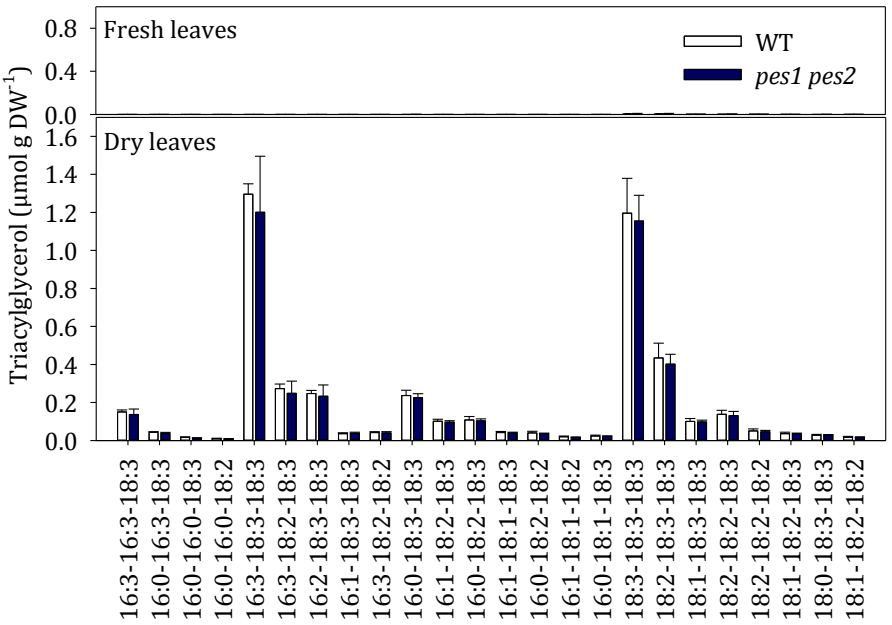

Figure 25 Molecular Species of TAG in WT and *pes1 pes2* During Drought Stress.

Lipids were measured in leaves from plants grown on soil. Fresh leaves were directly harvested from plants and frozen in liquid nitrogen for lipid extraction. Dry leaves were (after detachment from the plants) transferred to a petri dish and dried over-night under constant air stream. TAG was measured using direct infusion Q-TOF MS/MS. Data represent the mean and SD of 4 replicates.

In TAG harvested from leaves under –N conditions, 16:3-containing molecular species are hardly detected, but 16:0-18:3-18:3 is the most abundant molecular 16:0-containing species. Other stress conditions trigger an accumulation of 16:3-containing TAGs, for example freezing stress, drought stress and osmotic stress (Moellering and Benning, 2010).

To test if TAG accumulation is affected in *pes1 pes2* under conditions where 16:3 is enriched, WT and *pes1 pes2* plants were grown on soil and after 6 weeks leaves were detached from the plants and dried overnight under constant air flow. Afterwards TAGs were measured using direct infusion Q-TOF MS/MS (Figure 25). TAGs accumulated in the leaves after drought stress. 16:3-18:3-18:3 and 18:3-18:3-18:3 were the most abundant molecular species of TAG in contrast to -N stress, where16:0-18:3-18:3 and 18:3-18:3-18:3 accumulated. However, the level and the molecular species composition of TAGs in *pes1 pes2* during drought stress were unaltered.

The only other lipid which contains 16:3 under normal conditions in *Arabidopsis* is MGDG, which makes up over 50% of chloroplast lipids (Browse and Somerville, 1994). In green *Arabidopsis* leaves, MGDG contains about 30% 16:3, 60% 18:3 and small amounts of other fatty acids. Under –N conditions, MGDG is reduced by more than 90% (Figure 26B). MGDG degraded during growth of *Arabidopsis* on –N could serve as acyl donor for fatty acid phytyl ester synthesis.

As shown above (3.2.2), the transfer of WT plants to +N medium after nitrogen deprivation results in degradation of fatty acid phytyl esters and tocopherol. Therefore, phytol deposition in the form of phytyl esters and tocopherol is reversible. Fatty acid phytyl esters might be hydrolyzed to

provide phytol for the re-synthesis of chlorophyll and fatty acids for the re-synthesis of membrane glycerolipids when conditions have improved. To analyze this possible mechanism, WT and *pes1 pes2* plants were grown on +N and –N conditions and returned from –N to +N after several days (-+N) as described. Chlorophyll, fatty acid phytyl esters and membrane glycerolipids were measured in the leaves. As observed before, the chlorophyll content was completely re-established after returning WT plants to +N conditions, while the fatty acid phytyl esters increases and decreases again (Figure 26). In *pes1 pes2*, the chlorophyll content was lower after returning the plants to +N as compared to WT under the same conditions. This might at least in part be caused by the inability to store phytol in the form of fatty acid phytyl esters for the re-synthesis of chlorophyll in the *pes1 pes2* mutant (Figure 26B).

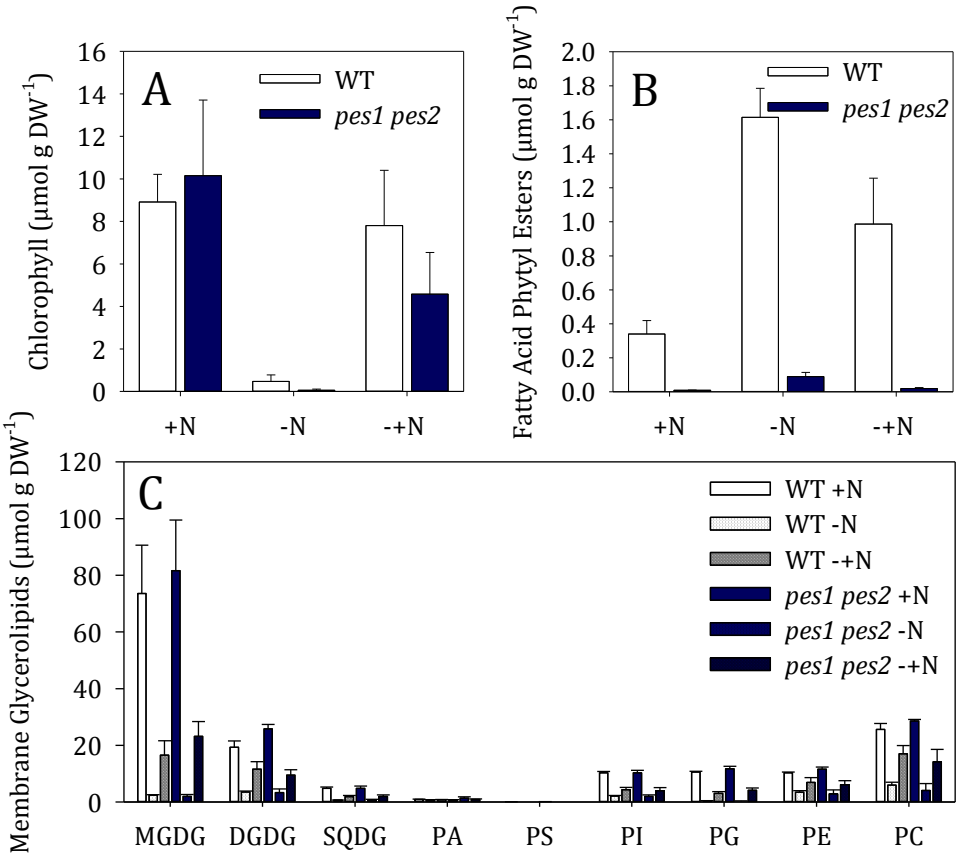

Figure 26 Membrane and Phytyl Lipids in WT and *pes1 pes2* in Nitrogen Deprivation.

Lipids were measured under normal conditions (+N), during nitrogen deprivation (-N) and after transfer back to +N conditions (-+N) on synthetic medium. (A) Chlorophyll content was determined photometrically. (B) Fatty acid phytyl esters were analysed using direct infusion Q-TOF MS/MS. (C) Phospholipids/galactolipids were measured using direct infusion Q-TOF MS/MS. Data represent the mean and SD of 4 replicates.

Membrane glycerolipids were degraded in WT leaves under –N conditions and resynthesized again after transfer back to +N (-+N). No difference could be observed between WT and *pes1 pes2* (Figure 26C). Presumably, only a minor fraction of glycerolipids were synthesized after re-transfer to +N conditions (-+N) with fatty acids released from fatty acid phytyl esters, because the amount of fatty acid phytyl esters is rather small compared to the amount of membrane glycerolipids.

3.3.5 Synthesis of Fatty Acid Phytyl Esters in *Chlamydomonas reinhardtii*

Chlamydomonas reinhardtii (*C. reinhardtii*) contains three predicted genes with sequence similarities to PES1 and PES2. However, the presence of fatty acid phytyl esters in *C. reinhardtii* was not shown before. When grown under nitrogen starvation, *C. reinhardtii* exhibits a similar phenotype as observed in plant chloroplasts: chlorophyll is degraded, i.e. the cultures turn from green to yellow, and at the same time large lipid droplets appear in the cells, which are packed with TAGs (Fan *et al.,* 2011; Merchant *et al.,* 2012). Two different *C. reinhardtii* strains (dw15 and cc124) were grown in +N medium before transfer to –N medium for 2 days (Zäuner *et al.,* 2012). Lipids were extracted and fatty acid phytyl esters were purified. Measurements by Q-TOF MS/MS revealed that the two strains of *C. reinhardtii* contain a variety of fatty acid phytyl esters when grown under +N and -N conditions. Moreover, there was a strong accumulation of fatty acid phytyl esters in the two strains of *C. reinhardtii* during N deprivation.

Under +N conditions, 18:3 represents the main fatty acid found in fatty acid phytyl esters in *C. reinhardtii*. Lower amounts of 18:0-phytol, 18:1-phytol and also 18:2-phytol were detected. 18:4-phytol (coniferonyl-phytol) is absent from plants, but present in small amounts in *C. reinhardtii.* The fatty acid composition of fatty acid phytyl esters is similar to that of TAG in *C. reinhardtii* dw15 grown under +N conditions (Zäuner *et al.*, 2012), but is distinct from the fatty acid phytyl ester composition in *Arabidopsis* leaves. Medium-chain fatty acids and C16 fatty acids are hardly detected in *C. reinhardtii*. In particular, 16:3 and 16:4 which are derived from the *C. reinhardtti* chloroplast are barely found in phytyl esters, in contrast to *Arabidopsis* which contains large amounts of 16:3-phytol. When transferred to –N conditions, the fatty acid phytyl ester composition changes: the most abundant fatty acid phytyl ester is 18:1-phytol, followed by 18:0-phytol, 18:2-phytol and 16:0-phytol. The relative amount of 18:3-phytol is decreased.

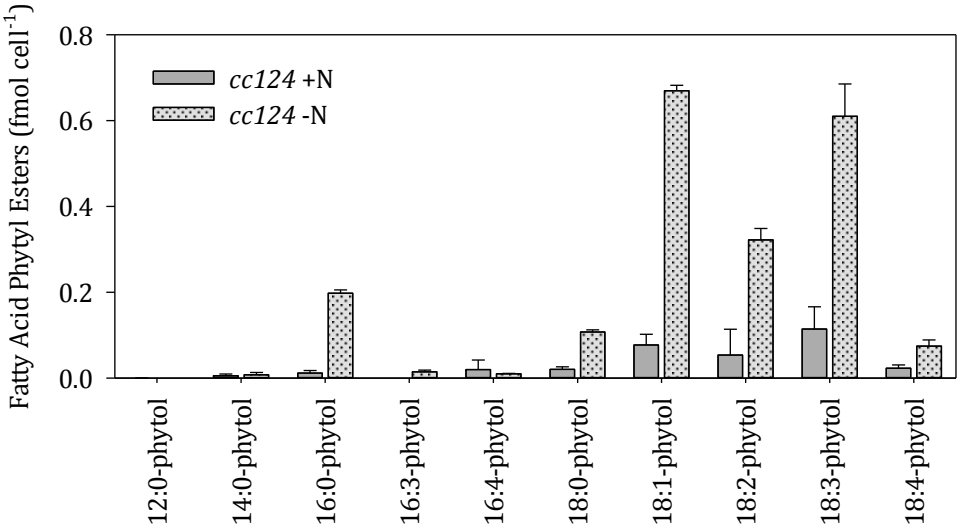

Figure 27 Fatty Acid Phytyl Esters During Nitrogen Deprivation in *C. reinhardtii*.

Fatty acid phytyl esters were measured in *C. reinhardtii* strain cc24 under normal conditions and after 2 days of nitrogen deprivation using direct infusion Q-TOF MS/MS. Data represent the mean and standard deviation of 4 replicates.

3.4 Characterization of the Putative Phytyl-Phosphate Kinase

The enzyme catalyzing the second phosphorylation step of the phytol phosphorylation pathway, the synthesis of phytyl-PP, was previously unknown. The *Arabidopsis* gene At1g78620, a member of the COG1836 sequence group, was identified as a candidate for phytyl-P kinase employing the SEED database. Orthologous sequences for this putative phytyl-P kinase can be found in plants (*Arabidopsis*, *Oryza sativa* (rice)), mosses (*P. patens*), algae (*Chlorella*, *Chlamydomonas*, *Bathycoccus*, *Selaginella*, *Chondrus*), photosynthetic bacteria (*Synechocystis*, *Synechococcus*, *Anabaena*, *Nostoc*), non-photosynthetic bacteria (*Symbiobacterium*, *Chlorobium*, *Pelodyction*) and archaea (*Archaeoglobus*, *Thermoplasma*) (Figure 28).

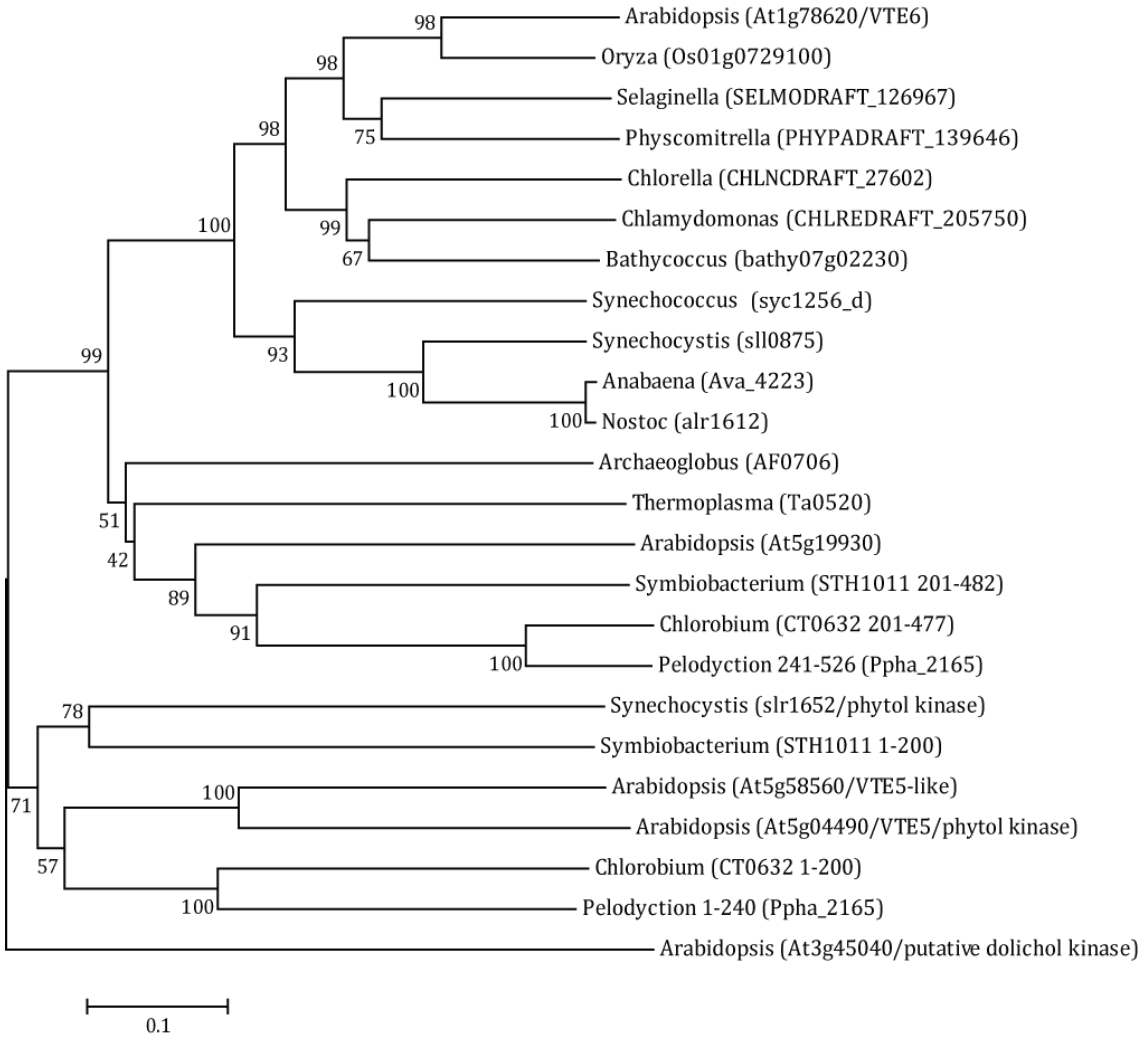

Figure 28 Phylogenetic Tree of Phytol Kinase and Putative Phytyl-P Kinase Sequences.

Phylogenetic analysis of phytol kinase and putative phytyl-P kinase (COG1836) sequences from plants and bacteria using MEGA6 (Felsenstein, 1985; Saitou and Nei, 1987; Nei and Kumar,; Tamura *et al.,* 2011). Protein sequences from *Arabidopsis*, *O. sativa*, *P. patens*, *S. moellendorfii*, *Chlorella*, *C. reinhardtii*, *Bathycoccus*, *Synechococcus*, *Synechocystis*, *Anabaena*, *Nostoc*, *Archeoglobus*, *Thermoplasma*, *Symbiobacterium*, *Chlorobium* and *Pelodyction* were obtained from GenBank. The phylogenetic analysis was done using the neighbour-joining-method and evolutionary distances were computed using the p-distance method (number of amino acid differences per site). Bootstrap values were calculated from 1000 replicates.

The amino acid sequence of At1g78620 is more similar to the homologous sequences in algae and cyanobacteria than to those in bacteria. The *Synechocystis* ORF *sll0875* shows high similarity with *Arabidopsis* At1g78620. An amino acid sequence alignment is shown in Figure 29 (Appendix). The *Arabidopsis* homolog At5g19930 also contains a domain of unknown function, DUF92, as all other COG1836 sequences. The phytol kinase sequences from *Arabidopsis* (*VTE5*, At5g04490) and cyanobacteria (*Synechocystis*, *slr1652*; *Symbiobacterium*, STH1011 1-200) reveal a low similarity with COG1836 sequences including At1g78620, Similarly, the sequence for the putative dolichol kinase (At3g45040), another putative long-chain isoprenyl-phosphate kinase, shows only low similarity with COG1836 sequences.

Two possible ORFs with different lenghts are predicted for the *Arabidopsis* gene At1g78620 from the TAIR database (www.*arabidopsis*.org), At1g78620.1 and At1g78620.2. The two ORFs differ by nine amino acids (27 bases) present in At1g78620.2 starting from amino acid 141, which are absent from At1g78620.1. The insertion is present at the end of a predicted exon (exon 3). Therefore, the two ORFs differ in the prediction of the position for one intron/exon splicing site. An expressed sequence tag cDNA clone was obtained from the RIKEN center and re-sequenced. It turned out that the cDNA sequence of this clone corresponds to At1g78620.1, the shorter version of the predicted ORF. In addition, the shorter ORF version of At1g78620 corresponds to the COG1836 sequence in Synechocystis, sll0875, which also lacks this insertion. Furthermore, semi-quantitative RT-PCR was done with first strand cDNA snythesized to RNA isolated from *Arabidopsis* WT leaves. For this RT-PCR experiment, a forward primer binding to exon 1 of At1g78620 and a reverse primer binding to the 27 bases (possible intron sequence) of the additional sequence in At1g78620.2 were used. However, it was not possible to amplify an RT-PCR product with this primer combination, suggesting that the extra 27 bases are absent from the cDNA sequence of At1g78620. As a control, the same cDNA was successfully employed to amplify a fragment of At1g78620 with the primers bn577 and bn578 that were used for expression analysis of At1g78620 shown in Figure 30B. Taken together, it can be concluded that At1g78620.1 represents the authentic ORF for the gene At1g78620.

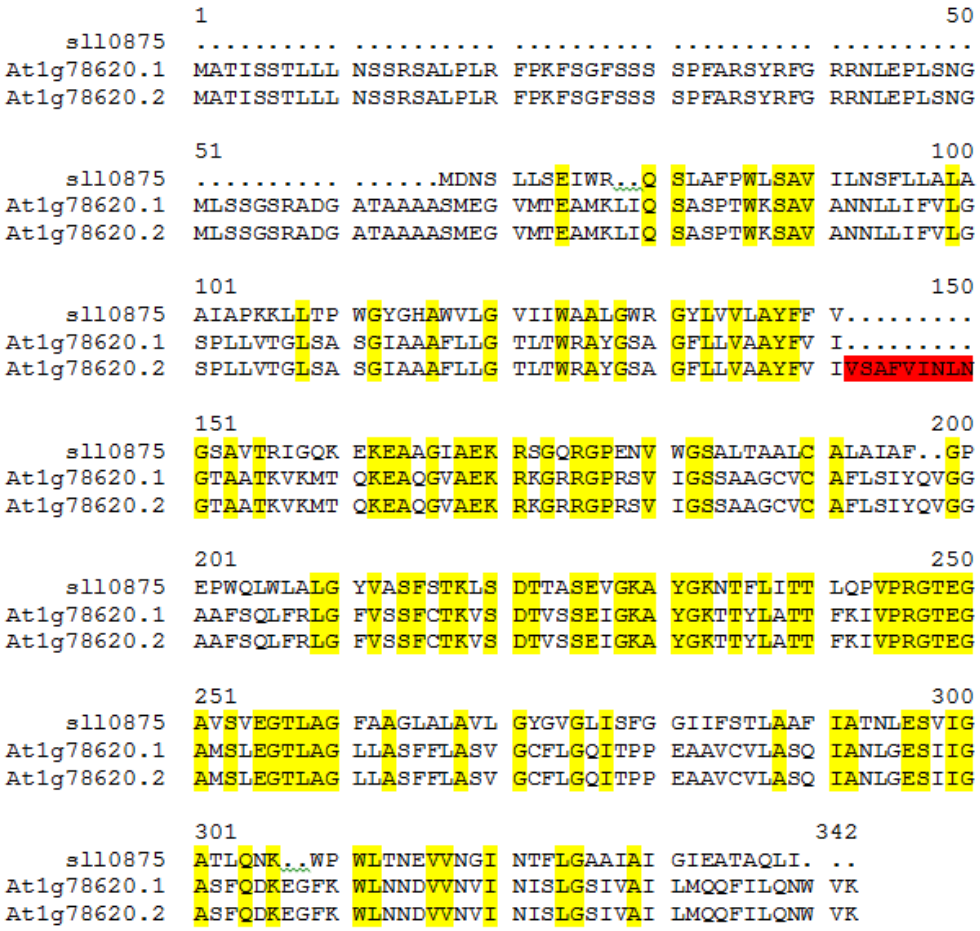

Figure 29 Alignment of *Arabidopsis* and *Synechocystis* COG1836 Sequences.

Amino acid sequences of *Arabidopsis* At1g78620 and *Synechocystis* sll0875 were aligned with the Multalin online tool (http://multalin.toulouse.inra.fr/multalin/) and the alignments were edited with Microsoft Office Word. Yellow letters indicate 100% sequence identity. Two ORFs for At1g78620 were predicted by TAIR (www.*arabidopsis*.org), At1g78620.1 and At1g78620.2 which differ in nine amino acids, indicated in red.

3.4.1 Growth of the *Arabidopsis* At1g78620 Mutant Is Strongly Retarded

To analyze the function of the putative phytyl-P kinase encoded by At1g78620, two insertional mutants were obtained from the RIKEN stock center, pst15134 and pst00121. These lines carry transposon insertions in the first exon of the At1g7862 gene. Seeds of a heterozygous plant were provided by the stock center. Homozygous mutant plants were identified by PCR screening. Interestingly, the homozygous mutant plants exhibited a severe growth phenotype when grown on MS sucrose medium: they were small, pale and bushy. They did not produce flowers and seeds and died shortly after transfer to soil. As a consequence, homozygous mutant plants were always grown from seeds of a heterozygous plant and identified using PCR analysis of genomic leaf DNA. To test whether the insertions in the first exon lead to null mutations of At1g78620, RNA was isolated from homozygous mutant plants and semi-quantitative RT-PCR was performed. Actin (ACT2) was used as control. No residual RT-PCR band was detected for the wild type copy of At1g78620 in the two homozygous mutant lines. Therefore pst15134 and pst00121 are likely null mutations. In a more sensitive approach, qPCR analysis also revealed no expression of At1g78620 in pst15134 (Figure 30B).

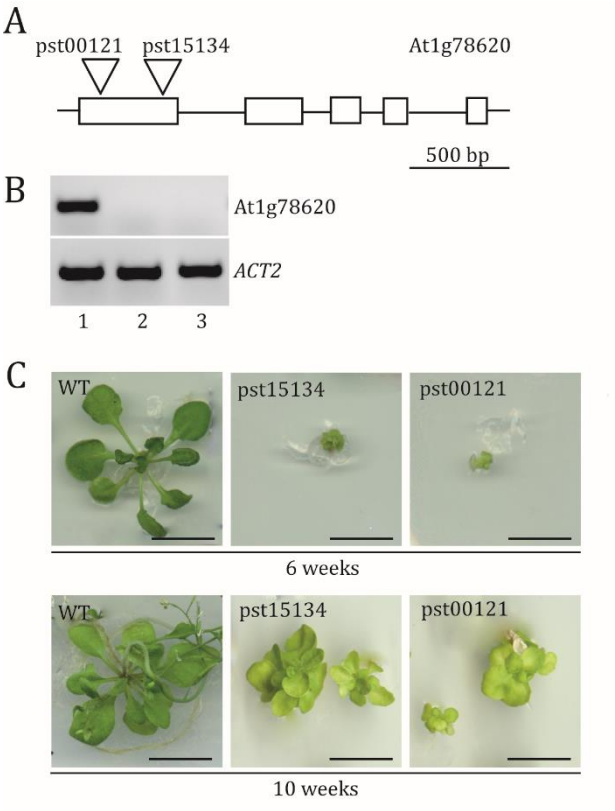

Figure 30 *Arabidopsis* Insertional Mutant Plants for At1g78620/VTE6.

(A) The gene locus At1g78620 from *Arabidopsis* showing the positions of insertions in the different mutant alleles. Exons are indicated by boxes. Bar = 500 bp. (B) Expression analysis (RT-PCR) of At1g78620 in 1, WT; 2, pst15134; 3, pst00121. Actin (*ACT2*) was used as control. (C) Growth of *Arabidopsis* insertional mutant plants for At1g78620. Plants of WT, pst15134 and pst00121 were grown on MS medium containing sucrose for 6 and 10 weeks. The mutant plants for At1g78620 were homozygous as shown by PCR. Bar = 1 cm.

3.4.2 At1g78620 Mutant Plants are Tocopherol-Deficient

Tocopherol levels were determined by fluorescence HPLC in leaves of WT and the insertion lines pst15134 and pst00121 grown on MS medium (Figure 31). In WT *Arabidopsis* leaves, the most abundant tocopherol form is α-tocopherol, and low amounts of β-, γ- and δ-tocopherol and PC-8 were detected. Interestingly, pst15134 and pst00121 reveal a strong decrease in tocopherol content, mostly due to the reduction of α-tocopherol by 98% (Figure 31). Because of the severe tocopherol decrease in leaves of the two insertion lines, they were named *vitamin E deficient 6* (*vte6-1*, pst15134; *vte6-2*, pst00121).

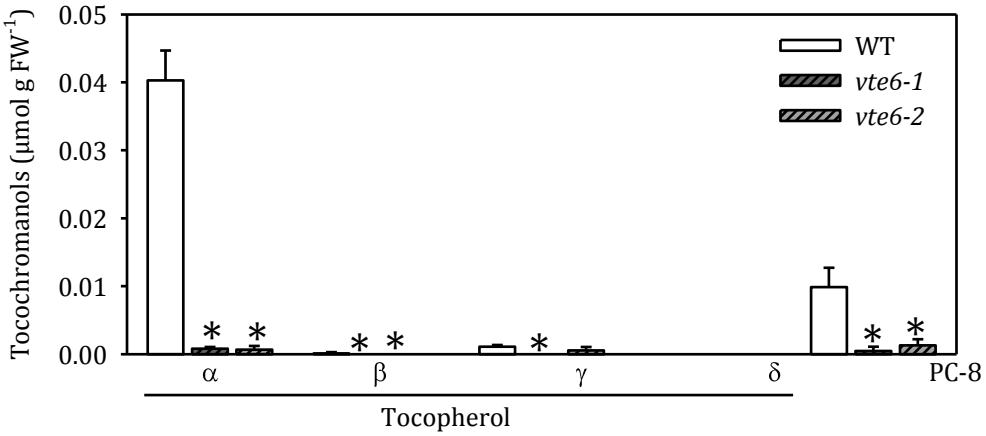

Figure 31 Tocopherol Contents in Leaves of WT and *vte6* Insertion Lines.

Tocopherol was measured using HPLC-FLD in leaves of *Arabidopsis* WT and *vte6* plants grown on MS medium. The genotypes of *vte6-1* and *vte6-2* were confirmed using PCR. The data represent mean and SD of 3-4 replicates. Asterisks indicate values significantly different to WT (* P<0.05) (Student's t-test).

3.4.3 *Vte6* Insertion Lines Show Reduced Seed Longevity

The *Arabidopsis* mutants *vte1* and *vte2* were previously characterized (Collakova and DellaPenna, 2001; Porfirova *et al.,* 2002; Kanwischer *et al.,* 2005). Seeds and leaves of *vte1* and *vte2* mutants are tocopherol-free. Their growth is comparable to WT, apart from a slightly delayed germination of *vte2* plants (Sattler *et al.,* 2004). In addition, seedlings of vte2 sporadically exhibit deformations of one of the two cotyledons. However, in particular *vte2* seeds exhibit a severe longevity phenotype. When exposed to accelerated ageing (high temperature, high humidity), the germination rate of *vte2* seeds is reduced by about 100% compared to WT (Sattler *et al.,* 2004). To observe whether tocopherol-deficiency results in a similar phenotype in the *vte6* mutants, the germination rate of seeds from a heterozygous vte6/*VTE6* plant was analyzed (Table 14) and the distribution of genotypes among the seedlings (WT, *vte6*/*VTE6*, *vte6*/*vte6*) was determined using PCR. To this end, freshly harvested seeds or seeds that had been stored for 6 months, from WT, heterozygous *vte6-1* and *vte6-2* plants, were sown on MS medium. Almost all fresh or stored WT

seeds germinated (96 and 89%). For freshly harvested seeds of heterozygous *vte6-1* plants, the germination rate was reduced to 76%. The germination rate of seeds from heterozygous *vte6-2* plants was similar to WT. In seeds that had been stored for 6 months, the two *vte6* insertion lines showed a reduced germination rate (76 and 67%). It is striking that the number of homozygous, germinating *vte6* plants derived from fresh seeds of a heterozygous *vte6/VTE6* plant, is low (about 11% as opposed to 25% according to Mendelian segregation). No homozygous *vte6-1 or vte6-2* plant germinated when *vte6-1/VTE6 or vte6-2/VTE6* seeds were stored. Therefore VTE6 plays an important role in seed longevity.

Table 14 Germination Rates of Seeds from WT, *vte6-1/VTE6* and *vte6-2/VTE6* Plants.

Seeds harvested from WT and heterozygous *vte6-1* and *vte6-2* plants were sown on MS medium (at least 250 seeds for each line) and the germination rate was determined. Fresh seeds were sown directly after harvesting and stored seeds were sown after storage for 6 months at 4°C in a dry environment. Data represent mean and SD of 5-6 biological replicates, one biological replicate is an MS plate with 50 seeds).

	Germination rate [%]	
	Fresh seeds	Stored seeds
WT Col-0	96±3	89±5
vte6-1/VTE6	76±6	76±7
vte6-2/VTE6	91±3	67±8

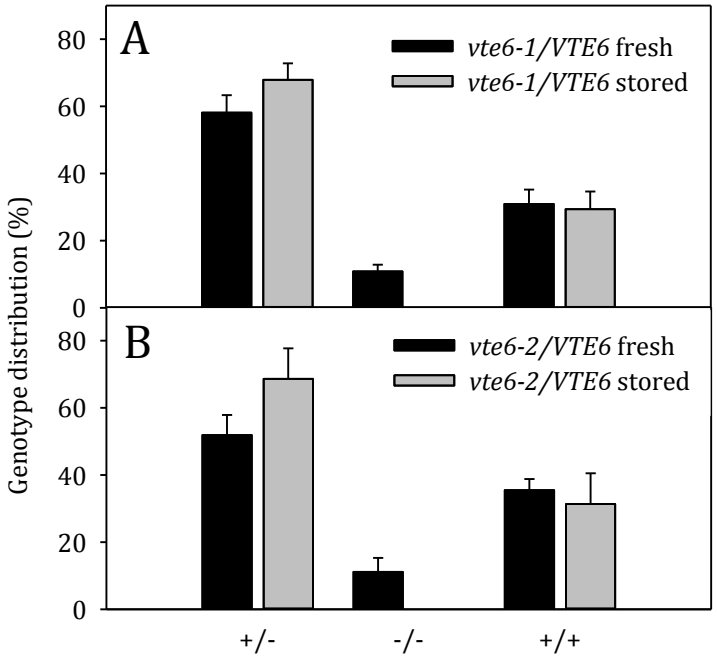

Figure 32 Genotype Distribution of of Plants Germinating from Seeds from Heterozygous *vte6-1/VTE6 or vte6-2/VTE6* Plants.

Seeds from a heterozygous *vte6-1/VTE6* or *vte6-2/VTE6* plant were grown on MS medium and the genotypes of the progeny were determined by PCR. (A) Genotype distribution of germinated seedlings from a *vte6-1/VTE6* plant. (B) Genotype distribution of germinated seedlings from a *vte6-2/VTE6* plant. 250 seeds for each *vte6-1/VTE6* and *vte6-2/VTE6* were tested (50 seeds per replicate) and the genotype distribution of germinated seedlings was determined for each replicate. Data represent the mean and SD of 6 replicates.

3.4.4 Phytyl-P Accumulates in *Arabidopsis vte6* Mutant Leaves

The severe growth retardation, developmental defects and chlorotic leaf color cannot be explained by the mere reduction in leaf tocopherol content, as growth and development of other tocopherol deficient mutants (*vte1*, *vte2*) is not affected. The deficiency in phytyl-P kinase activity in *vte6* mutant plants is expected to lead to a block of phytyl-P phosphorylation and as a result to an increased level of phytyl-P. Isoprenyl-phosphates were measured in leaves of WT and *vte6-1* mutant plants following the LC-MS method as described above (3.1.2). Leaves of *Arabidopsis* WT contain mostly phytyl-PP and GG-PP (45 and 8 nmol g FW^{-1}, respectively) and smaller amounts of phytyl-P and GG-P (0.25 and 0.08 nmol g FW^{-1}, respectively). Likely, phytyl-P levels are low because it is readily converted to phytyl-PP by VTE6. However, in leaves of *vte6-1,* the level of phytyl-P is increased about 5-fold, probably because it is not converted into phytyl-PP. In line with this scenario, the amount of phytyl-PP is reduced to 18 nmol g FW^{-1} in *vte6-1*. Additionally, GG-P is increased in *vte6-1*, maybe because *VTE6* can also accept GG-P as substrate as it is structurally similar to phytyl-P.

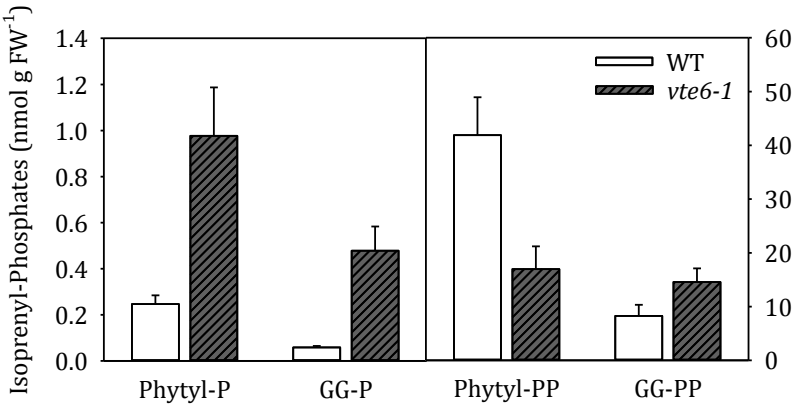

Figure 33 Isoprenyl-Phosphates in *Arabidopsis vte6-1*.

WT and *vte6-1* plants were grown on MS medium for 8 weeks. Phytyl-P, GG-P, phytyl-PP and GG-PP were quantified in leaves of these plants using LC-Q-TOF MS/MS by comparison with internal standards (3.1.2). Bars represent mean and SD of 4-5 replicates.

3.4.5 The Amounts of Phytol and Fatty Acid Phytyl Esters are Altered in *vte6*

The tocopherol content is strongly reduced in leaves of homozyogous *vte6-1* and *vte6-2* plants, presumably because of a decrease in phosphorylation of phytyl-P to phytyl-PP accompanied with reduced amounts of phytyl-P. Furthermore, the vte6 mutation might also lead to increased levels of phytol and fatty acid phytyl esters. Moreover, phytyl-PP and chlorophyllide are used for chlorophyll synthesis by ChlG. Thus the chlorophyll content might also be affected in *vte6*. Measurements of phytyl lipids revealed that the chlorophyll content in *vte6-1* leaves was reduced to nearly 50%, free phytol and fatty acid phytyl ester levels were increased by 6-fold and 3.5-fold

as compared to WT, respectively (Figure 34), in line with the presumed role of *VTE6* in phytyl-P phosphorylation.

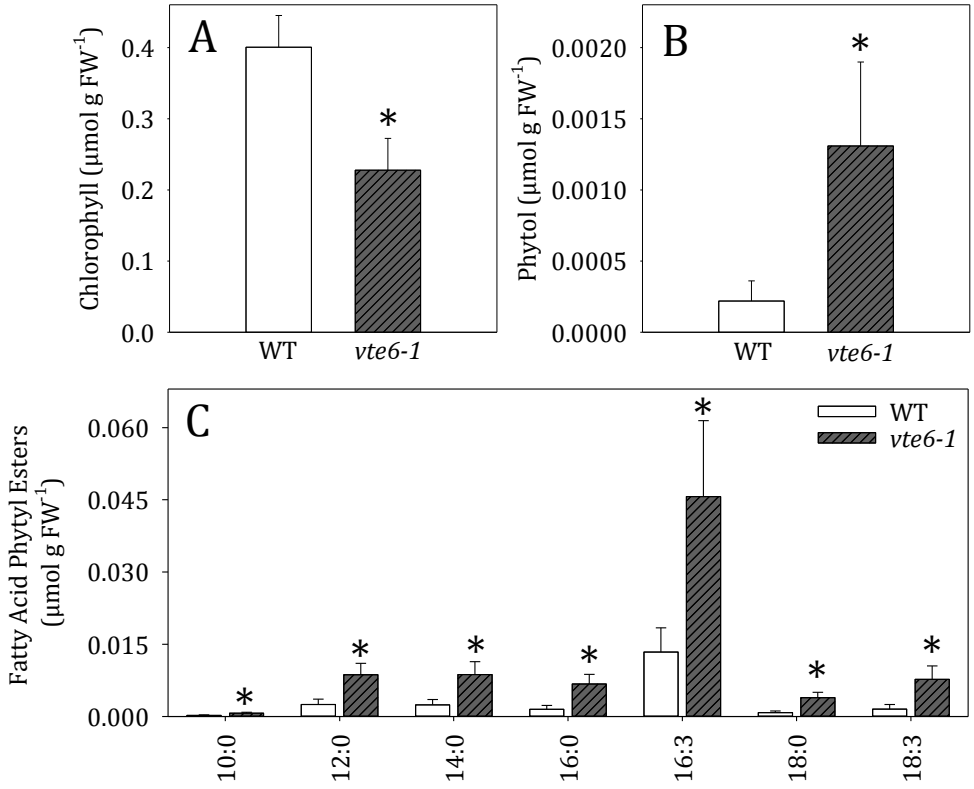

Figure 34 Phytyl Lipids in Leaves of WT and *vte6-1*.

Arabidopsis WT and *vte6-1* plants were germinated on MS medium and grown for 8 weeks. Homozygous *vte6-1* plants were identified by PCR. Leaves were harvested and phytyl-lipids were analysed. (A) Chlorophyll was measured photometrically. (B) Tocopherol was measured by fluorescence HPLC. (C) Phytol was quantified by GC-MS. (D) Fatty acid phytyl esters were measured by direct infusion Q-TOF MS/MS. The data show mean and SD of 4 measurements. Asterisks indicate significant differences to WT (* $P<0.05$) (Student's t-test).

3.4.6 VTE6 Exhibits Phytyl-P Kinase Activity in *Arabidopsis*

To test whether VTE6 encodes a functional phytyl-P kinase in *Arabidopsis*, seedlings of WT and *vte6-1* were grown on MS medium for 6 weeks and then incubated in 20 mM MES-KOH buffer in the presence of 0.1% (v/v) phytol or in 20 mM MES-KOH without phytol (control) for 48 h. Afterwards, the seedlings were washed to remove residual phytol from the leaves and isoprenyl-phosphates were isolated as described in 2.3.3.6. When WT seedlings were fed with excess phytol, levels of phytyl-PP increased about 3-fold compared to the control. In *vte6-1*, phytyl-PP levels were only slightly increased after feeding of phytol. In fact, the phytyl-PP levels in *vte6-1* were below 5% of WT phytyl-PP levels with and without feeding of synthetic phytol. Phytyl-P on the other hand accumulates in *vte6-1* compared to WT phytyl-P levels after phytol feeding. Therefore the insertional mutant *vte6-1* exhibits a block in the sequestration of phytol to phytyl-PP, which proves that VTE6 likely encodes a phytyl-P kinase in *Arabidopsis*.

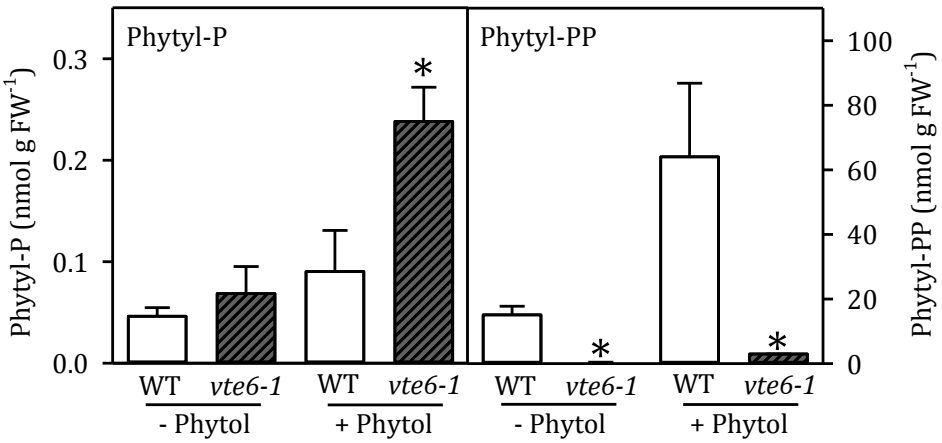

Figure 35 Synthesis of Isoprenyl-Phosphates in *vte6-1* After Feeding of Synthetic Phytol.

Seedlings of WT and *vte6-1* were grown in the presence (+phytol) or absence (control) of 0.1% (v/v) synthetic phytol for 48 h. Isoprenyl-phosphates were isolated from these seedlings and quantified by LC-MS/MS. Data represent the mean and SD of 3 replicates. Asterisks indicate significantly different to WT (* $P < 0.05$) (Student's t test).

3.4.7 The Amounts and Molecular Species Compositions of Membrane Glycerolipids are Unchanged in *Arabidopsis vte6-1* Plants

The tocopherol-deficient mutant *vte2* exhibits decreased membrane lipid desaturation under cold stress. After prolonged growth at 4°C, a shift from 18:2 to 18:3 was observed in PC of WT, but not in *vte2* (Maeda *et al*., 2008). To address the question whether membrane glycerolipid content or composition are altered in *vte6* as in *vte2*, phospholipids and galactolipids were measured in leaves of WT, *vte6-1* and *vte6-2* by direct infusion Q-TOF MS/MS.

Compared to WT, the relative amounts of the plastidial lipids MGDG and PG are reduced in the *vte6* mutants, in line with reduced chorophyll contents, pointing towards a reduced abundance of thylakoid membranes in these plants. In line with this result, the relative levels of PC are slightly increased (Figure 36A). Analysis of the molecular species composition of PC revealed that the desaturation of 18:3 is not affected in the *vte6* mutants. In contrast, the amount of 36:6-(18:3-18:3-)PC is even increased as compared to WT, indicating that the degree of 18:2 desaturation is increased, not decreased, in *vte6*.

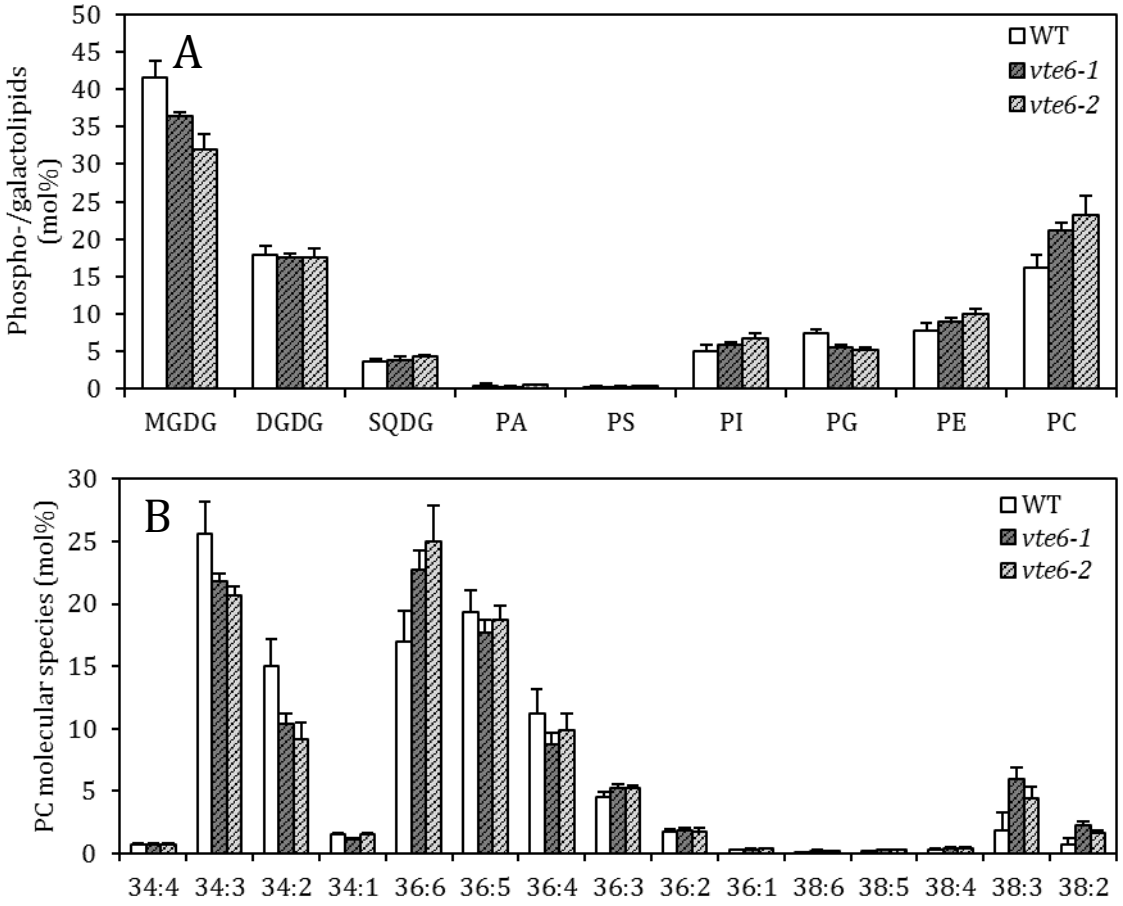

Figure 36 Phospholipids and Galactolipids in Leaves of WT and *vte6-1* and *vte6-2*.

(A) Phospholipids and galactolipids were quantified in leaves of WT, *vte6-1* and *vte6-2* using direct infusion Q-TOF MS/MS. Data are presented in mol%. (B) The molecular species composition of PC in mol%. Bars represent the means and SD of 4 measurements. Asterisks indicate significantly different to WT (* $P < 0.05$) (Student's t test).

3.4.8 The Growth Retardation of *vte6-1* is Partially Rescued in the *vte5-2 vte6-1* Double Mutant

The strong growth retardation of *vte6* plants cannot be explained by the reduced tocopherol content per se, as other tocopherol mutants (*vte1*, *vte2*) grow normally. As shown above, phytol and phytyl-P accumulate in the *vte6* mutant (Figure 33). To test whether the increased levels of phytol or phytyl-P contribute to the growth defect, a double mutant of phytol kinase (VTE5) and *VTE6* was generated by crossing a homozygous *vte5-2* mutant to a heterozygous *vte6-1* plant. Seeds of this cross were provided by Dr. Georg Hölzl, IMBIO, University of Bonn. The *vte5-2* (pst12490) mutant is a transposon insertion line obtained from the RIKEN seed stock center. The insertion lies within the first exon of At5g04490/*VTE5* (Figure 37A). The resulting *vte5-2* plants showed no residual expression of VTE5 mRNA as demonstrated by RT-PCR (Figure 37B). WT and *vte5-2* grew similarly, in line with previous results for *vte5-1* which also grows similarly to WT (Valentin *et al.*, 2006). After crossing, double homozygous plants were identified by PCR of genomic DNA from leaves of F2 plants, using the oligonucleotides described in Table 15.

Seeds from plants homozygous for *vte5-2* and heterozygous for *vte6-1* were germinated on MS sucrose medium. When transferred to soil these plants survived, unlike *vte6-1* and *vte6-2* plants, and developed further (Figure 37C). The double homozygous *vte5-2 vte6-1* plants were bushy and smaller than WT and *vte5-2* single mutant plants, but they grew better than *vte6-1*, which did not survive on soil (Figure 37C). The *vte5-2 vte6-1* plants were not chlorotic, similar to WT and *vte5-2*. Interestingly, the development of *vte5-2 vte6-1* was retarded. After 6 weeks, the plants were much smaller than WT, but they showed an extended life time. After 4 months, the WT and *vte5-2* plants had died, yet the *vte5-2 vte6-1* plants were still growing. They still exhibited the bushy phenotype as observed for the younger *vte5-2 vte6-1* plants. The leaf tips started to dry out, but senescence (i.e. chlorosis) could never be observed in *vte5-2 vte6-1*. Similar to the single mutants *vte6-1* and *vte6-2*, the *vte5-2 vte6-1* double mutant could not produce flowers and seeds.

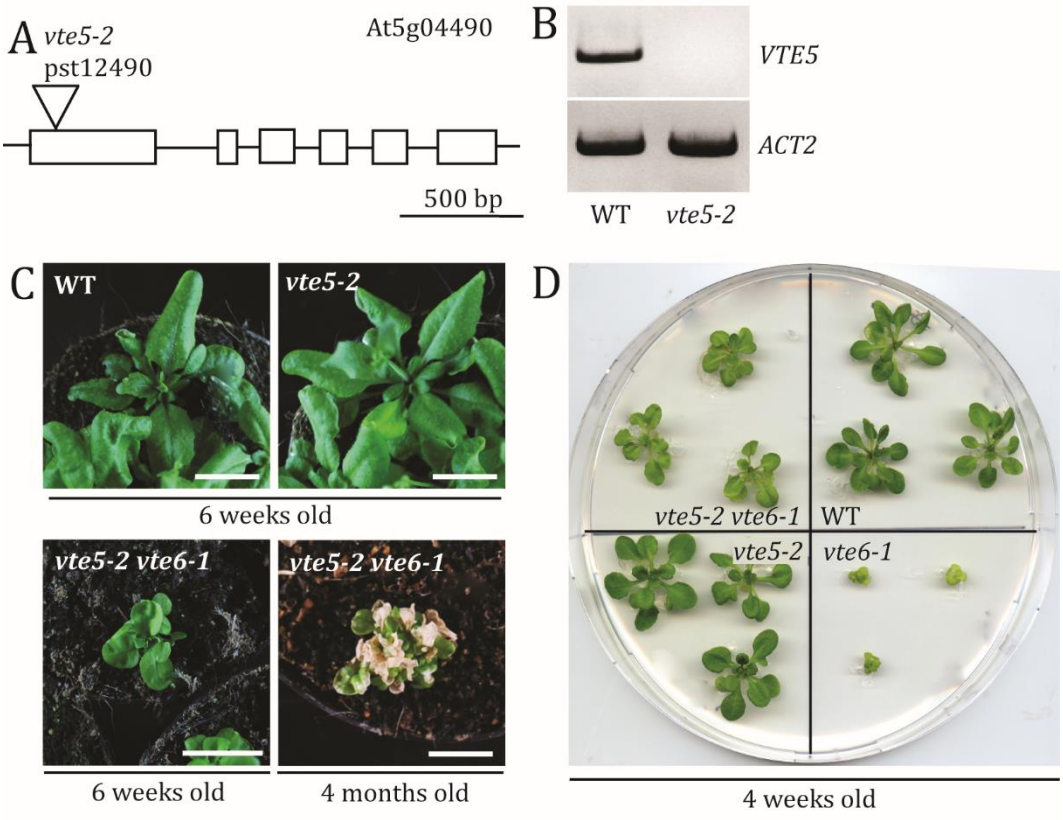

Figure 37 ***Arabidopsis vte5-2 vte6-1*** **Mutant.**

(A) Genome structure of At5g04490/*VTE5,* including the position of the transposon insertion in *vte5-2* (pst12490) (RIKEN stock center). (B) Semiquantitative RT-PCR of *VTE5* and *ACT2* using cDNA produced from RNA isolated from leaves of WT and *vte5-2* plants. (C) Plants of WT, *vte5-2* and *vte5-2 vte6-1* grown on soil for 6 weeks, and *vte5-2 vte6-1* plants grown for 4 months. (D) WT, *vte6-1*, *vte5-2* and *vte5-2 vte6-1* (clockwise) plants grown on MS sucrose medium for 4 weeks.

On MS sucrose medium (Figure 37D), the differences in growth and leaf color of *vte5-2 vte6-1* are even more striking. Growth of *vte5-2 vte6-1* is only slightly impaired and chlorophyll content is similar to WT and *vte5-2*, while *vte6-1* is much smaller and paler. Taken together, these observations show that blocking the initial phosphorylation step of the phytol phosphorylation pathway (phytol kinase reaction) by introducing the *vte5-2* mutation into the *vte6-1* background improves the growth and development as compared to the *vte6-1* single mutant.

3.4.9 The *Arabidopsis vte5-2 vte6-1* Double Mutant Is Tocopherol-Deficient

To determine whether the introduction of the *vte5-2* mutation into the *vte6-1* mutant background also affects the phytyl lipid content, tocopherol, chlorophyll, free phytol and fatty acid phytyl esters were quantified as described above (Figure 12). WT and *vte5-2* plants were used as controls. Plants were grown on MS medium for 6 weeks and *vte5-2 vte6-1* plants were identified by PCR. Changes in the tocopherol content were most striking. The tocopherol content of *vte5-2* leaves was reduced by ca. 50% compared to WT (0.05 and 0.1 µmol g FW^{-1}, respectively), yet in the *vte6-1* and *vte5-2 vte6-1* plants, tocopherol levels were below the detection limit (Figure 31). Therefore, the double mutant *vte5-2 vte6-1* revealed a more severe decrease in tocopherol content than *vte5-2*.

The chlorophyll content was, reduced by 90% in *vte6-1,* but only slightly lower in *vte5-2 vte6-1* while it was not changed in *vte5-2* as compared to WT. Phytol, however, was significantly increased in *vte6-1* compared to WT, but not in *vte5-2* and *vte5-2 vte6-1*. Fatty acid phytyl ester synthesis can serve as an alternative route for phytol metabolism if the phytol phosphorylation pathway is blocked. In line with this scenario, fatty acid phytyl ester levels were 2-3-fold higher in *vte5-2*, *vte6-1* and *vte5-2 vte6-1* (0.034, 0.051 and 0.045 µmol g FW^{-1}, respectively) compared to WT (0.018 µmol g FW^{-1}). The most drastic changes were observed for the fatty acid phytyl esters with 12:0-, 14:0- and 16:0-fatty acids.

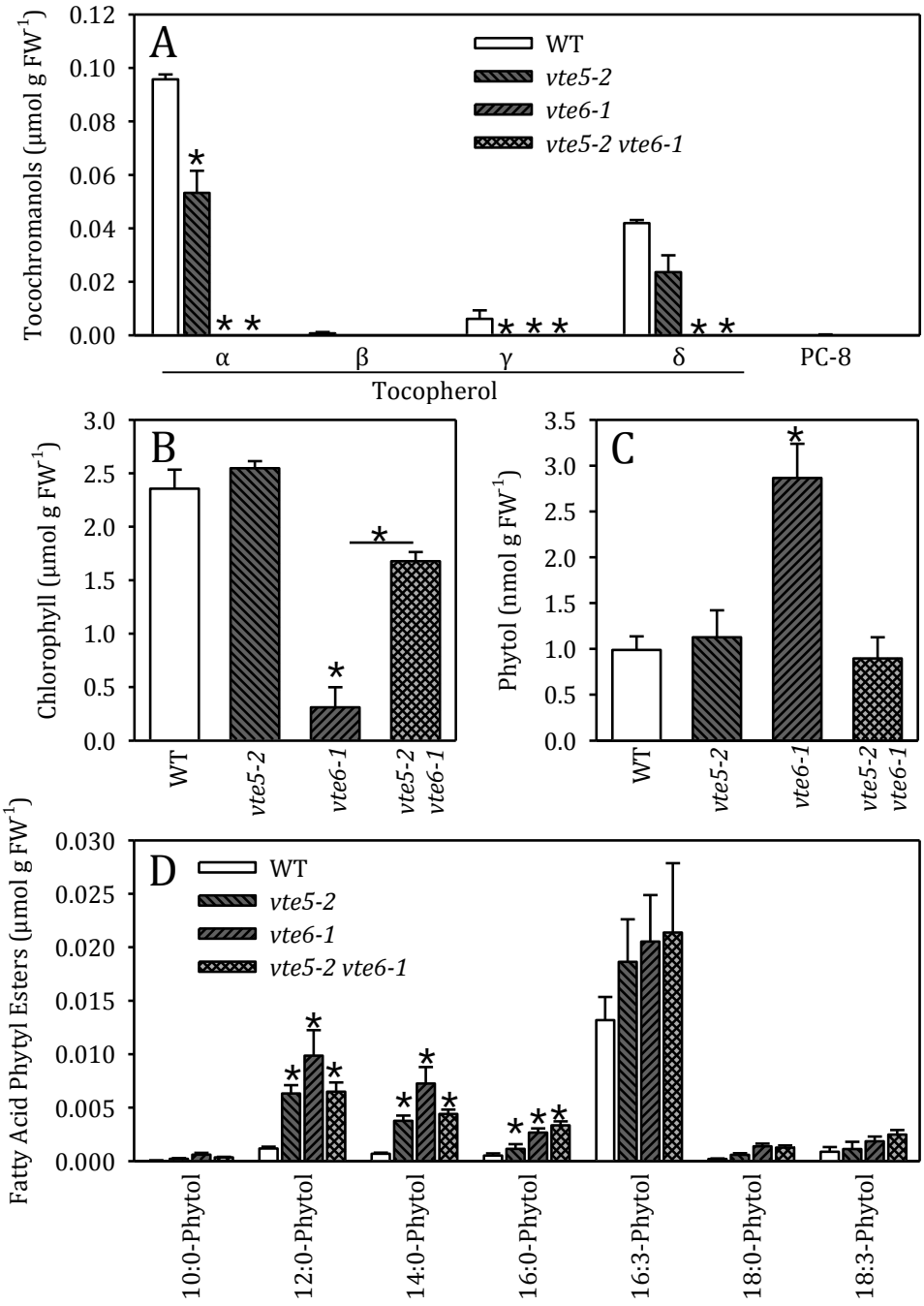

Figure 38 Phytol-Containing Lipids in Leaves of WT and *vte5-2 vte6-1*.

Plants (WT, *vte5-2* and *vte5-2 vte6-1*) were grown on MS medium containing sucrose for 6 weeks. Leaves were harvested and analyzed for phytyl lipids. (A) Tocopherol was measured by fluorescence HPLC. (B) Chlorophyll was measured photometrically. (C) The amount of free phytol was quantified by GC-MS. (D) Fatty acid phytyl esters were measured by Q-TOF MS/MS. The data show mean and SD of 4 measurements. Asterisks indicate values significantly different to WT (* $P<0.05$) (Student's t-test) or significantly different from *vte6-1* as indicated in (B).

3.4.10 Phytyl-P Does Not Accumulate in the *vte5-2 vte6-1* Double Mutant

As shown above, the severe growth retardation and decrease in chlorophyll content of *vte6-1* and *vte6-2* was partially rescued by crossing *vte6-1* to *vte5-2*. The accumulation of phytol or phytyl-P in leaves of *vte6* was considered as a possible reason for the growth retardation, because these metabolites could have an inhibitory or toxic function for plant metabolism. In *vte5-2 vte6-1*, the accumulation of the metabolites should be prevented because the phytol kinase that produces phytyl-P is absent. To test this scenario, isoprenyl-phosphates were measured in WT and *vte5-2 vte6-1* using LC-Q-TOF-MS/MS. Phytyl-P was not altered in *vte5-2* and *vte5-2 vte6-1* as compared to WT (0.08 nmol g FW^{-1} in *vte5-2*, 0.12 nmol g FW^{-1} in *vte5-2 vte6-1* and 0.1 nmol g FW^{-1} in WT). Phytyl-PP was reduced in *vte5-2*, *vte6-1* and *vte5-2 vte6-1.* Leaves contained 14 nmol phytyl-PP g FW^{-1} in WT, 5.5 nmol g FW^{-1} in *vte5-2*, 7.7 nmol g FW^{-1} in *vte6-1* and 5.7 nmol g FW^{-1} in *vte5-2 vte6-1*. GG-PP levels were unaffected, likely because GG-PP is mostly synthesized *de novo* from condensation of two geranyl-PP moieties.

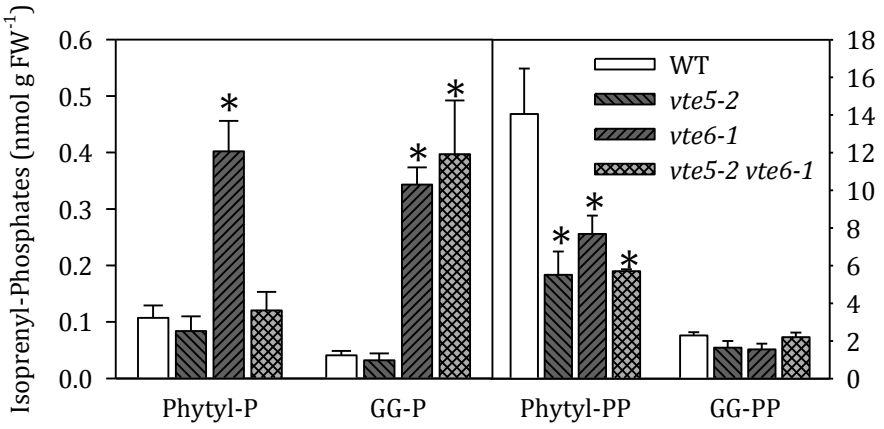

Figure 39 Isoprenyl-Phosphates in WT, *vte5-2*, *vte6-1* and *vte5-2 vte6-1*.

Isoprenyl-phosphates were measured using LC-Q-TOF-MS/MS in leaves of WT and *vte5-2 vte6-1* grown on MS medium for 6 weeks. Data represent the mean and SD of 4-5 replicates.

3.4.11 Overexpression of VTE6 Results in Accumulation of Phytyl-PP and Tocopherol in *Arabidopsis* Seeds

Phytyl-PP synthesized via the phytol phosphorylation pathway strongly contributes to tocopherol biosynthesis in leaves and seeds (Valentin et al., 2006) (this work). VTE6 was introduced under the control of the CaMV 35S promoter in *Arabidopsis* WT plants after floral dipping of plants with pL-35S-VTE6-DsRed. Trangenic seeds were selected based on fluorescence of the DsRed marker. Isoprenyl-phosphates were analyzed in transgenic seeds of empty vector (eV) and two overexpression lines, VTE6#3 and VTE6#4, by LC-MS/MS and tocochromanols were measured by fluorescence HPLC.

In the VTE6-overexpressing lines VTE6#3 and VTE6#4, phytyl-PP levels were significantly increased (509 and 514 nmol g seeds^{-1}) compared to the empty vector (eV) control (247 nmol g seeds^{-1}) (Figure 41A). The levels of phytyl-P and GG-PP were unaffected by overexpression of VTE6 (Figure 41A). Interestingly, the γ-tocopherol content was significantly increased in the VTE6-overexpression lines (1.5 and 1.6 µmol g seeds^{-1}) compared to the empty vector line (1.3 µmol g seeds^{-1}) (Figure 41B).

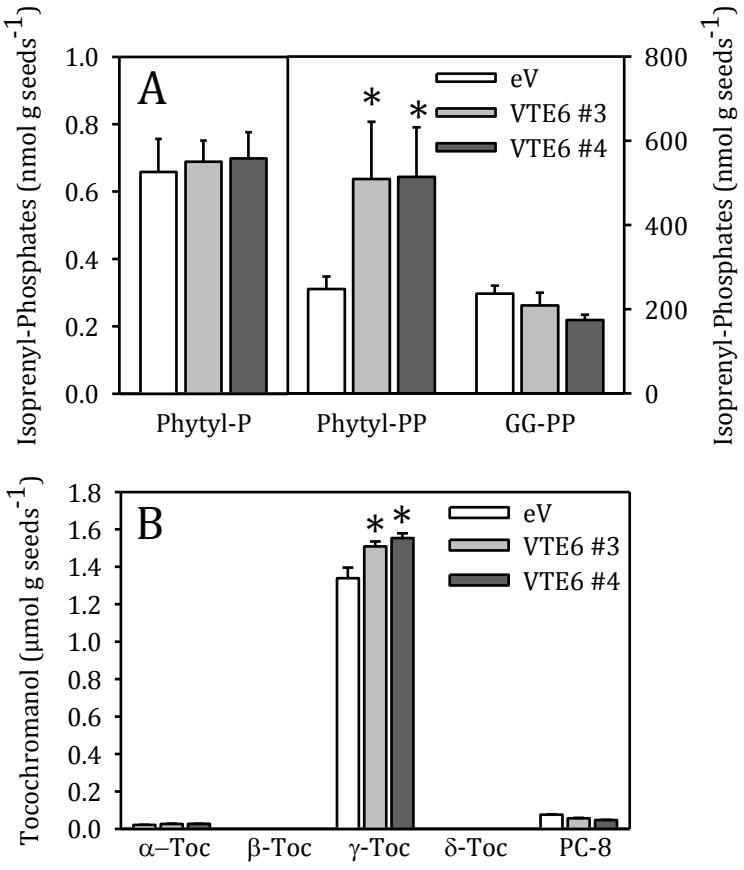

Figure 40 Isoprenyl-Phosphates and Tocopherol in Seeds of VTE6-Overexpression Lines.

Seeds of *Arabidopsis* WT plants, empty vector (eV) control and two lines overexpressing *VTE6* (VTE6#3 and VTE6#4) were harvested from plants simultaneously grown on soil. (A) Isoprenyl-phosphates were isolated from seeds and quantified by LC-MS/MS. (B) Tocochromanols were measured by fluorescence HPLC. Data show mean and SD of 3-4 measurements. *Significantly different to WT; $p < 0.05$; Student's t test.

3.4.12 Expression Analysis of Tocopherol- and Isoprenoid-Biosynthetic Genes in the *Arabidopsis vte6-1* Mutant via Quantitative PCR (qPCR)

After analyzing the phytol-containing metabolites in *Arabidopsis vte6-1* and *vte6-2*, *vte5-2* and *vte5-2 vte6-1*, several questions on the flux of chlorophyll-derived phytol remain unanswered. In all phytol phosphorylation mutants, phytyl-PP levels are reduced, yet phytyl-PP is not completely absent. However, tocopherol is hardly detectable in these plants. Therefore the remaining phytyl-PP presumably cannot be used for tocopherol synthesis. Expression levels of genes encoding enzymes for tocopherol biosynthesis (*VTE1*, *VTE2*/*HPT1*, *VTE3*, *VTE4, VTE5* and *VTE6*),

chlorophyll synthesis (*ChlG*) and isoprenyl-phosphate *de novo* synthesis (plastidial GG-PP synthase, *GGPS3,* and *GGR*) were determined in WT and *vte6-1* using qPCR. *ACT2* and *UBI* were used as housekeeping genes and the efficiency of all primer sets was evaluated. Synthetic oligonucleotides for qPCR were designed with Primer3 (Koressaar and Remm, 2007; Untergasser *et al.,* 2012) if not indicated otherwise (Table 15). Analysis by qPCR revealed that expression of *VTE6* in *vte6-1* was not detectable in agreement with the previous result that *vte6-1* represents a null mutant (Figure 41). Most of the tested genes were differentially expressed in *vte6-1*. The strongest down-regulation was measured for *VTE1*, which is hardly expressed in *vte6-1*. Expression of *VTE4*, *VTE5*, *ChlG*, *GGR* and *GGPS3* was also significantly reduced. Interestingly, expression of *VTE2* was similar to WT, and expression of *VTE3* was also only slightly reduced.

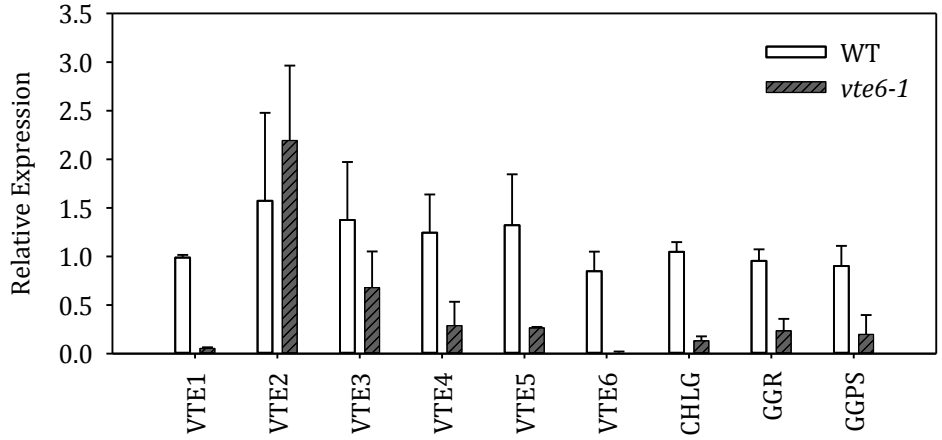

Figure 41 Expression Analysis of Genes of Isoprenoid, Chlorophyll and Tocopherol Biosynthesis in the *vte6-1* Mutant.

RNA was isolated from leaves of WT and *vte6-1* plants grown on MS medium and employed for qPCR measurements. Data represent the mean and SD of 3 biological replicates. The expression was calculated relative to the first WT replicate, which was set to the value 1.

3.4.13 Heterologous Expression of Protein Encoded By At1g78620

To determine whether the protein encoded by *VTE6* exhibits phytyl-P kinase activity, the coding sequence of At1g78620 was cloned into vectors for heterologous expression of the recombinant protein in *E. coli*, yeast and *N. benthamiana*.

For *E. coli* expression, the coding sequence of At1g78620 without the predicted transit peptide was amplified from a cDNA clone and ligated into different expression vectors, i.e. pQE-80L (Qiagen), pMal_C4x (New England Biolabs) and pET22b(+) (Novagen). Two versions of *VTE6* without transit peptide (woTP) were considered. The predicted length of the transit peptide is 65 amino acids when using the ChloroP 1.1 server, yet other prediction tools suggest a length of 47 amino acids. Therefore VTE6woTP47 and VTE6woTP65 were expressed in *E. coli*.

When protein expression in cells with pQE-80L or pMal_C4x constructs was induced with IPTG, cell division ceased, while cells harboring the empty vector continued to grow. This growth inhibition is often caused by toxic effects of the recombinant protein. To overcome this problem, the putative phytyl-P kinase was expressed in pET22b(+), which adds a leader sequence to the protein that translocates the protein to the periplasmic space. Thus, the toxic effect of the recombinant protein should be diminished. In fact, the putative phytyl-P kinase protein was detected after expression with pET22b(+) by western blot (Bachelor thesis Omnia El-Sayeed, 2013), but no phytyl-P kinase activity was measured in protein extracts (Figure 42A).

Furthermore, *S. cerevisiae* was used as eukaryotic expression system. Here, the coding sequence of At1g78620 without transit peptide (woTP65) was cloned into the expression vector pDR196 (Rentsch *et al.,* 1995). However, no enzyme activity was detected in protein extracts from yeast expressing At1g78620 (Figure 42B).

In addition, the coding sequence of At1g78620 including the predicted transit peptide was expressed in a modified pLH9000 vector with 35S promoter and DsRed marker (pL-nD1cM1-DsRed, Dr. Georg Hölzl, IMBIO, University of Bonn) in *N. benthamiana*. The recombinant protein harbors a C-terminal TAP-tag (CTAP) and therefore can be purified by tandem affinity chromatography. The phytyl-P kinase activity in crude protein extracts from *N. benthamiana* leaves expressing At1g78620was very high and indistinguishable form empty vector control, presumably because the activity of endogenous enzymes with phytyl-P kinase activity was too high. Atempts to enrich the recombinant kinase activity by TAP-tag affinity chromatography failed.

Enzyme assays were performed with protein extracts from *E. coli*, yeast and *N. benthamiana* as described in Ischebeck *et al.* (2006). Two experimental setups were used.

A non-radioactive assay was done with synthetic phytyl-P and nucleotide triphosphates (NTPs) (2.3.3.1). The reaction products were measured using LC-Q-TOF MS/MS as described above.

Furthermore, a radioactive assay was performed with synthetic phytyl-P and γ-^{32}P-CTP (2.3.3.1). The reaction products were separated on a TLC plate and analyzed using a phosphorimager. In none of the two assay systems, the conversion of phytyl-P to phytyl-PP could be detected after expression of *VTE6* in *E. coli* (pET-VTE6-woTP construct), yeast (pDR-VTE6-woTP construct) or *N. benthamiana* (pL-VTE6-CTAP).

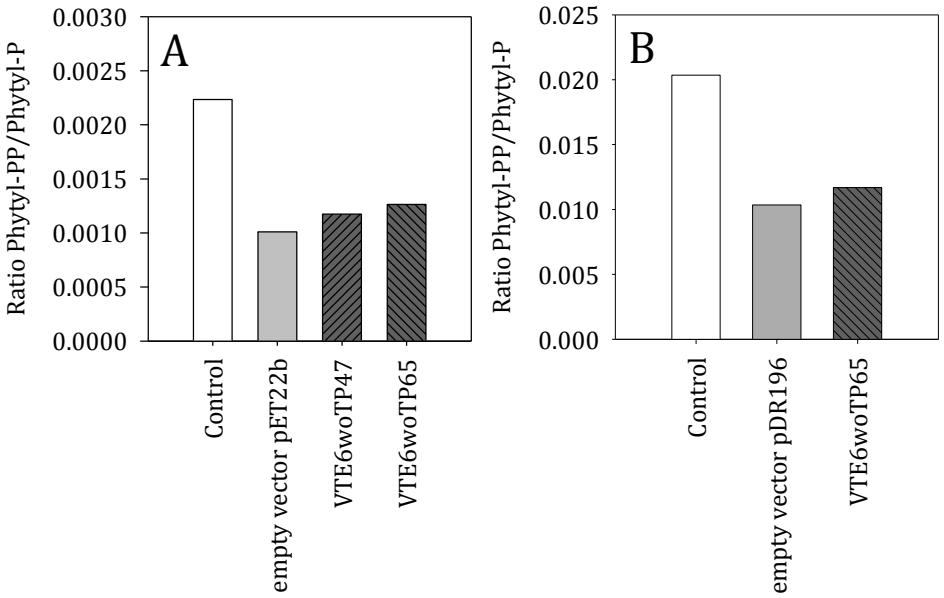

Figure 42 Non-Radioactive Phytyl-P-Kinase Assay With Recombinant Protein From *E. coli* and Yeast.

Protein extracts from *E. coli* and yeast were incubated with phytyl-P and NTPs as described in 2.3.3.1. A control was performed without the addition of a protein extract to the reaction mixture. After 30 min, the reaction was stopped and isoprenyl-phosphates were isolated from the reaction mixture. Isoprenyl-phosphates were analysed by LC-MS. The ratio of phytyl-PP versus phytyl-P was calculated and plotted for *E. coli* (A) and yeast (B).

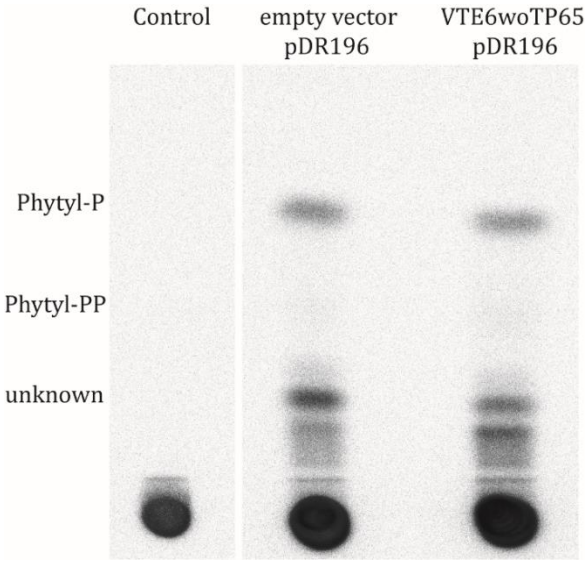

Figure 43 Radioactive Phytyl-P-Kinase Assay With Recombinant Protein From Yeast.

Protein extracts from yeast were incubated with phytyl-P and γ-^{32}P-CTP as described in 2.3.3.1. The reaction was stopped after 30 min by addition of methanol and the reaction products were separated on a TLC plate as described in 2.3.3.1. Afterwards the TLC plate was exposed to a phosphorimager screen for 48 h.

4 Discussion

Chlorophyll, the photosynthetically active pigment of plants and algae, is one of the most abundant molecules in nature. Therefore, phytol, the hydrophobic side chain of chlorophyll, presumably is the most abundant isoprenoid in the biosphere. During chlorotic stress, large amounts of phytol are released by hydrolysis of chlorophyll. Several metabolic pathways have been proposed to prevent accumulation of free phytol in the chloroplasts of plant cells. Ischebeck *et al.* (2006) showed that phytol is incorporated into different compounds: prenylquinones (tocopherol and phylloquinone), chlorophyll and fatty acid phytyl esters. Synthesis of chlorophyll, tocopherol and phylloquinone requires the phosphorylation of phytol to phytyl-P and then to phytyl-PP via phytol kinase and phytyl-P kinase. Fatty acid phytyl esters are directly produced by acylation of free phytol. In this work, the biochemical and functional characterization of some of the enzymes of phytol metabolism in *Arabidopsis* is presented: *Arabidopsis* insertion lines for Phytyl Esters Synthases (PES1, PES2) and for a putative Phytyl-P Kinase were characterized with regard to growth and development as well as their phytyl lipid composition. Furthermore, analytical methods were established that provide the means to understand the flux of phytol and its related compounds under stress conditions and in mutants with metabolic blocks in phytol metabolism.

4.1 A Comprehensive Method For Phytyl Lipid Analysis is Crucial To Understand Phytol Metabolism in Plants

Methods were already described for the quantitative analysis of several phytyl lipids, for example analysis of chlorophyll with a spectrophotometer (Porra *et al.,* 1989) or by HPLC, tocopherol measurement by fluorescence HPLC (Balz *et al.,* 1992; Zbierzak *et al.,* 2010), phytol determination using GC-MS (Ischebeck *et al.,* 2006) and fatty acid phytyl ester analysis using GC-MS (Ischebeck *et al.,* 2006; Gaude *et al.,* 2007). The Q-TOF mass spectrometer represents a highly sensitive instrument for the analysis of non-polar plant components. Using direct-infusion Q-TOF MS/MS after purification by solid-phase-extraction, fatty acid phytyl esters could be measured in very small sample amounts (10-20 mg). This is crucial for the analysis of leaves of mutants with a growth defect (e.g. *vte6* plants) or for seeds, which contain very low amounts of fatty acid phytyl esters.

The profile of fatty acid phytyl esters in seeds acquired by direct infusion Q-TOF MS/MS is presented in this work for the first time (Figure 16). The fatty acid composition of phytyl esters from seeds strongly differs from that in leaves. The most prominent molecular species in seeds is 18:3-phytol, followed by 18:2-phytol and 18:1-phytol. Smaller amounts of 16:3-phytol and 16:0-phytol were also detected. The medium-chain fatty acids that make up a large proportion of leaf fatty acid phytyl esters are of very low abundance in seeds. The fatty acid phytyl ester composition

of seeds is similar to the total fatty acid composition of seeds, because seeds contain mainly 16:0, 18:1, 18:2 and 18:3, but in contrast to phytyl esters, also substantial amounts of 20:1 (20% of total seed fatty acids) (Li *et al.,* 2006). 20:1-is mainly found in extraplastidic TAGs and is therefore not incorporated into plastid-localized fatty acid phytyl esters.

Increased sensitivity is provided by LC separation prior to mass spectrometry, because only one compound is eluted and measured at a time. This is important for the quantification of isoprenyl-phosphates. As isoprenyl-phosphates are polar due to the presence of one or two phosphate groups, they are difficult to extract from samples. Furthermore, they are of low abundance in most tissues.

The exact amounts of the C20-isoprenyl-phosphates phytyl-P, GG-P, phytyl-PP and GG-PP in *Arabidopsis* could be determined in this work for the first time. In the leaves and seeds of *Arabidopsis*, phytyl-PP is the most abundant isoprenyl-phosphate, yet the amount of phytyl-PP is six times higher in seeds than in leaves. The amount of tocopherol is also much higher in seeds than in leaves. Seeds contain 1.8 µmol g FW^{-1} and leaves 0.03 µmol g FW^{-1} of tocopherol. Therefore, a clear relationship between the amount of the substrate phytyl-PP and the product tocopherol exists in leaves and seeds. GG-PP is about 4-5 times less abundant than phytyl-PP in leaves and seeds. The phytylated and geranylgeranylated monophosphates (phytyl-P and GG-P) are much less abundant than the diphosphates. Phytyl-P and GG-P are likely of low abundance as they represent metabolic intermediates which are readily metabolized by phytyl-P kinase. It has long been discussed as to which extent phytyl-PP derived from GG-PP contributes to tocopherol biosynthesis. The data obtained in this study indicate that in leaves, the route of phytyl-PP synthesis through phytyl-P is far more relevant than the reduction of GG-PP. In conclusion, the LC-MS based method is a powerful tool to determine important intermediates in chlorophyll and prenylquinone metabolism. Together with the previously described methods, a comprehensive phytyl lipid profile can now be obtained, providing the means to understand the flow of phytol between different pathways under stress or in *Arabidopsis* mutants.

4.2 Fatty Acid Phytyl Ester Synthesis in *Arabidopsis* and *C. reinhardtii*

Fatty Acid Phytyl Esters in Arabidopsis

In *Arabidopsis*, PES1 and PES2 localize to plastoglobules of chloroplasts (Lippold *et al*., 2012). Therefore, substrates for phytyl ester synthesis are derived from chloroplast lipids only. Fatty acid phytyl esters produced in yellow leaves of *Arabidopsis* contain mostly 16:3 and medium-chain fatty acids. Feeding of WT and *pes1 pes2* plantlets with synthetic phytol also leads to accumulation of fatty acid phytyl esters. However, the fatty acid phytyl ester composition differs from that under nitrogen starvation. Medium-chain fatty acids and 16:3 are also synthesized in large amounts. However, 18:1 and 18:3 make up about one third of fatty acid phytyl esters after phytol feeding,

while they are hardly present in leaves under –N conditions or in purified plastoglobule fractions of control plants. In *pes1 pes2*, synthesis of 18:1-phytol is not affected after feeding of phytol, and 16:0-phytol also accumulates, but all other fatty acid phytyl esters were absent. Lippold *et al.* (2012) showed that the levels of 16:0-phytol, 18:1-phytol and 18:3-phytol are also unchanged in *pes1 pes2* during nitrogen starvation. A possible explanation is the presence of the four other *Arabidopsis* genes that belong to the family of ELT genes (ELT3, ELT4, ELT5 and ELT6) and could be responsible for the synthesis of the remaining fatty acid phytyl esters in *pes1 pes2*. The localization and expression pattern of the ELT enzymes needs to be studied to resolve the role of this pathway. All ELT protein sequences contain predicted transit peptides and therefore are likely localized to the chloroplast, similar to PES1 and PES2. Therefore, ELT enzymes might compensate for the loss of PES1 and PES2 in *pes1 pes2*.

The question of the *in vivo* acyl donor for PES1 and PES2 cannot be answered at this point. Phytol is released from chlorophyll in the thylakoid membranes. Medium-chain fatty acids are produced in the process of fatty acid *de novo* synthesis, bound to ACP (Harwood, 1996). Fatty acid *de novo* synthesis in plants is mainly localized to the stroma of the chloroplast. Therefore, the medium-chain (10:0, 12:0 and 14:0) acyl-ACPs might be direct substrates for fatty acid phytyl ester synthesis.

16:3-fatty acids in *Arabidopsis* occur nearly exclusively at the *sn-2* position of MGDG which is synthesized by the plastidial prokaryotic pathway (Ohlrogge and Browse, 1995). The fatty acid moiety of 16:3-phytol might be directly derived from the *sn-2* position of MGDG. However, 18:3 is highly abundant in MGDG of *Arabidopsis* as well, even at the *sn-2* position, yet is not incorporated into fatty acid phytyl esters under chlorotic stress. It is unlikely that PES1/PES2 have a specificity for the *sn-2* position of MGDG, because in the *Arabidopsis act1* mutant, where 18:3 is exclusively bound to the *sn-2* position of MGDG, 18:3 is still not incorporated into fatty acid phytyl esters (Gaude *et al.,* 2007). Therefore, it is more likely that either PES2 is specific for the direct transfer of 16:3 from MGDG to phytol, or that 16:3 is first hydrolyzed from MGDG by a 16:3 specific lipase and then activated by transfer to ACP or CoA. A comprehensive analysis of acyl-CoAs and acyl-ACPs in *Arabidopsis* chloroplasts would help to address the question of the substrate specificity of PES1 and PES2.

Acyltransferase Activity of PES1 and PES2 in Plants

In *Arabidopsis*, TAG is mostly produced in seeds, where it accounts for 94% of total lipids (Li-Beisson *et al.,* 2010; Bates and Browse, 2011). The enzymes responsible for TAG biosynthesis, DGAT1 and PDAT, are localized at the ER (Routaboul *et al.,* 1999; Zhang *et al.,* 2009). The TAGs produced by DGAT1 and PDAT are stored in lipid droplets that are derived from the ER membranes (Horn *et al.,* 2011). Leaves contain only small amounts of TAG under normal conditions (Chapman and Ohlrogge, 2012). However, under stress conditions (e.g. osmotic stress,

drought stress or freezing stress) TAGs accumulate also in *Arabidopsis* leaves (Moellering *et al.,* 2010).

PES1 and PES2 localize to plastoglobules of chloroplasts. Their expression is induced upon chlorotic stress. To analyze the contribution of PES1 and PES2 to TAG synthesis, *Arabidopsis* WT and *pes1 pes2* were grown under +N and –N conditions on synthetic medium and TAGs were quantified. In WT and *pes1 pes2*, TAG strongly accumulated under –N conditions while it is hardly detected in +N samples. In *pes1 pes2* the total amount of TAG is about 30% lower than in WT on –N. Therefore, PES1 and PES2 contribute to plastidial TAG synthesis under nitrogen deprivation. However, the contribution of PES1 and PES2 to total leaf TAG synthesis is minor because the bulk of TAG presumably is synthesized by DGAT1 and PDAT at the ER. During drought stress, TAG accumulation was also observed, however the molecular species composition of TAGs is distinct from that under nitrogen starvation. Large amounts of 16:3-18:3-18:3 and 16:3-16:3-18:3 were found, both of these molecular species are hardly present in plants grown under normal conditions or in chlorotic leaves derived from -N deprivation experiments.

Osmotic stress (vacuum-infiltration with $MgCl_2$) resulted in the same accumulation of 16:3-enriched TAGs as drought stress (data not shown). The amount of TAG after drought stress or osmotic stress increased in *pes1 pes2* but was unchanged as compared to WT, likely as the upregulation of *PES1* and *PES2* expression is specific to chlorotic stress. TAG accumulation after drought stress and osmotic stress stimulates galactolipid:galactolipid galactosyltransferase activity (GGGT, SRF2) (Moellering *et al.,* 2010) which results in the enrichment of TAGs with a high proportion of 16:3 at the plastidial envelopes.

In the last two years, additional functions for the PES enzymes were described. Aslan *et al.* (2014) transiently expressed AtPES2 together with fatty acid reductases (FAR) from *Arabidopsis* and *Marinobacter* in *N. benthamiana*, thereby efficiently producing wax esters enriched in medium-chain fatty acids. Nagel *et al.* (2014) discovered geranylgeranylated fatty acids and an increased production of GG-PP in spruce after overexpression of IDS enzymes. They assumed that these fatty acid geranylgeranyl esters are synthesized by the spruce orthologs of PES1 and PES2. Finally, Ariizumi *et al.* (2014) characterized the tomato gene *PYP1*, a homolog to *PES1* and *PES2*, which is responsible for esterification of xanthophyll in tomato flowers (Ariizumi *et al.,* 2014).

Considering the broad range of substrates that are used by PES1 and PES2, it is possible that these enzymes are also responsible for the esterification of other isoprenoids in plants, for example carotenoid esters in plastoglobules of senescent leaves (Steinmüller and Tevini, 1985; Tevini and Steinmüller, 1985).

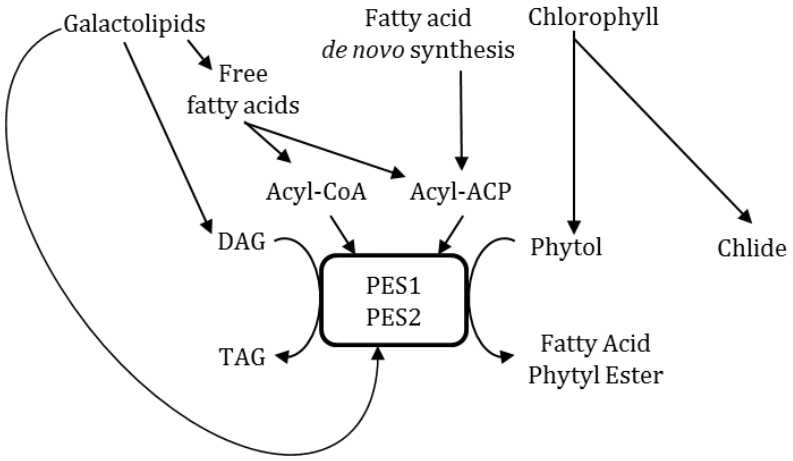

Figure 44 The Role of PES1 and PES2 in Lipid Metabolism of *Arabidopsis* Leaves.

PES1 and PES2 can use a variety of substrates as shown by enzyme assays after heterologous expression in yeast. *In planta*, fatty acid phytyl esters are synthesized by PES1/PES2 from phytol that results from cleavage of chlorophyll during chlorotic stress. The *in vivo* fatty acid donor still needs to be clearly identified. Fatty acids might be derived from degradation of galactolipids and could be incorporated into fatty acid phytyl esters directly, or after activation as acyl-CoA and acyl-ACP (modified from Lippold *et al.*, 2012).

4.3 Biological Function of Fatty Acid Phytyl Ester Synthesis

Fatty acid phytyl esters are produced in response to stress conditions or senescence. The block of fatty acid phytyl ester synthesis in the *pes1 pes2* double mutant does not affect growth or plant development. Only leaf senescence is slightly delayed. To understand the biological function of fatty acid phytyl esters, *Arabidopsis* WT plants were exposed to different stress conditions, and the physiological and biochemical response after returning the plants to normal growth conditions was tested. Plants were grown on MS medium with full nutrition, transferred to –N medium until nearly all chlorophyll was degraded, and returned to +N conditions until the leaves were green again. This experiment showed that fatty acid phytyl esters and tocopherol are synthesized from phytol derived from chlorophyll degradation under nitrogen deprivation in agreement with previous results (Ischebeck *et al.*, 2006). Moreover, after transfer from –N to +N conditions, the levels of chlorophyll increases as the levels of fatty acid phytyl esters decrease again, indicating a relationship between fatty acid phytyl ester degradation and chlorophyll synthesis. Interestingly, the same effect was observed in tocopherol levels determined under +N, -N and -+N conditions. However, it has to be noted that the levels of chlorophyll are ten-times and five-times higher than the levels of accumulating fatty acid phytyl esters and tocopherols, respectively. Therefore only a small proportion of the phytol is incorporated into fatty acid phytyl esters and tocopherol in chlorotic leaves.

Chlorophyll turnover in leaves is a continuous process and is strongly enhanced under stress (Alberte *et al.,* 1977; Dannehl *et al.,* 1995; Beisel *et al.,* 2010). Chlorophyll levels are varying based on the diurnal rhythm and in response to different light conditions (Yentsch and Ryther, 1957). Yentsch and Ryther (1957) demonstrated that a change in light radiation rapidly results in

reduced chlorophyll synthesis in phytoplankton. A similar mechanism could be present in plants and algae as well. Short-term variations in light intensitymight lead to decreased chlorophyll synthesis and increased chlorophyll turnover and fatty acid phytyl esters might be produced as a result.

Therefore it is possible that fatty acid phytyl esters and tocopherol represent intermediate sinks for the chlorophyll catabolite phytol during short term alterations in chlorophyll content caused by changes in irradiation. However, their levels are too low to provide enough storage capacity for the total amount of phytol released under stress conditions.

Mechanisms for the re-use of free phytol for incorporation into chlorophyll from fatty acid phytyl esters and tocopherol have never been described. However it is possible that a yet unknown hydrolase can de-esterify fatty acid phytyl esters, producing free phytol and free fatty acids as building blocks for chlorophyll and membrane lipid biosynthesis. The generation of free phytol from tocopherol is more complicated as carbon-carbon bonds need to be broken, and is therefore unlikely.

The function of fatty acid phytyl esters deposition during senescence or other stress conditions is not yet completely understood. The accumulation of free alcohols and free fatty acids is detrimental to membrane stability. Therefore, they have to be further metabolized or degraded. Acylation renders a compound less polar and therefore might help to translocate it to a nonpolar compartment such as the plastoglobules. Moreover, an ester linkage is easily broken down when the two components needs to be released.

Fatty Acid Phytyl Esters in C. reinhardtii

Homologs to ELT genes could be determined in higher plants, mosses, lycophytes and algae. Interestingly, putative ELT genes were also found in *C. reinhardtii*, a unicellular eukaryotic alga. The lipid biosynthesis and distribution in *C. reinhardtii* differs from that in *Arabidopsis*. PC is absent from *C. reinhardtii* and is functionally replaced by diacylglyceroltrimethylhomoserine (DGTS). Moreover, *C. reinhardtii* contains fatty acids that are absent from *Arabidopsis*. The fatty acid 16:4 can be found in the plastidial galactolipid MDGD in *C. reinhardtii* and replaces 16:3, which is bound at the *sn-2* position of MGDG in *Arabidopsis*. 16:4 is unique to MGDG in *C. reinhardtii*. Another unusual fatty acid found in *C. reinhardtii* is 18:4 (coniferonic acid), which is mainly found in extraplastidic lipids like diacylglyceroltrimethylhomoserine and TAG. *C. reinhardtii* accumulates large amounts of TAG during nitrogen starvation in lipid droplets (Boyle *et al.,* 2012). Therefore it represents a most interesting resource for the production of TAGs for the potential use as biofuels (Chisti, 2007; Griffiths and Harrison, 2009; Merchant *et al.,* 2012).

Fatty acid phytyl esters were measured in *C. reinhardtii* under +N and –N conditions using Q-TOF MS/MS. A variety of fatty acid phytyl esters could be detected. This is to our knowledge the first demonstration of the presence of fatty acid phytyl esters in algae. Under nitrogen deprivation, the

amount of fatty acid phytyl esters increases strongly, similar to the situation in *Arabidopsis*. The acyl composition of phytyl esters is very similar as that of TAGs in *C. reinhardtii* cells grown under the same conditions. The most abundant fatty acids are 16:0, 18:1, 18:2 and 18:3. Smaller amounts of 18:4 and 18:0 can be detected. 16:3 and 16:4 can hardly be detected in fatty acid phytyl esters. In *C. reinhardtii* as in *Arabidopsis*, TAGs can be synthesized in the plastid in addition to extraplastidial TAG biosynthesis (Merchant *et al.,* 2012). However, plastidial TAG accumulation in *C. reinhardtii* is minor and can only be observed under stress or in the *sta6* mutant, which over-accumulates TAGs (Goodson *et al.,* 2011). The lipid composition of *C. reinhardtii* TAGs also reflects the extraplastidic localization of the TAG biosynthetic pathway. Very little plastid-specific 16:4 is incorporated into TAG. In analogy, very little plastid-specific 16:3 is incorporated into TAGs in *Arabidopsis* under normal conditions or under chlorotic stress.

The fatty acid composition of fatty acid phytyl esters in *C. reinhardtii* is very different from fatty acids in MGDG. MGDG consists mainly of 16:4 and 18:3 under –N conditions.

The aycl composition of *C. reinhardtii* fatty acid phytyl esters differs strongly from that in *Arabidopsis* under –N conditions. Medium-chain fatty acids are hardly present in phytyl esters of *C. reinhardtii*. Moreover, 16:3 and 16:4 are hardly present in *C. reinhardtii* fatty acid phytyl esters, while 16:3-phytol is by far the most abundant fatty acid phytyl ester in chlorotic *Arabidopsis* leaves. Therefore, MGDG is most likely not a preferred acyl donor for fatty acid phytyl ester synthesis in *C. reinhardtii*. Based on the fatty acid composition of fatty acid phytyl esters, extraplastidic acyl-CoAs or glycerolipids could serve as acyl donor. 18:1, 18:3 and 18:4, which accumulate in fatty acid phytyl esters of *C. reinhardtii* are otherwise mainly found in extraplastidic lipids as diacylglyceroltrimethylhomoserine and TAG.

The fact that fatty acid phytyl esters accumulate under nitrogen deprivation indicates that the ELT sequences found in the *C. reinhardtii* genome, Cre01.g017100, Cre08.g365950 and Cre12.g521650 likely encode functional fatty acid phytyl ester synthases. Heterologous expression of these genes and enzyme assays with purified proteins could resolve their function and substrate specificities. Noticeably, the amounts of fatty acid phytyl esters accumulating in *C. reinhardtii* under –N conditions (about 2 fmol $cell^{-1}$) are more than 50-fold lower than the amounts of TAGs or MGDG (about 100 fmol $cell^{-1}$) (Fan *et al.,* 2011).

4.4 At1g78620 Encodes Phytyl-P Kinase in *Arabidopsis*

This work includes the characterization of a candidate gene for phytyl-P kinase in *Arabidopsis*, At1g78620, that was identified taking advantage of the SEED database (Overbeek *et al.,* 2005; Seaver *et al.,* 2014). The protein encoded by At1g78620 likely localizes to plastids (Ferro *et al.,* 2003). The *Arabidopsis* insertion lines *vte6-1* and *vte6-2* have strongly reduced phytyl-PP and tocopherol content, while the substrate for phytyl-P kinase, phytyl-P, accumulates (Figure 31 and

Figure 33). Therefore, At1g78620 likely encodes a functional phytyl-P kinase and was renamed VTE6 (for vitamin E deficient 6).

Heterologous Expression of VTE6

Attempts to detect phytyl-P kinase activity after heterologous expression of *VTE6* in *E. coli*, yeast and *N. benthamiana* were unsuccessful so far. The inability to record enzymatic activity after heterologous expression might be derived from different problems. It is possible that the cleavage site of the predicted *VTE6* transit peptide was incorrect, i.e. that the sequence omitted for heterologous expression was too short or too long. This could affect protein structure and the localization of *VTE6* in *E. coli* or yeast. In addition, the availability of co-factors or other important factors (ions, pH) may be limited in recombinant systems. Finally, the enzyme activity could be below detection limit for the radioactive and non-radioactive methods. Enrichment of the recombinant protein by column purification (e.g. via Ni-affinity chromatography using the His-tag) could be used to enrich enzyme activity. In addition to assays with proteins extracts, enzyme activity was tested employing a substrate feeding experiment to living cells. In this experiment, cells expressing *VTE6* (*E. coli*) were incubated with non-radioactive synthetic phytyl-P after induction of recombinant protein expression. However, no phytyl-P kinase activity could be measured. A possible explanation for the absence of phytyl-P kinase activity might be that any phytyl-PP that was synthesized in the cells expessing VTE6 could have been further metabolized in *E. coli* and therefore the levels might have been below detection limit after the feeding experiment.

In Vivo Activity of VTE6

A feeding experiment was carried out to test if phytyl-P kinase activity is inhibited in insertion lines of VTE6 using seedling of WT and *vte6-1* that were incubated with synthetic phytol. In fact, phytyl-PP accumulated in WT after feeding of phytol compared to the control (without phytol), while *vte6-1* did not accumulate phytyl-PP. At the same time, *vte6-1* seedlings accumulated phytyl-P compared to WT after phytol feeding.

Phytyl-P and GG-P increase approximately 5-fold higher in *vte6-1* compared to WT. Interestingly, the amounts of GG-P and GG-PP are also altered in *vte6* plants. The WT level of GG-P however is much lower than that of phytyl-P. GG-PP levels are slightly higher in *vte6-1* but not significantly altered. This effect cannot be explained by an increased rate of GG-PP synthesis via isoprenoid *de novo* synthesis as the gene expression of GGPS, the enzyme responsible for GG-PP synthesis, is strongly downregulated in *vte6-1* (Figure 41). The chlorophyll synthase ChlG can use both phytyl-PP and GG-PP as substrates to prenylate chlorophyllide a, thereby producing chlorophyll a and GG-chlorophyll a, respectively (Keller *et al.,* 1998). This can be explained by the high similarity

between phytol and geranylgeraniol, because they differ by only three double bonds (Figure 2). Therefore, *VTE6* might also be able to phosphorylate GG-P, producing GG-PP, and a block of *VTE6* activity could explain the accumulation of GG-PP. Shpilyov *et al.* (2013) also suspected a possible promiscuity of the phytol kinase and phytyl-P kinase activities for the respective geranylgeranylates phosphates.

The synthesis of geranylgeranylated and phytylated chlorophyll could present a "backup" metabolic pathway in plants. Under normal conditions, plants contain very little GG-chlorophyll. In *ggr* mutants chlorophyll is replaced by GG-chlorophyll and tocopherol by tocotrienol, but these plants are much smaller and paler than the control plants (Tanaka *et al.,* 1999; Yang *et al.,* 2011). This shows that plants grow poorly when phytylated compounds are missing. The functions of the phytylated forms (chlorophyll, tocopherol) in the chloroplasts can only partially be compensated for by the geranylgeranylated forms.

In *vte6-1* plants, phytyl-PP is reduced by about 60%. In turn, 40%, i.e. 18 nmol g FW^{-1}, of phytyl-PP levels remain in *vte6-1* leaves. The residual amount of phytyl-PP might be derived from reduction of GG-PP by GGR. GG-PP levels are unaffected in the *vte6* mutant. Therefore, GGR provides a steady supply of substrate for phytyl-PP synthesis. Intriguingly, the residual phytyl-PP pool is not sufficient to maintain tocopherol normal levels in *vte6-1* leaves. It can be deduced that tocopherol biosynthesis in leaves depends on phytol phosphorylation.

The situation in seeds is probably similar, because seeds of the *vte5-1* mutant have 80% less tocopherol than WT seeds (Valentin *et al.,* 2006). Intriguingly, overexpression of VTE6 in *Arabidopsis* seeds results in a 2-fold increase in phytyl-PP and in increased tocopherol levels. Therefore, phytol phosphorylation provides the predominant proportion of phytyl-PP for tocopherol biosynthesis in seeds.

Phytyl-PP is also an important substrate for chlorophyll synthesis: chlorophyll synthase prenylates chlorophyllide using phytyl-PP. In leaves of *vte5-2 vte6-1*, phytyl-PP is reduced by 86%, yet chlorophyll synthesis remains mainly unaffected: the leaves are green and chlorophyll levels are not significantly reduced. Therefore, it can be deduced that the residual phytyl-PP is used for chlorophyll synthesis in these plants and the decrease in phytyl-PP amount affects tocopherol but not chlorophyll synthesis. Possibly, the relative flux of phytyl-PP into chlorophyll is increased when phytyl-PP is limited in the *vte5-2 vte6-1* mutant to maintain photosynthesis in these plants.

4.5 Tocopherol Synthesis in *Arabidopsis* Leaves Requires Phytyl-PP from the Phytol Phosphorylation Pathway

Sequences homologous to VTE5 and *VTE6* can be found in plants, mosses, lycophytes, algae, archaea and bacteria (Valentin *et al.,* 2006) (this study). Therefore, the phytol phosphorylation pathway is conserved, similar to the phytol esterification pathway (Lippold *et al.*, 2012).

In leaves of *vte5*, *vte6* and *vte5-2 vte6-1* plants, tocopherol levels are lower than in WT (33%, 13% and 4% of WT amounts, respectively). Therefore, all mutants carry a block in the phytol phosphorylation pathway, and this block is strongest in the *vte5-2 vte6-1* double mutant. This shows that the phytol phosphorylation pathway for phytyl-PP production is almost the exclusive source of phytyl-PP for tocopherol production in the leaves. Phytyl-PP synthesized by reduction of GG-PP by GGR plays a minor role for tocopherol synthesis in *Arabidopsis* leaves.

VTE5 and VTE5-like

In *vte6-1* a 5-fold increase in phytyl-P levels compared to WT was measured. This increase was not detected in *vte5-2* and *vte5-2 vte6-1* plants where phytyl-P levels are lower than it WT. Therefore, VTE5 is responsible for the synthesis of the bulk of phytyl-P produced in the phytol phosphorylation pathway. The remaining phytyl-P might be produced by the VTE5-like enzyme At5g58560. Interestingly, an attempt to produce a *vte5-2 vte5-like* double mutant in our lab was not successful. Only plants homozygous for *vte5-2* and heterozygous for *vte5-like* or vice versa were obtained (unpublished results, Dr. Georg Hölzl, IMBIO, University of Bonn), suggesting that the flux of phytol through the phytol phosphorylation pathway is essential for plant development. The At5g58560 enzyme was previously implicated in farnesol phosphorylation, but its putative involvement in phytyl-P synthesis has not been studied (Fitzpatrick *et al.,* 2011). The presence of a *VTE5-LIKE* gene in addition to *VTE5* could explain that *vte5* mutants exhibit no growth retardation. It is possible that the levels of phytol accumulating in the *vte5-2 vte5-like* double mutant reach a toxic level that is lethal to gametes or to the embryo. High levels of free alcohols are detrimental to membrane stability (Löbbecke and Cevc, 1995).

The direct substrate for VTE5, PES1/PES2 and likely for VTE5-like is phytol, and in *vte5-2* and *pes1 pes2* mutants phytol accumulates. However, as described previously, there are several pathways to metabolize phytol: esterification, phosphorylation and degradation by α- and β-oxidation in peroxisomes and mitochondria. Therefore, accumulation of phytol to a toxic level is prevented in the single mutants, but this may not be the case in the *vte5-2 vte5-like* double mutant.

Seed Longevity Defect in vte6 Mutants

As shown in this work, seed longevity is affected in *vte6-1* and *vte6-2*. When stored for a period longer than three months, *vte6* seeds lose their germination capability. This effect was already described for *vte1* and in particular for *vte2,* and was explained by an increased nonenzymatic lipid peroxidation in seed TAGs and in seedlings (Sattler *et al.,* 2004). Lipid peroxidation in *vte1* was much less severe. This was explained by the accumulation of DMPBQ, which can compensate for the absence of tocopherols as antioxidant (Porfirova *et al.,* 2002; Sattler *et al.,* 2004). DMPBQ did not accumulate in leaves of *vte6* (data not shown).

Tocopherol levels could not be determined in homozygous seeds of *vte6* plants. Homozyogous *vte6* plants cannot produce seeds. The tocopherol analysis in single segregating seeds of a heterozygous *vte6* plant was technically impossible. However, the seed longevity phenotype which is similar to the tocopherol-deficient *vte2* mutant, together with the decreased tocopherol levels in leaves, indicate that seeds of *vte6* most likely have a strongly reduced tocopherol content.

Contents and molecular species composition of galactolipids and phospholipids in vte6-1

In wild type plants, 18:3 increases in the total fatty acid pool after long term growth at low temperature. This increase was particularly prominent in PC, as 18:3 containing molecular species (18:3-18:3) increased. However, the increase in 18:3 in total fatty acids, and of 18:3-18:3-PC at low temperature in *vte2* mutant plants was abolished (Sattler *et al.,* 2004; Maeda *et al.,* 2008; Mehrshahi *et al.,* 2013). Furthermore, *vte2* plants show a strong growth retardation at low temperature which was explained by the inability to increase the 18:3 content in this plant (Maeda et al., 2008). This effect was associated with tocopherol deficiency, but was independent from oxidative stress. On the other hand, the tocopherol-deficient *vte6* mutant also showed a reduced growth, already at normal temperatures (20°C). Therefore, it was possible that the *vte6* mutant also suffered from the incapability to produce sufficent amounts of 18:3, similar to the *vte2* mutant plant. When grown under normal temperatures, the amount of 18:3-18:3-PC in *vte6-1* and *vte6-2* was even higher than in WT. Therefore, *vte6* plants have a sufficient capacity for 18:3 production, and the alterations in growth and development of *vte6* are not associated with the decrease in 18:3-18:3- PC, in contrast to other tocopherol-deficient mutants (*vte2*) which show reduced growth under low temperature.

Furthermore, membrane glycerolipids are mainly unaffected in *vte6* plants. The amounts of MGDG and PG are reduced, likely as they are abundant in chloroplast membranes, and PC leaves are increased. The reduction in the amounts of chloroplast lipids might be explained by the fact that chloroplast physiology is affected in the *vte6* mutant resulting in decreased amounts of thylakoid lipids, thus affecting chlorophyll and galactolipid contents.

Accumulation of Phytol and Phytyl-P is Associated with Decreased Plant Growth and Developmental Perturbations

As shown in this work, *vte6* mutant plants show a severe growth defect. They are small, bushy and pale, can only grow on sucrose-supplemented medium and are infertile. This phenotype is not observed in *vte5-2* plants, which are null mutants for VTE5 as shown by RT-PCR. Moreover, *vte5-2 vte6-1* double mutant plants show a strong improvement of growth and development as compared to *vte6* single mutant plants. They can grow on soil and are taller and greener than the *vte6* plants.

The accumulation of phytol and phytyl-P is unique to *vte6* plants compared to WT, *vte5-2* and *vte5-2 vte6-1*, and presumably results in a severe growth defect. The defects observed in growth and development of *vte6* cannot be explained by the reduction of tocopherol as neither *vte1* nor *vte2* nor the double mutant *vte5-2 vte6-1* have a similar phenotype. The tocopherol levels in leaves of these mutants are below detection limit (Sattler *et al.,* 2004; Kanwischer *et al.,* 2005) (this study). The effect of the block in VTE6 in combination with the increased phytol and phytyl-P levels on plant metabolism is striking. As mentioned before, accumulation of free phytol could be harmful to the plants as it might compromise the integrity of biological membranes, e.g. thylakoids and envelopes of the plastid (Löbbecke and Cevc, 1995). The mechanism by which phytyl-P exerts its detrimental effect is unclear. Phytyl-P might directly act as signaling molecule negatively regulating growth and development. Other phosphorylated long-chain alcohols, for example long-chain base 1-phosphate, are potent signaling molecules in plants and animals (Lee *et al.,* 1999; Markham and Hille, 2001; Spiegel and Milstien, 2003; Scherer *et al.,* 2009; Guo *et al.,* 2012). Long-chain base 1-phosphate in *Arabidopsis* leaves of soil grown plants account for about 0.04 nmol g FW^{-1}. The amount of phytyl-P is higher (0.2 nmol g FW^{-1}) but still vely low as compared to other metabolites e.g. phytyl-PP.

In addition, phytyl-P itself could be toxic, in agreement with the fact that it is maintained at very low levels in *Arabidopsis*. For example, phytyl-P could interfere with important enzymatic reactions, because it might act as an inhibitor. Phytyl-P could also be metabolized to other compounds that are toxic to plant cells.

Feeding of WT plants grown on MS medium with phytyl-P could be used to address the question whether the growth retardation of *vte6-1* is due to phytyl-P toxicity. However, this experiment is difficult to perform as phytyl-P has to be chemically synthesized in large quantities and the yield during synthesis is low. Furthermore, it is unknown whether phytyl-P can be taken up by plants, and whether it can reach the leaf cells and the chloroplasts where it usually occurs.

A major difference between *vte6* and the other tocopherol-deficient mutants is the reduction in the chlorophyll content in *vte6* (Figure 34) which is hardly observed *vte1*, *vte2*, *vte5-2* and *vte5-2 vte6-1* (Figure 38). Therefore, it is possible that chlorophyll synthesis is affected in *vte6*, but it is obviously not affected in *vte5-2 vte6-1*. The fact that the amount of phytyl-PP is reduced cannot explain the reduction in chlorophyll synthesis of *vte6*, as phytyl-PP is also low in *vte5-2 vte6-1,* but this plant is not chlorotic. It is possible that chlorophyll synthesis is affected by phytol and phytyl-P accumulation via pleiotropic toxic effects on plastid metabolism. Another possible explanation might be the reduction in chlorophyll synthase activity, either caused by reduced gene expression or reduced enzyme activity. Expression data performed in this work show a strong reduction of chlorophyll synthase expression in *vte6-1* (Figure 41). It is also possible that phytyl-P directly inhibits chlorophyll synthase activity by binding to the chlorophyll synthase protein. Phytyl-P is structurally very similar to phytyl-PP, the direct substrate for chlorophyll synthase, and could

block the phytyl-PP binding site of chlorophyll synthase, thereby acting as competitive substrate inhibitor.

Expression analysis of tocopherol, chlorophyll and isoprenyl-phosphate synthetic enzymes was performed in *vte6-1*. Expression of VTE1, VTE4, VTE5, chlorophyll synthase, GGR (geranylgeranyl reductase) and GGPS3 (plastidial GG-PP synthase) was significantly decreased. VTE3 expression was slightly reduced and VTE2 expression was unchanged. Therefore, expression of most isoprenoid pathway genes is in general down-regulated in *vte6-1*. This finding points towards a pleiotropic effect of expression of chloroplast localized proteins in the *vte6-1* mutant, presumably originating from perturbations in the overall chloroplast metabolism of *vte6-1* plants. The strong alteration in chloroplast physiology might be caused by the toxic effects of phytol and phytyl-P accumulation. In combination, these negative effects on chloroplast metabolism might explain the strong growth defect and infertility: metabolic fluxes, gene expression and enzyme activities might be affected. Electron-micrographic pictures of chloroplasts from *vte6* plants might help to study the integrity of the plastids.

5 Summary and Outlook

The ability of a plant to convert light energy into chemical energy relies on the integrity and functionality of the photosynthetic membranes of the chloroplasts. Chlorophyll is one of the key players in photosynthesis as it is involved in capturing of photons and forms part of the electron transport chain. Therefore, its synthesis and turnover have to be tightly regulated. Upon chlorotic stress, large amounts of chlorophyll are hydrolyzed in chloroplasts and the breakdown products, phytol and pheophorbide, are further metabolized. In this work, two pathways for the metabolism of phytol after chlorophyll dephytylation were investigated: phytol esterification and phytol phosphorylation, resulting in the synthesis of fatty acid phytyl esters and isoprenyl-phosphates (phytyl-P and phytyl-PP), respectively.

First, a set of analytical tools was established to obtain a comprehensive profile of phytol-containing metabolites in *Arabidopsis*. Highly sensitive methods for the detection of fatty acid phytyl esters and isoprenyl-phosphates were developed, including optimization of sample preparation and direct infusion or liquid chromatography Q-TOF MS/MS analysis. These methods were used to quantify fatty acid phytyl esters and isoprenyl-phosphates in minute sample amounts and tissues of low abundance, where previous methods were unsuccessful because of lack of sensitivity. This work includes the first profile of isoprenyl-phosphates in *Arabidopsis* tissues. Using this set of methods, changes of phytol metabolism in mutants or during chlorotic stress could be determined.

Previous work showed that *PES1* and *PES2* encode functional Phytyl Ester Synthases in *Arabidopsis*, and that the *Arabidopsis pes1 pes2* mutant lacks the most abundant fatty acid phytyl esters. Therefore, the main route for fatty acid phytyl ester synthesis in *Arabidopsis* is via PES1 and PES2. In the present work, the biological function of fatty acid phytyl ester synthesis was investigated. When *Arabidopsis* was grown under nitrogen-deplete conditions, chlorophyll was degraded while fatty acid phytyl esters and tocopherol accumulated. When full nutrition was restored, fatty acid phytyl esters and tocopherol were degraded, possibly to provide phytol for synthesis of chlorophyll. Many photosynthetic organisms contain homologous sequences to *PES1* and *PES2*, for example *C. reinhardtii*. The present work demonstrated that *C. reinhardtii* produces fatty acid phytyl esters under nitrogen starvation. Therefore, the fatty acid phytyl ester synthesis pathway seems to be preserved from green algae to plants.

The role of PES1 and PES2 in TAG biosynthesis in chlorotic *Arabidopsis* leaves was further investigated. The double mutant *pes1 pes2* when grown under –N conditions accumulates 30% less TAG than WT plants under the same conditions. Therefore, a small proportion of TAG might

be synthesized by PES1 and PES2. Other stress conditions (drought, osmotic stress) did not result in a changed TAG accumulation in *pes1 pes2*. These data indicate that plastidial TAG production by PES1 and PES2 contributes only little to the total TAG pool, which is mostly derived from extraplastidic enzymes. To study plastidial TAG biosynthesis by PES1/PES2 in detail, the enzymes could be purified from *Arabidopsis* or *N. benthamiana* after expression with a protein tag and used for an enzyme assay.

A candidate gene for a *PHYTYL-P KINASE* in *Arabidopsis* was characterized in this work to study its role in the phytol phosphorylation pathway. The *Arabidopsis* insertion mutants for the gene At1g78620 (*vte6-1*, *vte6-2*) are tocopherol-deficient. Therefore, this gene was named *VITAMIN E DEFICIENT 6* (*VTE6*). Growth of *vte6-1* and *vte6-2* is strongly affected and homozygous seeds have a decreased longevity. Quantification of isoprenyl-phosphates using the method developed in this work revealed a strong accumulation of phytyl-P in *vte6-1,* while phytyl-PP was decreased. This indicates that At1g78620 encodes a phytyl-P kinase, because the level of phytyl-P increases as a result of a block in this pathway. Phytol and fatty acid phytyl ester levels were increased in *vte6-1* in agreement with the scenario that the phytol phosphorylation pathway is blocked. Overexpression of VTE6 results in an increase in phytyl-PP and tocopherol in seeds of *Arabidopsis*, giving additional evidence to the identity of VTE6 as phytyl-P kinase. Introduction of an additional mutation in phytol kinase (VTE5) activity into *vte6-1* by generating a *vte5-2 vte6-1* double mutant strongly improved the growth defect of the *vte6-1* plants. The double mutant plants are greener and larger than *vte6-1* and can grow on soil. This double mutant does not accumulate phytyl-P, as phytol phosphorylation is blocked. The *vte5-2 vte6-1* plants are tocopherol-deficient like *vte6-1*. Therefore, the tocopherol deficiency does not explain the severe phenotype of *vte6-1* and *vte6-2.* Instead, the growth retardation of *vte6-1* and *vte6-2* might result from a toxic effect exerted by phytol or phytyl-P. In the future, a phytol and phytyl-P feeding experiment will be performed with *Arabidopsis* WT plants to determine whether high levels of phytol or phytyl-P affect plant growth.

In conclusion, the highly sensitive methods developed in this work provided the means to establish a detailed overview of phytol metabolism under normal conditions, in stress and in *Arabidopsis* mutants. Moreover, it could be shown that phytol-P phosphorylation is essential for tocopherol biosynthesis in *Arabidopsis*. Phytol esterification is not essential for *Arabidopsis* metabolism but presumably represents a sink for small amounts of phytol during short-termed fluctuations in the chlorophyll content.

6 References

Alberte, R. S.; Thornber, J. P. and E. L. Fiscus (1977). Water stress effects on the content and organization of chlorophyll in mesophyll and bundle sheath chloroplasts of maize. Plant Physiology **59:** 351–353.

Almeida, J.; Asis, R.; Carrari, F.; Lira, B. S.; Molineri, V. N.; Sestari, I.; Pereira Peres, L. E. and M. Rossi (2015). Fruits from ripening impaired, chlorophyll degraded and jasmonate insensitive tomato mutants have altered tocopherol content and composition. Phytochemistry **111**.

Anderson, J. M. and A. Melis (1983). Localization of different photosystems in separate regions of chloroplast membranes. Proceedings of the National Academy of Sciences of the United States of America **80:** 745–749.

Ariizumi, T.; Kishimoto, S.; Kakami, R.; Maoka, T.; Hirakawa, H.; Suzuki, Y.; Ozeki, Y.; Shirasawa, K.; Bernillon, S.; Okabe, Y.; Moing, A.; Asamizu, E.; Rothan, C.; Ohmiya, A. and H. Ezura (2014). Identification of the carotenoid modifying gene *PALE YELLOW PETAL 1* as an essential factor in xanthophyll esterification and yellow flower pigmentation in tomato (*Solanum lycopersicum*). Plant Journal **79:** 453–465.

Aslan, S.; Sun, C.; Leonova, S.; Dutta, P.; Dörmann, P.; Domergue, F.; Stymne, S. and P. Hofvander (2014). Wax esters of different compositions produced via engineering of leaf chloroplast metabolism in *Nicotiana benthamiana*. Metabolic Engineering **25:** 103–112.

Austin, J. R.; Frost, E.; Vidi, P.-A.; Kessler, F. and L. A. Staehelin (2006). Plastoglobules are lipoprotein subcompartments of the chloroplast that are permanently coupled to thylakoid membranes and contain biosynthetic enzymes. Plant Cell **18:** 1693–1703.

Balz, M.; Schulte, E. and H.-P. Thier (1992). Trennung von Tocopherolen und Tocotrienolen duch die HPLC. Fat Science Technology **94:** 209–213.

Bates, P. D. and J. Browse (2011). The pathway of triacylglycerol synthesis through phosphatidylcholine in *Arabidopsis* produces a bottleneck for the accumulation of unusual fatty acids in transgenic seeds. Plant Journal **68:** 387–399.

Beisel, K. G.; Jahnke, S.; Hofmann, D.; Köppchen, S.; Schurr, U. and S. Matsubara (2010). Continuous turnover of carotenes and chlorophyll a in mature leaves of *Arabidopsis* revealed by $^{14}CO_2$ pulse-chase labeling. Plant Physiology **152:** 2188–2199.

Benedict, C. and R. Benedict (1978). Nature of obligate photoautotrophy. Annual Review of Plant Physiology **29:** 67–93.

Block, M. A.; Dorne, A. J.; Joyard, J. and R. Douce (1983). Preparation and characterization of membrane fractions enriched in outer and inner envelope membranes from spinach chloroplasts. II. Biochemical characterization. Journal of Biological Chemistry **258:** 13281–13286.

Boyle, N. R.; Page, M. D.; Liu, B.; Blaby, I. K.; Casero, D.; Kropat, J.; Cokus, S. J.; Hong-Hermesdorf, A.; Shaw, J.; Karpowicz, S. J.; Gallaher, S. D.; Johnson, S.; Benning, C.; Pellegrini, M.; Grossman, A. and S. S. Merchant (2012). Three acyltransferases and nitrogen-responsive regulator are implicated in nitrogen starvation-induced triacylglycerol accumulation in *Chlamydomonas*. Journal of Biological Chemistry **287:** 15811–15825.

Cahoon, E. B.; Hall, S. E.; Ripp, K. G.; Ganzke, T. S.; Hitz, W. D. and S. J. Coughlan (2003). Metabolic redesign of vitamin E biosynthesis in plants for tocotrienol production and increased antioxidant content. Nature Biotechnology **21:** 1082–1087.

Chapman, K. D. and J. B. Ohlrogge (2012). Compartmentation of triacylglycerol accumulation in plants. Journal of Biological Chemistry **287:** 2288–2294.

Charrier, B.; Champion, A.; Henry, Y. and M. Kreis (2002). Expression profiling of the whole *Arabidopsis* shaggy-like kinase multigene family by real-time reverse transcriptase-polymerase chain reaction. Plant Physiology **130:** 577–590.

Chen, A.; Dale Poulter, C. and P. A. Kroon (1994). Isoprenyl diphosphate synthases: Protein sequence comparisons, a phylogenetic tree, and predictions of secondary structure. Protein Science **3:** 600–607.

Chisti, Y. (2007). Biodiesel from microalgae. Biotechnology Advances **25:** 294–306.

Chow, C. K. (1991). Vitamin E and oxidative stress. Free Radical Biology and Medicine **11:** 215–232.

Clough, S. J. and A. F. Bent (1998). Floral dip: a simplified method for *Agrobacterium*-mediated transformation of *Arabidopsis thaliana*. The Plant Journal **16:** 735–743.

Collakova, E. and D. DellaPenna (2001). Isolation and functional analysis of homogentisate phytyltransferase from *Synechocystis* sp. PCC 6803 and *Arabidopsis*. Plant Physiology **127:** 1113–1124.

Collakova, E. and D. DellaPenna (2003). Homogentisate phytyltransferase activity is limiting for tocopherol biosynthesis in *Arabidopsis*. Plant Physiology **131:** 632–642.

Csupor, L. (1971). Das Phytol in vergilbten Blättern. Planta Med **19:** 37–41.

Dannehl, H.; Herbik, A. and D. Godde (1995). Stress-induced degradation of the photosynthetic apparatus is accompanied by changes in thylakoid protein turnover and phosphorylation. Physiologia Plantarum **93:** 179–186.

de la Torre, F.; El-Azaz, J.; Avila, C. and F. M. Cánovas (2014). Deciphering the role of aspartate and prephenate aminotransferase activities in plastid nitrogen metabolism. Plant Physiology **164:** 92–104.

Dyall, S. D.; Brown, M. T. and P. J. Johnson (2004). Ancient Invasions: from endosymbionts to organelles. Science **304:** 253–257.

Eckhardt, U.; Grimm, B. and S. Hörtensteiner (2004). Recent advances in chlorophyll biosynthesis and breakdown in higher plants. Plant Molecular Biology **56:** 1-14.

Erbilgin, N.; Krokene, P.; Christiansen, E.; Zeneli, G. and J. Gershenzon (2006). Exogenous application of methyl jasmonate elicits defenses in Norway spruce (*Picea abies*) and reduces host colonization by the bark beetle *Ips typographus*. Oecologia **148:** 426-436.

Fan, J.; Andre, C. and C. Xu (2011). A chloroplast pathway for the de novo biosynthesis of triacylglycerol in *Chlamydomonas reinhardtii*. FEBS Letters **585:** 1985–1991.

Felsenstein, J. (1985). Confidence limits on phylogenies: an approach using the bootstrap. Evolution **39:** 783–791.

Ferro, M.; Salvi, D.; Brugiere, S.; Miras, S.; Kowalski, S.; Louwagie, M.; Garin, J.; Joyard, J. and N. Rolland (2003). Proteomics of the chloroplast envelope membranes from *Arabidopsis thaliana*. Molecular Cell Proteomics **2:** 325–345.

Fitzpatrick, A. H.; Bhandari, J. and D. N. Crowell (2011). Farnesol kinase is involved in farnesol metabolism, ABA signaling and flower development in *Arabidopsis*. Plant Journal **66:** 1078–1088.

Gasulla, F.; Vom Dorp, K.; Dombrink, I.; Zähringer, U.; Gisch, N.; Dörmann, P. and D. Bartels (2013). The role of lipid metabolism in the acquisition of desiccation tolerance in *Craterostigma plantagineum*: a comparative approach. Plant Journal **75:** 726–741.

Gaude, N.; Brehelin, C.; Tischendorf, G.; Kessler, F. and P. Dormann (2007). Nitrogen deficiency in *Arabidopsis* affects galactolipid composition and gene expression and results in accumulation of fatty acid phytyl esters. Plant Journal **49:** 729–739.

Girotti, A. W. (1998). Lipid hydroperoxide generation, turnover, and effector action in biological systems. Journal of Lipid Research **39:** 1529–1542.

Goodson, C.; Roth, R.; Wang, Z. T. and U. Goodenough (2011). Structural correlates of cytoplasmic and chloroplast lipid body synthesis in *Chlamydomonas reinhardtii* and stimulation of lipid body production with acetate boost. Eukaryotic Cell **10:** 1592–1606.

Griffiths, M. J. and S. T. L. Harrison (2009). Lipid productivity as a key characteristic for choosing algal species for biodiesel production. Journal of Applied Phycology **21:** 493–507.

Grob, E. C. and L. Csupor (1967). Zur Kenntnis der Blattlipide von *Acer platanoides L.* während der herbstlichen Vergilbung. Experientia **23:** 1004-1005.

Gunning, B. E. S. (1965). The fine structure of chloroplast stroma following aldehyde osmium-tetroxide fixation. The Journal of Cell Biology **24:** 79–93.

Guo, L.; Mishra, G.; Markham, J. E.; Li, M.; Tawfall, A.; Welti, R. and X. Wang (2012). Connections between sphingosine kinase and phospholipase D in the abscisic acid signaling pathway in *Arabidopsis*. Journal of Biochemistry **287:** 8286–8296.

Guyer, L.; Hofstetter, S. S.; Christ, B.; Lira, B. S.; Rossi, M. and S. Hörtensteiner (2014). Different mechanisms are responsible for chlorophyll dephytylation during fruit ripening and leaf senescence in tomato. Plant Physiology **166:** 44–56.

Harwood, J. L. (1996). Recent advances in the biosynthesis of plant fatty acids. Biochimica et Biophysica Acta (BBA) - Lipids and Lipid Metabolism **1301:** 7–56.

Havaux, M.; Eymery, F.; Porfirova, S.; Rey, P. and P. Dörmann (2005). Vitamin E protects against photoinhibition and photooxidative stress in *Arabidopsis thaliana.* Plant Cell **17:** 3451–3469.

Hendry, G.; Houghton, J. D. and S. B. Brown (1987). Tansley review No. 11 - The degradation of chlorophyll - a biological enigma. New Phytologist **107:** 255–302.

Hiltbrunner, A.; Bauer, J.; Vidi, P.-A.; Infanger, S.; Weibel, P.; Hohwy, M. and F. Kessler (2001). Targeting of an abundant cytosolic form of the protein import receptor at Toc159 to the outer chloroplast membrane. The Journal of Cell Biology **154:** 309–316.

Holtzapple, E. and C. Schmidt-Dannert (2007). Biosynthesis of isoprenoid wax ester in *Marinobacter hydrocarbonoclasticus* DSM 8798. Journal of Bacteriology **189:** 3804–3812.

Horn, P. J.; Ledbetter, N. R.; James, C. N.; Hoffman, W. D.; Case, C. R.; Verbeck, G. F. and K. D. Chapman (2011). Visualization of lipid droplet composition by direct organelle mass spectrometry. Journal of Biological Chemistry **286:** 3298–3306.

Hörtensteiner, S. (1999). Chlorophyll breakdown in higher plants and algae. Cellular and Molecular Life Sciences **59:** 330–347.

Hörtensteiner, S. (2006). Chlorophyll degradation during senescence. Annual Review of Plant Biology **57:** 55–77.

Hörtensteiner, S. and B. Kräutler (2011). Chlorophyll breakdown in higher plants. Regulation of electron transport in chloroplasts **1807:** 977–988.

Hunter, W. N. (2007). The non-mevalonate pathway of isoprenoid precursor biosynthesis. Journal of Biological Chemistry **282:** 21573–21577.

Ischebeck, T.; Zbierzak, A. M.; Kanwischer, M. and P. Dörmann (2006). A salvage pathway for phytol metabolism in *Arabidopsis.* Journal of Biological Chemistry **281:** 2470–2477.

Jedlicki, E.; Jacob, G.; Faini, F.; Cori, O. and C. A. Bunton (1972). Stereospecificity of isopentenylpyrophosphate isomerase and prenyl transferase from Pinus and Citrus. Archives of Biochemistry and Biophysics **152:** 590–596.

Joo, C. N.; Park, C. E.; Kramer, J. K. and M. Kates (1973). Synthesis and acid hydrolysis of monophosphate and pyrophosphate esters of phytanol and phytol. Canadian Journal of Biochemistry **51:** 1527–1536.

Kandlbinder, A.; Finkemeier, I.; Wormuth, D.; Hanitzsch, M. and K.-J. Dietz (2004). The antioxidant status of photosynthesizing leaves under nutrient deficiency: redox regulation, gene expression and antioxidant activity in *Arabidopsis thaliana*. Physiologia Plantarum **120:** 63–73.

Kanwischer, M. (2006). Phytol aus dem Chlorophyllabbau ist limitierend für die Tocopherol (Vitamin E)-Synthese. PhD Thesis. Max Planck Institute of Molecular Plant Physiology, Golm, Germany.

Kanwischer, M.; Porfirova, S.; Bergmüller, E. and P. Dörmann (2005). Alterations in tocopherol cyclase activity in transgenic and mutant plants of *Arabidopsis* affect tocopherol content, tocopherol composition, and oxidative stress. Plant Physiology **137:** 713–723.

Karunanandaa, B.; Qi, Q.; Hao, M.; Baszis, S. R.; Jensen, P. K.; Wong, Y.-H. H.; Jiang, J.; Venkatramesh, M.; Gruys, K. J.; Moshiri, F.; Post-Beittenmiller, D.; Weiss, J. D. and H. E. Valentin (2005). Metabolically engineered oilseed crops with enhanced seed tocopherol. Metabolic Engineering **7:** 384–400.

Keeling, C. I. and J. Bohlmann (2006a). Diterpene resin acids in conifers. Phytochemistry **67:** 2415–2423.

Keeling, C. I. and J. Bohlmann (2006b). Genes, enzymes and chemicals of terpenoid diversity in the constitutive and induced defence of conifers against insects and pathogens. New Phytologist **170:** 657–675.

Keller, Y.; Bouvier, F.; d'Harlingue, A. and B. Camara (1998). Metabolic compartmentation of plastid prenyllipid biosynthesis. Evidence for the involvement of a multifunctional geranylgeranyl reductase. European Journal of Biochemistry **251:** 413.

Kim, S.; Schlicke, H.; van Ree, K.; Karvonen, K.; Subramaniam, A.; Richter, A.; Grimm, B. and J. Braam (2013). *Arabidopsis* chlorophyll biosynthesis: an essential balance between the methylerythritol phosphate and tetrapyrrole pathways. Plant Cell **25:** 4984–4993.

Kobayashi, N. and D. DellaPenna (2008). Tocopherol metabolism, oxidation and recycling under high light stress in *Arabidopsis*. Plant Journal **55:** 607–618.

Koressaar, T. and M. Remm (2007). Enhancements and modifications of primer design program Primer3. Bioinformatics (Oxford, England) **23:** 1289–1291.

Lange, M.; Rujan, T.; Martin, W. and R. Croteau (2000). Isoprenoid biosynthesis: The evolution of two ancient and distinct pathways across genomes. Proceedings of the National Academy of Sciences of the United States of America **97:** 13172–13177.

Larson, T. R. and I. A. Graham (2001). Technical advance: A novel technique for the sensitive quantification of acyl CoA esters from plant tissues. Plant Journal **25:** 115–125.

Lee, O. H.; Kim, Y. M.; Lee, Y. M.; Moon, E. J.; Lee, D. J.; Kim, J. H.; Kim, K. W. and Y. G. Kwon (1999). Sphingosine 1-phosphate induces angiogenesis: its angiogenic action and signaling mechanism in human umbilical vein endothelial cells. Biochemical and Biophysical Research Communications **264:** 743–750.

Leth, T. and H. Søndergaard (1977). Biological activity of vitamin E compounds and natural materials by the resorption-gestation test, and chemical determination of the vitamin E activity in foods and feeds. The Journal of Nutrition **107:** 2236–2243.

Li, Y.; Beisson, F.; Pollard, M. and J. Ohlrogge (2006). Oil content of *Arabidopsis* seeds: the influence of seed anatomy, light and plant-to-plant variation. Phytochemistry **67:** 904–915.

Li, Y.; Zhou, Y.; Wang, Z.; Sun, X. and K. Tang (2010). Engineering tocopherol biosynthetic pathway in *Arabidopsis* leaves and its effect on antioxidant metabolism. Plant Science **178:** 312–320.

Li-Beisson, Y.; Shorrosh, B.; Beisson, F.; Andersson, M. X.; Arondel, V.; Bates, P. D.; Baud, S.; Bird, D.; Debono, A.; Durrett, T. P.; Franke, R. B.; Graham, I. A.; Katayama, K.; Kelly, A. A.; Larson, T.; Markham, J. E.; Miquel, M.; Molina, I.; Nishida, I.; Rowland, O.; Samuels, L.; Schmid, K. M.; Wada, H.; Welti, R.; Xu, C.; Zallot, R. and J. Ohlrogge. Acyl-lipid metabolism. The *Arabidopsis* Book **11:** e0161. 2013.

Lichtenthaler, H. K. (1999). The 1-deoxy-D-xylose-5-phosphate pathway of isoprenoid biosynthesis in plants. Annual Review of Plant Physiology and Plant Molecular Biology **50:** 47–65.

Lichtenthaler, H. K.; Prenzel, U.; Douce, R. and J. Joyard (1981). Localization of prenylquinones in the envelope of spinach chloroplasts. Biochimica et Biophysica Acta (BBA) - Biomembranes **641:** 99–105.

Lichtenthaler, H. K.; Rohmer, M. and J. Schwender (1997). Two independent biochemical pathways for isopentenyl diphosphate and isoprenoid biosynthesis in higher plants. Physiologia Plantarum **101:** 643–652.

Liebler, D. C. (1993). The role of metabolism in the antioxidant function of vitamin E. Critical Reviews in Toxicology **23:** 147–169.

Liebler, D. C.; Burr, J. A.; Philips, L. and A. J. L. Ham (1996). Gas chromatography–mass spectrometry analysis of vitamin E and its oxidation products. Analytical Biochemistry **236:** 27–34.

Linn, T. C. (1967). The demonstration and solubilization of β-hydroxy-β-methylglutaryl coenzyme A reductase from rat liver microsomes. Journal of Biological Chemistry **242:** 984–989.

Lippold, F.; Vom Dorp, K.; Abraham, M.; Hölzl, G.; Wewer, V.; Lindberg-Yilmaz, J.; Lager, I.; Montandon, C.; Besagni, C.; Kessler, F.; Stymne, S. and P. Dörmann (2012). Fatty acid phytyl ester synthesis in chloroplasts of *Arabidopsis*. Plant Cell **24:** 2001–2014.

Livak, K. J. and T. D. Schmittgen (2001). Analysis of relative gene expression data using real-time quantitative PCR and the 2−ΔΔCT method. Methods **25:** 402–408.

Löbbecke, L. and G. Cevc (1995). Effects of short-chain alcohols on the phase behavior and interdigitation of phosphatidylcholine bilayer membranes. Biochimica et Biophysica Acta (BBA) - Biomembranes **1237:** 59–69.

Maeda, H.; Sage, T. L.; Isaac, G.; Welti, R. and D. DellaPenna (2008). Tocopherols modulate extraplastidic polyunsaturated fatty acid metabolism in *Arabidopsis* at low temperature. Plant Cell **20:** 452–470.

Markham, J. E. and J. Hille (2001). Host-selective toxins as agents of cell death in plant-fungus interactions. Molecular Plant Pathology **2:** 229–239.

Markham, J. E.; Li, J.; Cahoon, E. B. and J. G. Jaworski (2006). Separation and identification of major plant sphingolipid classes from leaves. Journal of Biological Chemistry **281:** 22684–22694.

Mehrshahi, P.; Stefano, G.; Andaloro, J. M.; Brandizzi, F.; Froehlich, J. E. and D. DellaPenna (2013). Transorganellar complementation redefines the biochemical continuity of endoplasmic reticulum and chloroplasts. Proceedings of the National Academy of Sciences of the United States of America **110:** 12126–12131.

Mène-Saffrané, L.; Jones, A. D. and D. DellaPenna (2010). Plastochromanol-8 and tocopherols are essential lipid-soluble antioxidants during seed desiccation and quiescence in *Arabidopsis*. Proceedings of the National Academy of Sciences of the United States of America **107:** 17815–17820.

Merchant, S. S.; Kropat, J.; Liu, B.; Shaw, J. and J. Warakanont (2012). TAG, you're it! *Chlamydomonas* as a reference organism for understanding algal triacylglycerol accumulation. Current Opinion in Biotechnology **23:** 352–363.

Miriyala, S.; Subramanian, T.; Panchatcharam, M.; Ren, H.; McDermott, M. I.; Sunkara, M.; Drennan, T.; Smyth, S. S.; Spielmann, H. P. and A. J. Morris (2010). Functional characterization of the atypical integral membrane lipid phosphatase PDP1/PPAPDC2 identifies a pathway for interconversion of isoprenols and isoprenoid phosphates in mammalian cells. Journal of Biological Chemistry **285:** 13918–13929.

Moellering, E. R. and C. Benning (2010). RNA interference silencing of a major lipid droplet protein affects lipid droplet size in *Chlamydomonas reinhardtii*. Eukaryotic Cell **9:** 97–106.

Moellering, E. R.; Muthan, B. and C. Benning (2010). Freezing tolerance in plants requires lipid remodeling at the outer chloroplast membrane. Science **330:** 226–228.

Munné-Bosch, S. (2005). The role of α-tocopherol in plant stress tolerance. Journal of Plant Physiology **162:** 743–748.

Nagel, R.; Berasategui, A.; Paetz, C.; Gershenzon, J. and A. Schmidt (2014). Overexpression of an isoprenyl diphosphate synthase in spruce leads to unexpected terpene diversion products that function in plant defense. Plant Physiology **164:** 555–569.

Nagel, R.; Gershenzon, J. and A. Schmidt (2012). Nonradioactive assay for detecting isoprenyl diphosphate synthase activity in crude plant extracts using liquid chromatography coupled with tandem mass spectrometry. Analytical Biochemistry **422:** 33–38.

Nei, M. and S. Kumar (2000). Molecular evolution and phylogenetics. Oxford University Press **2**.

Norris, S. R.; Barrette, T. R. and D. DellaPenna (1995). Genetic dissection of carotenoid synthesis in *Arabidopsis* defines plastoquinone as an essential component of phytoene desaturation. Plant Cell **7:** 2139–2149.

Ogura, K.; Nishino, T. and S. Seto (1968). The purification of prenyltransferase and isopentenyl pyrophosphate isomerase of pumpkin fruit and their some properties. Journal of Biochemistry **64:** 197–203.

Ohlrogge, J. and J. Browse (1995). Lipid biosynthesis. Plant Cell **7:** 957–970.

Oster, U.; Bauer, C. E. and W. Rüdiger (1997). Characterization of chlorophyll a and bacteriochlorophyll a synthases by heterologous expression in *Escherichia coli*. Journal of Biological Chemistry **272:** 9671–9676.

Overbeek, R.; Begley, T.; Butler, R. M.; Choudhuri, J. V.; Chuang, H. Y.; Cohoon, M.; Crecy-Lagard, V. de; Diaz, N.; Disz, T.; Edwards, R.; Fonstein, M.; Frank, E. D.; Gerdes, S.; Glass, E. M.; Goesmann, A.; Hanson, A.; Iwata-Reuyl, D.; Jensen, R.; Jamshidi, N.; Krause, L.; Kubal, M.; Larsen, N.; Linke, B.; McHardy, A. C.; Meyer, F.; Neuweger, H.; Olsen, G.; Olson, R.; Osterman, A.; Portnoy, V.; Pusch, G. D.; Rodionov, D. A.; Ruckert, C.; Steiner, J.; Stevens, R.; Thiele, I.; Vassieva, O.; Ye, Y.; Zagnitko, O. and V. Vonstein (2005). The subsystems approach to genome annotation and its use in the project to annotate 1000 genomes. Nucleic Acids Research **33:** 5691–5702.

Pageau, K.; Reisdorf-Cren, M.; Morot-Gaudry, J.-F. and C. Masclaux-Daubresse (2006). The two senescence-related markers, GS1 (cytosolic glutamine synthetase) and GDH (glutamate dehydrogenase), involved in nitrogen mobilization, are differentially regulated during pathogen attack and by stress hormones and reactive oxygen species in *Nicotiana tabacum L.* leaves. Journal of Experimental Botany **57:** 547–557.

Patterson, G. W.; Hugly, S. and D. Harrison (1993). Sterols and phytyl esters of *Arabidopsis thaliana* under normal and chilling temperatures. Phytochemistry **33:** 1381–1383.

Phillips, M. A.; D'Auria, J. C.; Gershenzon, J. and E. Pichersky (2008a). The *Arabidopsis thaliana* type I isopentenyl diphosphate isomerases are targeted to multiple subcellular compartments and have overlapping functions in isoprenoid biosynthesis. Plant Cell **20:** 677–696.

Phillips, M. A.; León, P.; Boronat, A. and M. Rodríguez-Concepción (2008b). The plastidial MEP pathway: unified nomenclature and resources. Trends in Plant Science **13:** 619–623.

Porfirova, S.; Bergmüller, E.; Tropf, S.; Lemke, R. and P. Dörmann (2002). Isolation of an *Arabidopsis* mutant lacking vitamin E and identification of a cyclase essential for all tocopherol biosynthesis. Proceedings of the National Academy of Sciences of the United States of America **99:** 12495–12500.

Porra, R. J.; Thompson, W. A. and P. E. Kriedemann (1989). Determination of accurate extinction coefficients and simultaneous equations for assaying chlorophylls a and b extracted with four different solvents. Biochimica et Biophysica Acta (BBA) - Lipids and Lipid Metabolism **975:** 384–394.

Pružinská, A.; Tanner, G.; Anders, I.; Roca, M. and S. Hörtensteiner (2003). Pheophorbide a oxygenase is a Rieske-type iron-sulfur protein, encoded by the accelerated cell death 1 gene. Proceedings of the National Academy of Sciences of the United States of America **100:** 15259–15264.

Pružinská, A.; Tanner, G.; Aubry, S.; Anders, I.; Moser, S.; Müller, T.; Ongania, K.-H.; Kräutler, B.; Youn, J.-Y.; Liljegren, S. J. and S. Hörtensteiner (2005). Chlorophyll breakdown in senescent *Arabidopsis* leaves. Characterization of chlorophyll catabolites and of chlorophyll catabolic enzymes involved in the degreening reaction. Plant Physiology **139:** 52–63.

Re, E. B.; Brugger, S. and M. Learned (1997). Genetic and biochemical analysis of the transmembrane domain of *Arabidopsis* 3-hydroxy-3-methylglutaryl coenzyme A reductase. Journal of Cellular Biochemistry **65:** 443–459.

Rentsch, D.; Laloi, M.; Rouhara, I.; Schmelzer, E.; Delrot, S. and W. B. Frommer (1995). NTR1 encodes a high affinity oligopeptide transporter in *Arabidopsis*. FEBS Letters **370:** 264–268.

Riewe, D.; Koohi, M.; Lisec, J.; Pfeiffer, M.; Lippmann, R.; Schmeichel, J.; Willmitzer, L. and T. Altmann (2012). A tyrosine aminotransferase involved in tocopherol synthesis in *Arabidopsis*. Plant Journal **71:** 850–859.

Rodríguez-Concepción, M. and A. Boronat (2002). Elucidation of the methylerythritol phosphate pathway for isoprenoid biosynthesis in bacteria and plastids. A metabolic milestone achieved through genomics. Plant Physiology **130:** 1079–1089.

Roessner, U.; Wagner, C.; Kopka, J.; Trethewey, R. N. and L. Willmitzer (2000). Simultaneous analysis of metabolites in potato tuber by gas chromatography-mass spectrometry. Plant Journal **23:** 131–142.

Rogers, D. (1983). Evidence that the essential sulfhydryl-group of HMG-CoA reductase is involved in the binding of HMG-CoA and not NADPH. Journal of Lipid Research **24:** 1412.

Rohmer, M. (1999). The discovery of a mevalonate-independent pathway for isoprenoid biosynthesis in bacteria, algae and higher plants. Natural Product Reports **16:** 565–574.

Rontani, J.-F.; Cuny, P. and V. Grossi (1996). Photodegradation of chlorophyll phytyl chain in senescent leaves of higher plants. Phytochemistry **42:** 347–351.

Routaboul, J. M.; Benning, C.; Bechtold, N.; Caboche, M. and L. Lepiniec (1999). The TAG1 locus of *Arabidopsis* encodes for a diacylglycerol acyltransferase. Plant Physiology and Biochemistry **37:** 831–840.

Saitou, N. and M. Nei (1987). The neighbor-joining method: a new method for reconstructing phylogenetic trees. Molecular Biology and Evolution **4:** 406–425.

Sattler, S. E.; Gilliland, L. U.; Magallanes-Lundback, M.; Pollard, M. and D. DellaPenna (2004). Vitamin E is essential for seed longevity and for preventing lipid peroxidation during germination. Plant Cell **16:** 1419–1432.

Savidge, B.; Weiss, J. D.; Wong, Y.-H. H.; Lassner, M. W.; Mitsky, T. A.; Shewmaker, C. K.; Post-Beittenmiller, D. and H. E. Valentin (2002). Isolation and characterization of homogentisate phytyltransferase genes from *Synechocystis* sp. PCC 6803 and *Arabidopsis.* Plant Physiology **129:** 321–332.

Scheibe, R. (1991). Redox-modulation of chloroplast enzymes. Plant Physiology **96:** 1–3.

Schelbert, S.; Aubry, S.; Burla, B.; Agne, B.; Kessler, F.; Krupinska, K. and S. Stefan Hörtensteiner (2009). Pheophytin pheophorbide hydrolase (pheophytinase) is involved in chlorophyll breakdown during leaf senescence in *Arabidopsis*. Plant Cell **21:** 767–785.

Scherer, M.; Schmitz, G. and G. Liebisch (2009). High-throughput analysis of sphingosine 1-phosphate, sphinganine 1-phosphate, and lysophosphatidic acid in plasma samples by liquid chromatography-tandem mass spectrometry. Clinical Chemistry **55:** 1218–1222.

Schmidt, A. and J. Gershenzon (2007). Cloning and characterization of isoprenyl diphosphate synthases with farnesyl diphosphate and geranylgeranyl diphosphate synthase activity from Norway spruce (*Picea abies*) and their relation to induced oleoresin formation. Phytochemistry **68:** 2649–2659.

Schüep, W. and R. Rettenmeier (1994). Analysis of vitamin E homologs in plasma and tissue: High-performance liquid chromatography. Methods Enzymology **234:** 294–302.

Seaver, S. M. D.; Gerdes, S.; Frelin, O.; Lerma-Ortiz, C.; Bradbury, L. M. T.; Zallot, R.; Hasnain, G.; Niehaus, T. D.; El Yacoubi, B.; Pasternak, S.; Olson, R.; Pusch, G.; Overbeek, R.; Stevens, R.; Crécy-Lagard, V. de; Ware, D.; Hanson, A. D. and C. S. Henry (2014). High-throughput comparison, functional annotation, and metabolic modeling of plant genomes using the PlantSEED resource. Proceedings of the National Academy of Sciences of the United States of America **111:** 9645–9650.

Shalygo, N.; Czarnecki, O.; Peter, E. and B. Grimm (2009). Expression of chlorophyll synthase is also involved in feedback-control of chlorophyll biosynthesis. Plant Molecular Biology **71:** 425–436.

Shpilyov, A. V.; Zinchenko, V. V.; Grimm, B. and H. Lokstein (2013). Chlorophyll a phytylation is required for the stability of photosystems I and II in the cyanobacterium *Synechocystis* sp. PCC 6803. Plant Journal **73:** 336–346.

Soll, J.; Schultz, G.; Joyard, J.; Douce, R. and M. A. Block (1985). Localization and synthesis of prenylquinones in isolated outer and inner envelope membranes from spinach chloroplasts. Archives of Biochemistry and Biophysics **238:** 290–299.

Spiegel, S. and S. Milstien (2003). Sphingosine-1-phosphate: an enigmatic signalling lipid. Nature Reviews Molecular Cell Biology **4:** 397–407.

Steinmüller, D. and M. Tevini (1985). Composition and function of plastoglobuli. I. Isolation and purification from chloroplasts and chromoplasts. Planta **163:** 201–207.

Tamura, K.; Peterson, D.; Peterson, N.; Stecher, G.; Nei, M. and S. Kumar (2011). MEGA5: molecular evolutionary genetics analysis using maximum likelihood, evolutionary distance, and maximum parsimony methods. Molecular Biology and Evolution **28:** 2731–2739.

Tanaka, R.; Oster, U.; Kruse, E.; Rüdiger, W. and B. Grimm (1999). Reduced activity of geranylgeranyl reductase leads to loss of chlorophyll and tocopherol and to partially geranylgeranylated chlorophyll in transgenic tobacco plants expressing antisense RNA for geranylgeranyl reductase. Plant Physiology **120:** 695–704.

Tevini, M. and D. Steinmüller (1985). Composition and function of plastoglobuli. II. Lipid composition of leaves and plastoglobuli during beech leaf senescence. Planta **163:** 91-96.

Thompson, J. D.; Gibson, T. J.; Plewniak, F.; Jeanmougin, F. and D. G. Higgins (1997). The CLUSTAL_X windows interface: flexible strategies for multiple sequence alignment aided by quality analysis tools. Nucleic Acids Research **25:** 4876–4882.

Tong, H.; Wiemer, A. J.; Neighbors, J. D. and R. J. Hohl (2008). Quantitative determination of farnesyl and geranylgeranyl diphosphate levels in mammalian tissue. Analytical Biochemistry **378:** 138–143.

Untergasser, A.; Cutcutache, I.; Koressaar, T.; Ye, J.; Faircloth, B. C.; Remm, M. and S. G. Rozen (2012). Primer3-new capabilities and interfaces. Nucleic Acids Research **40:** e115.

Vailleau, F.; Daniel, X.; Tronchet, M.; Montillet, J.-L.; Triantaphylidès, C. and D. Roby (2002). A R2R3-MYB gene, AtMYB30, acts as a positive regulator of the hypersensitive cell death program in plants in response to pathogen attack. Proceedings of the National Academy of Sciences of the United States of America **99:** 10179–10184.

Valentin, H. E.; Lincoln, K.; Moshiri, F.; Jensen, P. K.; Qi, Q.; Venkatesh, T. V.; Karunanandaa, B.; Baszis, S. R.; Norris, S. R.; Savidge, B.; Gruys, K. J. and R. L. Last (2006). The *Arabidopsis vitamin E pathway gene5-1* mutant reveals a critical role for phytol kinase in seed tocopherol biosynthesis. Plant Cell **18:** 212–224.

Valentin, H. E. and Q. Qi (2005). Biotechnological production and application of vitamin E: current state and prospects. Applied Microbiology and Biotechnology **68:** 436–444.

van den Brink, D. M.; van Miert, J. N.; Dacremont, G.; Rontani, J.-F. and R. J. Wanders (2005). Characterization of the final step in the conversion of phytol into phytanic acid. Journal of Biological Chemistry **280:** 26838–44.

Vidi, P. A.; Kanwischer, M.; Baginsky, S.; Austin, J. R.; Csucs, G.; Dormann, P.; Kessler, F. and C. Brehelin (2006). Tocopherol cyclase (VTE1) localization and vitamin E accumulation in chloroplast plastoglobule lipoprotein particles. Journal of Biological Chemistry **281:** 11225–11234.

Vom Dorp, K.; Dombrink, I. and P. Dörmann (2013). Quantification of diacylglycerol by mass spectrometry. Plant Lipid Signaling Protocols **1009:** 43-54.

Wanders, R. J.; Jansen, G. A. and M. D. Lloyd (2003). Phytanic acid alpha-oxidation, new insights into an old problem: a review. Biochimica et Biophysica Acta (BBA) - Molecular and Cell Biology of Lipids **1631:** 119–135.

Wanders, R. J. A.; Komen, J. and S. Ferdinandusse (2011). Phytanic acid metabolism in health and disease. Biochimica et Biophysica Acta (BBA)-Molecular and Cell Biology of Lipids **1811:** 498–507.

Wang, K. (2000). Isoprenyl diphosphate synthases. Biochimica et Biophysica Acta (BBA) - Molecular and Cell Biology of Lipids **1529:** 33–48.

Welti, R.; Li, W.; Li, M.; Sang, Y.; Biesiada, H.; Zhou, H.-E.; Rajashekar, C. B.; Williams, T. D. and X. Wang (2002). Profiling membrane lipids in plant stress responses. Role of phospholipase Da in freezing-induced lipid changes in *Arabidopsis.* Journal of Biological Chemistry **277:** 31994–32002.

Whatley, J. M. and F. R. Whatley (1981). Chloroplast evolution. New Phytologist **87:** 233–247.

Whistance, G. R. and D. R. Threlfall (1970). Biosynthesis of phytoquinones. Homogentisic acid: a precursor of plastoquinones, tocopherols and alpha-tocopherolquinone in higher plants, green algae and blue-green algae. Biochemical Journal **117:** 593–600.

Yang, W.; Cahoon, R. E.; Hunter, S. C.; Zhang, C.; Han, J.; Borgschulte, T. and E. B. Cahoon (2011). Vitamin E biosynthesis: functional characterization of the monocot homogentisate geranylgeranyl transferase. Plant Journal **65:** 206–217.

Yao, N.; Imai, S.; Tada, Y.; Nakayashiki, H.; Tosa, Y.; Park, P. and S. Mayama (2002). Apoptotic cell death is a common response to pathogen attack in oats. Molecular Plant-Microbe Interactions **15:** 1000–1007.

Yentsch, C. S. and J. H. Ryther (1957). Short-term variations in phytoplankton chlorophyll and their significance. Limnology and Oceanography **2:** 140–142.

Ytterberg, A. J.; Peltier, J. B. and van Wijk, K. J. (2006). Protein profiling of plastoglobules in chloroplasts and chromoplasts. A surprising site for differential accumulation of metabolic enzymes. Plant Physiology **140:** 984–997.

Zäuner, S.; Jochum, W.; Bigorowski, T. and C. Benning (2012). A cytochrome b5-containing plastid-located fatty acid desaturase from *Chlamydomonas reinhardtii*. Eukaryotic Cell **11:** 856–863.

Zbierzak, A. M.; Kanwischer, M.; Wille, C.; Vidi, P. A.; Giavalisco, P.; Lohmann, A.; Briesen, I.; Porfirova, S.; Brehelin, C.; Kessler, F. and P. Dormann (2010). Intersection of the tocopherol and plastoquinol metabolic pathways at the plastoglobule. Biochemical Journal **425:** 389–399.

Zhang, D. L. and C. D. Poulter (1993). Analysis and purification of phosphorylated isoprenoids by reversed-phase HPLC. Analytical Biochemistry **213:** 356–361.

Zhang, M.; Fan, J.; Taylor, D. C. and J. B. Ohlrogge (2009). DGAT1 and PDAT1 acyltransferases have overlapping functions in *Arabidopsis* triacylglycerol biosynthesis and are essential for normal pollen and seed development. Plant Cell **21:** 3885–3901.

Zhang, W.; Liu, T.; Ren, G.; Hörtensteiner, S.; Zhou, Y.; Cahoon, E. B. and C. Zhang (2014). Chlorophyll degradation: the tocopherol biosynthesis-related phytol hydrolase in *Arabidopsis* seeds is still missing. Plant Physiology **166:** 70–79.

Zhu, X.; Suzuki, K.; Saito, T.; Okada, K.; Tanaka, K.; Nakagawa, T.; Matsuda, H. and M. Kawamukai (1997). Geranylgeranyl pyrophosphate synthase encoded by the newly isolated gene GGPS6 from *Arabidopsis thaliana* is localized in mitochondria. Plant Molecular Biology **35:** 331–341.

7 Appendix

7.1 LC-MS Chromatograms of Isoprenyl-Phosphates

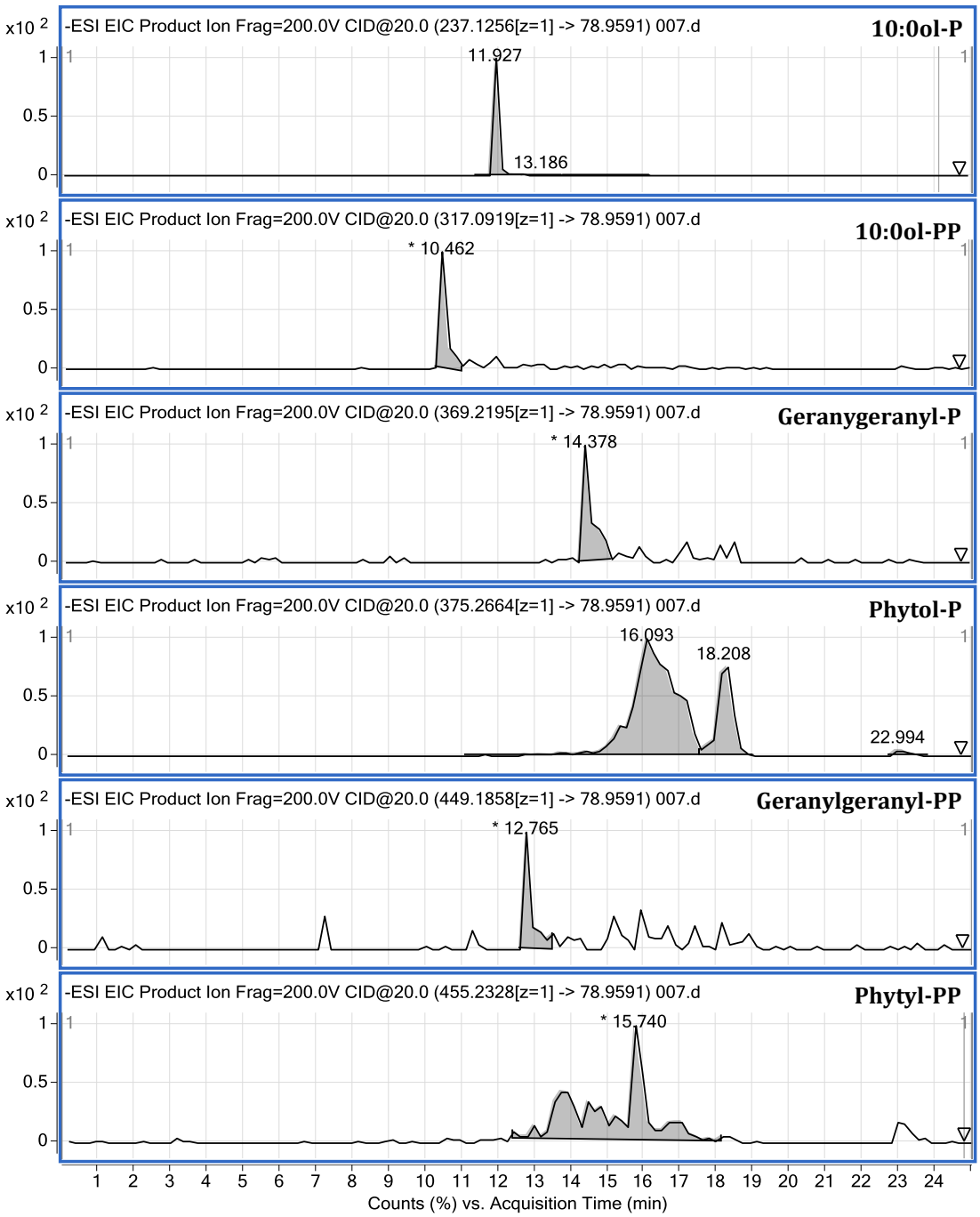

Figure 45 Chromatographic Separation of Standards and C20-Isoprenyl-Phosphates from *Arabidopsis* Leaves.

Isoprenyl-phosphates were isolated and measured as described in 3.1.2. All compounds can be separated based on chain length and the degree of phosphorylation. 10:0ol-P and 10:0ol–PP were added as internal standards. The y-axis shows the relative peak intensity (%).

7.2 Synthetic Oligonucleotides

Table 15 Synthetic Oligonucleotides.

Oligonucleotides used for this work were ordered from IDT Genomics (Leuven, BE). Restriction sites in the oligonucleotide sequences are underlined.

Primer	Sequence	Gene target
bn130	tccgttccgttttcgttttttac	Transposon primer Ds5-2a G-Edge
bn232	ccggatcgtatcggttttcg	Transposon primer Ds3-2a H-Edge
bn233	atggcaacgatttcgtcaactc	VTE6 forward (*vte6-1*, *vte6-2*)
bn234	gtccagccaatgttccttcaag	VTE6 reverse (*vte6-1*, *vte6-2*)
bn771	actgtacctccgtcaatcgcc	VTE5 forward (*vte5-2*)
bn772	aagcttaagacaagcgcgtatg	VTE5 reverse(*vte5-2*)
bn78	attttgccgatttcggaac	Left border primer SALK
bn358	gccatccaagctgttctctc	Forward RT primer ACT2
bn359	gaaccaccgatccagacact	Reverse RT primer ACT2
bn577	gcaacgaaggttaaaatgacgc	Forward RT primer VTE6
bn578	gaagcacctattatgctctctc	Reverse RT primer VTE6
bn410	caaactcagttccctccgtc	Forward RT primer VTE5
bn411	gtccgttaataacaagccttaag	Reverse RT primer VTE5
bn2109	attggttcaagtgctgctgg	VTE6-qPCR-fw
bn2110	agctccctctgttcctcttg	VTE6-qPCR-rev
bn2111	atttgcgatgatggccgtac	VTE1-qPCR-fw
bn2112	aactcaaacctttcaccgcc	VTE1-qPCR-rev
bn2113	ccctatcttccattggcatca	VTE2-qPCR-fw
bn2114	caatccacccaagccagaa	VTE2-qPCR-rev
bn2115	agggacgttgcttcaaatcttc	HPPD-qPCR-fw (Li *et al.,* 2010)
bn2116	caaaaccaccacatcctcca	HPPD-qPCR-rev (Li *et al.,* 2010)
bn2117	gaggggaataagggaagcgta	VTE3-qPCR-fw (Li *et al.,* 2010)
bn2118	aaaagaagcgagagagccagaa	VTE3-qPCR-rev (Li *et al.,* 2010)
bn2119	gcttttatgaccctgattcttctgt	VTE4-qPCR-fw (Li *et al.,* 2010)
bn2120	cacacccaacatccactactttct	VTE4-qPCR-rev (Li *et al.,* 2010)
bn2133	taagtgcatttgtgatcaacctgaatg	RT-PCR At1g78620.2 forward
bn2134	caggaagcagccaacagatg	RT-PCR At1g78620.2 reverse
bn2139	tcctcactttcatcagccgt	ACT2, fw
bn2140	catctcctgcaaatccagcc	ACT2, rev
bn2141	ggtaacattgtgctcagtggtgg	ACT2 (Charrier *et al.,* 2002)
bn2142	aacgaccttaatcttcatgctgc	ACT2 (Charrier *et al.,* 2002)
bn2143	ggccttgtataatccctgatgaataag	UBI-10, fw
bn2144	aaagagataacaggaacggaaacatagt	UBI-10, rev
bn2147	ctgtgccctagaaatggtgc	GGR-qPCR-fw
bn2148	atgagtctgaggatggtggc	GGR-qPCR-rev
bn2149	cactcaagatccacgaagcg	GGPS3-qPCR-fw
bn2150	gtgtgaatcatctcgacggc	GGPS3-qPCR-rev
bn2151	ctcaccggttctgttctcct	VTE5-qPCR-fw
bn2152	acgtcatgcaacagcgaatt	VTE5-qPCR-rev
bn2153	cactgtctccaccatccact	ChlG-qPCR-fw
bn2154	atcagtatcagtctccgccg	ChlG-qPCR-rev
bn2004	atactagtatggcaacgatttcgtcaac	VTE6 for TAP-tag fusion, *SpeI*
bn2005	gcggatcccttgacccagttctggagta	VTE6 for TAP-tag fusion, *BamHI*, wo stop codon
bn2006	gcggatccatggagagcagcagatgga	C-TAP for TAP-tag fusion, *BamHI*
bn2007	atctcgagtcactttggggcttgggcat	C-TAP for TAP-tag fusion, *XhoI*
bn1726	aggatccgatgctttccaacggaatgctttc	VTE6woTP47 for expression in *E. coli*, *BamHI*
bn1727	aggatccgatggaaggagtgatgacggaggc	VTE6woTP65 for expression in *E. coli*, *BamHI*
bn1728	agtcgaccttgacccagttctggagtataa	VTE6woTP65 for expression in *E. coli*, *BamHI*, wo stop codon

7.3 Targeted Lists for MS Analysis

Table 16 Targeted List for GC-MS Analysis of Isoprenyl Alcohols.

Phytol was quantified using GC-MS after derivatization with MSTFA and was measured as trimethylsilyl (TMS)-derivative. A product ion of the TMS group (m/z 73) was used to determine the amount of octadecenol, while a product ion of the silylated phytol moiety (m/z 143) was used for the quantification of phytol.

Isoprenyl Alcohols	Formula [M]	M	M+TMS	Product Ion m/z
Octadecenol (I.S.)	$C_{18}H_{36}O$	268.2766	340	73
Phytol	$C_{20}H_{40}O$	296.3079	368	143

Table 17 Targeted List for Q-TOF-MS/MS Analysis of Fatty Acid Phytyl Esters.

Fatty acid phytyl esters were measured as ammonium adducts (NH_4^+) using direct infusion Q-TOF MS/MS in the positive ion mode by neutral loss scanning of the phytol-H_2O moiety, 278.2974.

Fatty Acid Phytyl Esters	Formula [M]	M	Parental Ion $[M+NH_4]^+$	Neutral Loss $[Phytol-H_20]^+$
10:0-phytol	$C_{30}H_{58}O_2$	450.4437	468.4781	278.2974
12:0-phytol	$C_{32}H_{62}O_2$	478.475	496.5094	
14:0-phytol	$C_{34}H_{66}O_2$	506.5063	524.5407	
16:0-phytol	$C_{36}H_{70}O_2$	534.5376	552.572	
16:1-phytol	$C_{36}H_{68}O_2$	532.5219	550.5563	
16:2-phytol	$C_{36}H_{66}O_2$	530.5063	548.5407	
16:3-phytol	$C_{36}H_{64}O_2$	528.4906	546.525	
16:4-phytol	$C_{36}H_{62}O_2$	526.475	544.5094	
17:0-phytol	$C_{37}H_{72}O_2$	548.5532	566.5876	
18:0-phytol	$C_{38}H_{74}O_2$	562.5689	580.6033	
18:1-phytol	$C_{38}H_{72}O_2$	560.5532	578.5876	
18:2-phytol	$C_{38}H_{70}O_2$	558.5376	576.572	
18:3-phytol	$C_{38}H_{68}O_2$	556.5219	574.5563	
18:4-phytol	$C_{38}H_{66}O_2$	554.5063	572.5407	

Table 18 Targeted List for Q-TOF-MS/MS Analysis of Alcohol-Phosphates.

Alcohol-phosphates were measured as deprotonated ions by LC-Q-TOF-MS/MS in the negative ion mode by scanning for a fragment of the phosphate group, m/z 78.9591.

Alcohol-Phosphates	Formula [M]	M	Parental Ion $[M-H]^-$	Product Ion $[HPO_3]^-$
10:0ol-P (I.S.)	$C_{10}H_{23}O_4P$	238.1334	237.1256	m/z 78.9591
10:0ol-PP (I.S.)	$C_{10}H_{24}O_7P_2$	318.0997	317.0919	
16:0ol-P (I.S.)	$C_{16}H_{35}O_4P$	322.2273	321.2195	
16:0ol-PP (I.S.)	$C_{16}H_{36}O_7P_2$	402.1936	401.1858	
18:0ol-P (I.S.)	$C_{18}H_{39}O_4P$	350.2586	349.2508	
18:0ol-PP (I.S.)	$C_{18}H_{40}O_7P_2$	430.2249	429.2171	
20:0ol-P (I.S.)	$C_{20}H_{43}O_4P$	378.2899	377.2821	
20:0ol-PP (I.S.)	$C_{20}H_{44}O_7P_2$	458.2562	457.2484	
Geranylgeranyl-P	$C_{20}H_{35}O_4P$	370.2273	369.2195	
Geranylgeranyl-PP	$C_{20}H_{36}O_7P_2$	450.1936	449.1858	
Phytyl-P	$C_{20}H_{41}O_4P$	376.2742	375.2664	
Phytyl-PP	$C_{20}H_{42}O_7P_2$	456.2406	455.2328	

7.4 Constructs for Expression of VTE6 in *E.coli*, Yeast, *Arabidopsis* and *N. benthamiana*

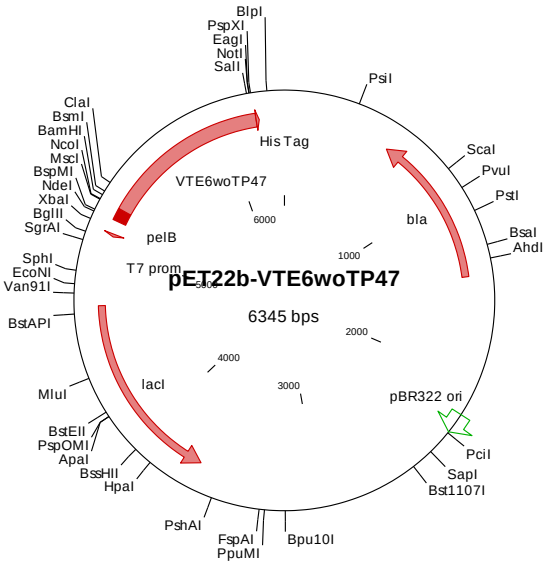

Figure 46 Construct for Expression of VTE6 without Transit Peptide in *E. coli.*

The coding sequence of *VTE6* without the predicted transit peptide was amplified by PCR with addition of restriction sites for BamHI/SalI and ligated into the pET22b(+) vector. Two different versions of VTE6 without transit peptide (VTE6woTP) were cloned, according to two different predictions: starting at amino acid 47 and 67.

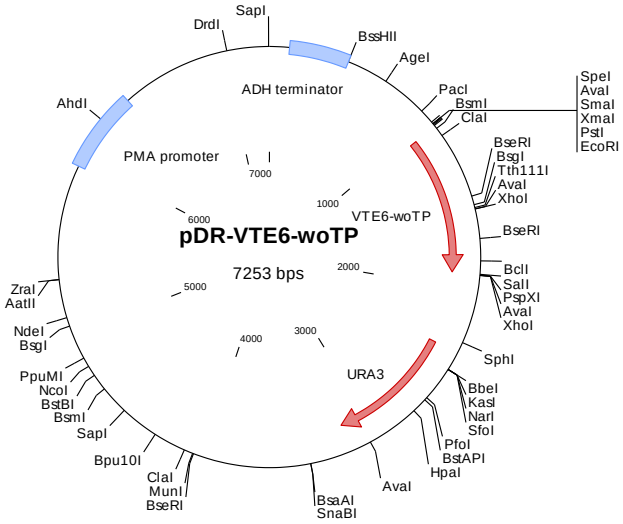

Figure 47 Construct for Expression of VTE6 without Transit Peptide in Yeast.

The coding sequence of *VTE6* without the predicted transit peptide (amino acids 1-65) was amplified by PCR with addition of restriction sites for EcoRI/SalI and ligated into the pDR196 vector.

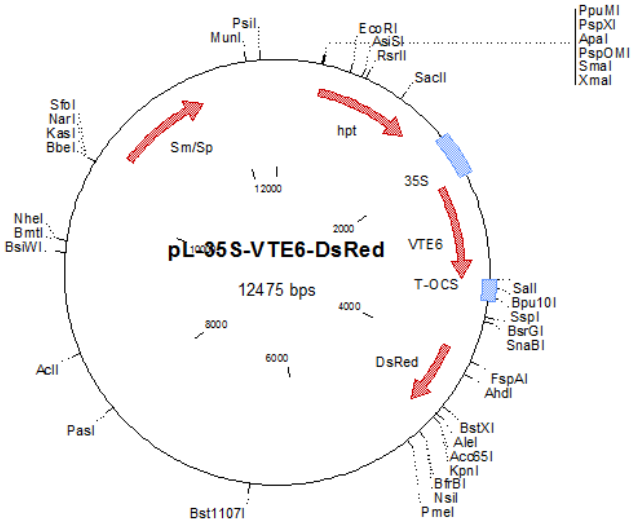

Figure 48 Construct for Overexpression of VTE6 in *Arabidopsis*.

The coding sequence of *VTE6* was amplified by PCR with addition of restriction sites for XbaI/SalI, respectively, and ligated into the modified pLH9000 vector with 35S promoter and DsRed marker (Dr. Georg Hölzl, 2009).

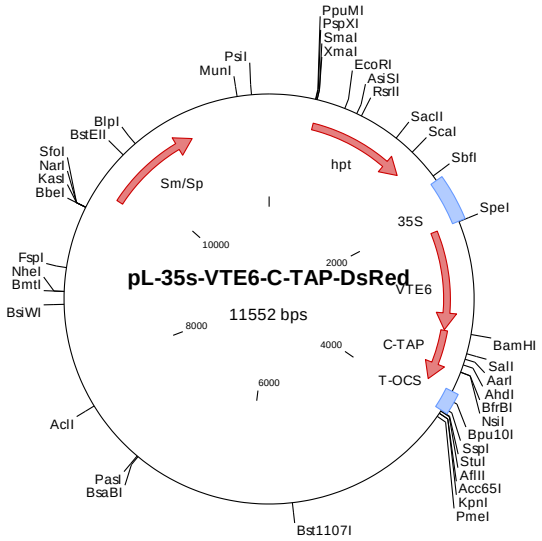

Figure 49 Construct for Expression of VTE6-TAP Fusion Protein in *N. benthamiana*.

The coding sequences of *VTE6* and C-TAP were amplified by PCR with addition of restriction sites for SpeI/BamHI and BamHI/SalI, respectively, and ligated into the modified pLH9000 vector with 35S promoter and DsRed marker in a single ligation step.

8 Publication List

Parts of this thesis were published in:

Lippold, F.*; vom Dorp, K.*; Abraham, M.; Hölzl, G.; Wewer, V.; Lindberg-Yilmaz, J.; Lager, I.; Montandon, C.; Besagni, C.; Kessler, F.; Stymne, S. and P. Dörmann (2012). Fatty acid phytyl ester synthesis in chloroplasts of *Arabidopsis.* Plant Cell **5**: 2001–2014 (* equal contributions).

vom Dorp, K.; Dombrink, I. and P. Dörmann (2013). Quantification of diacylglycerol by mass spectrometry. Plant Lipid Signaling Protocols **1009**: 43-54.

vom Dorp, K.; Hölzl, G.; Abraham, M.; Hanson, A.D. and P. Dörmann (2015). Remobilization of phytol from chlorophyll degradation is essential for tocopherol synthesis and growth of *Arabidopsis.* Plant Cell (doi:10.1105/tpc.15.00395).